PhD Thesis

Performance of a space-time coded multicarrier CDMA system in frequency-selective Rayleigh channel

Submitted by

Olanrewaju Bola Wojuola

In fulfilment of the degree of

Doctor of Philosophy in Electronic Engineering at the University of KwaZulu-Natal, Durban, South Africa

Date of submission

October 2014

Supervised by

Prof. Stanley H. Mneney

As the candidate's supervisor, I agree to the submission of this thesis.

Signed: ______________________________

Name: _______________________________ Date: ___________________

Dedication

Dedicated to God,
the merciful and gracious One;

and to
His Son Jesus Christ.

PREFACE

The research work reported in this thesis was performed by Olanrewaju Bola Wojuola under the supervision of Professor Stanley H. Mneney at the School of Engineering, University of KwaZulu-Natal, Durban, South Africa. The research work was supported by German Academic Exchange Programme (DAAD - Deutscher Akademischer Austausch Dienst), as well as the Center of Excellence (CoE), and the Centre for Engineering Postgraduate Studies (CEPS), both of the School of Engineering, University of KwaZulu-Natal, South Africa.

The whole thesis, unless otherwise indicated, is the author's work and has not been submitted in part, or in whole, to any other University for degree purposes.

ACKNOWLEDGEMENT

My sincere appreciation goes to my supervisor Professor S. H. Mneney for his patience, kindness guidance, and gentle approach. He is a source of help, encouragement and motivation.

Special thanks goes to my wife, Rosemary Nike Wojuola, for her kind support, sacrifice, supplication, patience, forbearance and encouragement throughout the PhD period. She has been a source of constant support and encouragement. Thank you for being always there for me. I also thank my son, Toluwanimi, for his endurance, affection and sacrifice. Special thanks go to Dr Aderemi Adewumi, Dr. Ilesanmi Oluwafemi and Dr Olutayo Oyerinde for their invaluable support, suggestions and encouragement from the time of admission and at different stages of the work. Thank you for every way you have made this PhD a reality.

I also wish to express my appreciation to my parents and siblings for their love, sacrifices, patience, concerns and care in making me who I am today. Thank you very much for every contribution you have made to my life. My gratitude also goes to the DLCF family in South Africa.

I wish to express my gratitude to the German Academic Exchange Programme (DAAD - Deutscher Akademischer Austausch Dienst), as well as the Center of Excellence (CoE), and the Centre for Engineering Postgraduate Studies (CEPS), both of the School of Engineering, University of KwaZulu-Natal for supporting this research work.

Thanks to all professors, lecturers and support staff of the university who offered support and help in the course of my PhD programme.

Above all, I give praise to God for His great mercies and help concerning this PhD programme.

ABSTRACT

The increasing demand for wireless services requires fast and robust broadband wireless communication for efficient utilisation of the scarce electromagnetic spectrum. One of the promising techniques for future wireless communication is the deployment of multi-input multi-output (MIMO) antenna system with orthogonal frequency division multiplexing (OFDM) coupled with multiple-access techniques. The combination of these techniques guarantees a much more reliable and robust transmission over the hostile wireless channel. This thesis investigates the performance of a multi-antenna space-time coded (STC) multi-carrier code-division multiple-access (MC-CDMA) system in a frequency-selective channel using Gold codes as spreading sequences.

Spreading codes are known to be central to the performance of spread spectrum systems, STC MC-CDMA systems inclusive. Initial phase of this research work investigates multiple-access performance of spreading codes for the communication system. The performance of different sets of Gold codes for increasing number of interfering users for up to a thousand users and eight different code lengths, ranging from 31 to 4095-chip Gold codes, were considered. Simulation results show that odd-degree Gold codes give better bit-error-rate performance than even-degree Gold codes. Whereas the odd-degree codes exhibited relatively marginal loss in performance when the system was loaded, their even-degree counterparts degraded rapidly in performance, resulting in early emergence of an error floor, culminating in premature system saturation.

Furthermore in this thesis, software simulations were carried to investigate the performance of a direct-sequence (DS) CDMA system in a flat-fading Rayleigh channel, and a multi-carrier (MC) CDMA system in a frequency-selective channel using different sets of Gold. The results showed that in a flat-fading channel, the Gold codes provide a constant coding gain close to that obtainable in a Gaussian channel. The results also showed that the impact of longer spreading codes was more pronounced for the MC-CDMA system in a frequency-selective channel as indicated by significant lowering of error floors. Also, frequency diversity associated with the use of longer codes coupled with multi-carrier modulation makes the MC-CDMA system resilient to multi-path effects.

Further still, this thesis investigated the performance of a space-time block-coded (STBC) CDMA system in a flat-fading channel. Results showed that at low signal-to-noise ratio, the coding gain provided by the codes surpasses the diversity advantage provided by the use of the multiple antennas. The results also showed that coding gain between no-diversity link and its Gold-coded counterpart is the same as that between the transmit-diversity link and its Gold–coded counterpart. The independence of the diversity advantage provided by multiple transmit antennas and the coding gain obtainable from the use of the spreading sequences enables the prediction of the performance of composite space-time block-coded CDMA systems.

Performance of a STBC OFDM system as well as a STBC MC-CDMA system in frequency-selective channel was also investigated. Results showed that the combination of diversity gain from the use of multiple antennas, coupled with coding gain provided by the Gold codes of the CDMA system, plus the diversity gain resulting from frequency diversity of multi-carrier transmission and the spectrum-spreading by the CDMA makes the composite STBC MC-CDMA system resilient to channel fading. This fact is particularly the case for long codes. For example, with reference to the OFDM transmission, the results showed that a 511-chip Gold-coded STC MC-CDMA system provided a factor of about 3,786 reduction in error floor.

TABLE OF CONTENTS

TABLE OF FIGURES

LIST OF TABLES

LIST OF ABBREVIATIONS

BER	-	Bit-Error Rate
BPSK	-	Binary Phase Shift Keying
CDMA		-Code-Division Multiple-Access
DS	-	Direct-Sequence
DS-CDMA	-	Direct Sequence CDMA
FDM	-	Frequency Division Multiplexing
FDMA		-Frequency-Division Multiple-Access
FFT	-	Fast Fourier Transform
FH-CDMA	-	Frequency-Hopping CDMA
GPS	-	Global Positioning System
IFFT	-	Inverse Fast Fourier Transform
ISI	-	Inter-Symbol Interference
LFSR	-	Linear Feedback Shift Register
LOS	-	Line-of-Sight
MAI	-	Multiple-Access Interference
MC	-	Multi-carrier
MC-CDMA	-	Multicarrier CDMA
MIMO		-Multiple-Input Multiple-Output
MT-CDMA	-	Multi-Tone CDMA
OFDM	-	Orthogonal Frequency-Division Multiplexing

PN	-	Pseudo-noise (PN)
PRN	-	Pseudo-Random Noise (PRN)
QPSK	-	Quadrature Phase Shift Keying
SOSTTC		-Super-Orthogonal STTC
SSMA	-	Spread-Spectrum Multiple Access
STBC	-	Space-Time Block Code
STC	-	Space-Time Coding
STTC	-	Space-Time Trellis Code
TDMA	-	Time-Division Multiple-Access
TH-CDMA	-	Time-Hopping CDMA
WCDMA	-	Wideband CDMA

Chapter 1

General Introduction

1.0 Background

Telecommunications in the current information age is increasingly relying on the wireless link. It is doubtless to say that wireless communication is one of the fastest-growing aspects of modern technology. This is particularly applicable to mobile communication. Wireless communication has made possible a variety of services ranging from voice to data, and now multimedia [1]. Consequently, demand for new wireless capacity is growing rapidly. Nevertheless, wireless communication system is constantly faced with diverse challenges. One of these has to do with numerous users having to share a common channel. Another challenge is the sparsely available radio frequency spectrum. Added to these is the hostile nature of the wireless propagation channel, coupled with the increasing demand for higher data rates and better quality of service.

This chapter gives a brief treatment of common access methods and evolving techniques for mitigating factors militating against the performance of mobile communication systems, more precisely the code-division multiple-access (CDMA), leading to an itemization of research objectives.

The rest of this chapter is organised as follows. Common access techniques are considered in Section 1.1. The research problem is described in Section 1.2, followed by aims and objectives in Section 1.3. Section 1.4 provides a summary of original contributions, with a list of published works resulting from this research. Organisation of the rest of this thesis is given in Section 1.5.

1.1 *Multiple access techniques*

Wireless communication often involves numerous users having to share a common channel, which might result in some conflicts among several users wanting to transmit at the same time. This calls for some form of multiple-access techniques in order to resolve the conflicts among users. In what follows, we shall be considering basic access techniques [2] in use today.

1.1.1 Time Division Multiple Access

One of the common access techniques is time-division multiple-access (TDMA), which involves the use of time slots. The time axis is divided into frames of time slots having certain duration, Fig. 1.1. Each time slot is allocated to a different user. During this time slot, the user has the whole channel bandwidth at his disposal. Time slots are separated by guard times in which transmission by a user is prohibited.

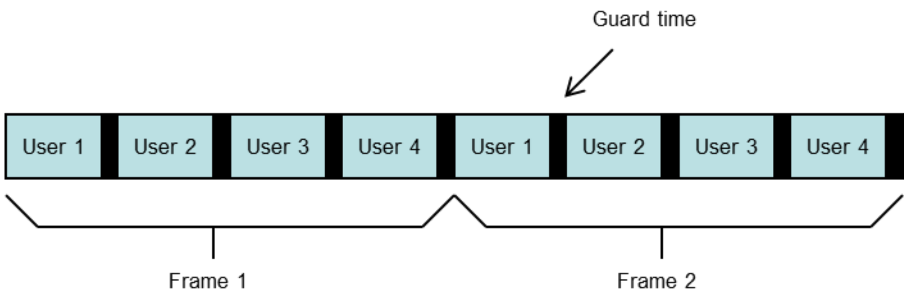

Fig. 1.1. Frame and time slot structure of TDMA

A user generating much less traffic wastes a lot of capacity, although a more generalized TDMA that allows a user to be assigned more than one time slot per frame, and also allows for time slots within a frame to be of different duration could minimise the waste. Despite the capacity-wasting property, TDMA is used today because of its relative simplicity. Another problem with TDMA is that of achieving necessary synchronization for each user to know when and how long the user can transmit.

1.1.2 Frequency-division multiple-access

Another common access technique is frequency-division multiple-access (FDMA). In FDMA, bandwidth of a common channel is divided into frequency bands, with guard bands in-between to achieve a separation between adjacent bands. Each user is assigned a particular frequency band for his own private use. Thus with FDMA, a user can be part of a transmission channel all the time.

FDMA has the same capacity-wasting property as TDMA, because if a user has nothing to transmit, his frequency band cannot be taken over by another user. However, it has an advantage over TDMA because no synchronization of the users is necessary.

1.1.3 Code-division multiple-access

Code-division multiple-access (CDMA) is another important access technique which relies on coding to achieve its multiple-access property. It brands each user by assigning each one with a unique code. Each user is assigned a unique code sequence that is used to encode the information-bearing signal. The receiver, knowing the code sequence of the user, decodes the received signal after reception to recover the original data.

The encoding enlarges (spreads) the spectrum of the signal and is therefore also known as spread-spectrum (SS) modulation. The resulting encoded signal is also called spread-spectrum signal, and CDMA is often denoted as spread-spectrum multiple access (SSMA). CDMA is an important communication technique today not only in mobile telephony but also in satellite navigation.

This thesis focuses on CDMA access technology due to its robustness to fading, and will invoke multi-carrier modulation to obtain some frequency diversity, and the use of multiple-antennas and space-time coding which provides space diversity and coding gain.

1.2 Problem definition & Research motivation

The performance of a CDMA system depends greatly on the properties of the code sequences used for the system. The type of code set bounds on the capability of the system, which can be changed only by changing the code. In line with this, earlier aspects of this thesis investigate the performance of certain spreading sequences in multi-user CDMA systems, to give new insights on the performance of the codes. We investigate the multiple-access performance of even- and odd-degree Gold codes, which to the best of our knowledge has not been reported in literature previously.

The limited radio frequency spectrum, the harsh mobile environment, and the ever-increasing demand for wireless applications calls for advanced techniques for combatting the hostile environmental factors and for more efficient use of the scarce radio spectrum. Among others, multicarrier modulation and the use of multiple-antennas have emerged as promising techniques for combatting certain problems associated with the hostile properties of the wireless channel. The combination of these two techniques with CDMA is a promising solution to high-speed future wireless communication systems. In consonance with this, this thesis models the performance of a multiple-input multiple-output (MIMO) space-time-coded (STC) orthogonal frequency-division multiplexing (OFDM) CDMA system in a fading channel. The motivation for investigating STC OFDM-CDMA system is because of the robustness of OFDM-CDMA against channel fading [3], and STC in harnessing diversity and coding gain for improved system performance [4]. OFDM converts a frequency-selective channel to a flat-fading channel [5-7]. Furthermore, the combination of OFDM and CDMA lowers the symbol rate in each subcarrier, the advantage being that a longer symbol duration makes it easier to quasi-synchronise the transmission, and also enables the use of a guard interval which helps in eliminating inter-symbol interference (ISI) [3, 4, 8-10].

Significant amount of work has been done on space-time-coded MC-CDMA systems, but most of existing works involve the use of Walsh-Hadamard codes as spreading sequences [11-62]. Only a few reported works-[63-66] involving the performance of Gold codes in such systems have been found, and we seek to add to this small collection. In this thesis, we investigate the performance of a series of Gold codes in a space-time coded CDMA system.

1.3 Aims & Objectives

This thesis aims at developing theoretical model(s) for predicting the performance of a space-time coded OFDM-CDMA communication system. Objectives of this thesis are:

- To study the characteristics of spreading sequences and to select an appropriate one for the system;
- To investigate multiple-access performance of Gold codes in multi-user CDMA systems;
- To model the performance of multi-user CDMA system in a flat-fading channel;

- To model the performance of multi-user, OFDM-CDMA systems in frequency-selective channel;
- To study and model the performance of a space-time coded OFDM-CDMA system in a fading channel.

1.4 Original contribution

Implementation of any CDMA-based system is impossible without the availability of spread-spectrum codes. Therefore among other things in this thesis, spreading sequences were generated and tested for use in the communication system. Different sets of Gold codes were obtained from appropriate combination of preferred pairs of *m*-sequences, using linear feedback shift registers. Software simulations on correlation properties of the codes were carried out towards to development of the proposed communication system. The codes were further validated by using them for signal transmission through a noisy channel.

This thesis also investigated multiple-access performance of even- and odd-degree Gold codes in a multi-user spread-spectrum system for different sets of Gold codes, ranging from 31-chip to 4095-chip Gold codes, from light to heavy system loading, involving up to about a thousand simultaneous users. This outcome of the work produced new insights on multiple-access performance of the codes.

Furthermore in this thesis, software simulations were carried to investigate the performance of a direct-sequence (DS) CDMA system in a Gaussian and flat-fading Rayleigh channels. Beginning with this model, multicarrier transmission was then introduced for the realisation of a multi-carrier (MC) CDMA system. The performance of the MC-CDMA system in a frequency-selective channel was modelled. The influence of code length on the system performance was investigated for a given number of tones and data rate for uncoded as well as coded data transmission.

Further still, by invoking the use of multiple antennas and space-time coding, this thesis models the performance of a space-time block coded (STBC) MC-CDMA system in a fading channel, and examines the relative effects or contributions of the system components on certain performance indicators such as coding gain, error floor and resilience to channel fading.

The work reported in this thesis has resulted in several research papers contributing to the field of wireless communication. These papers have either been presented at an international conference, accepted or submitted for publication in accredited, peer-reviewed journals. The list of papers is as follows:

Conference paper

[1] O. B. Wojuola and S. H. Mneney, "Performance of even-and odd-degree Gold codes in a multi-user spread-spectrum system," in *Wireless Communications, Vehicular Technology, Information Theory and Aerospace & Electronic Systems (VITAE), 2014 4th International Conference*, Aalborg, Denmark, 2014, pp. 1-5.

Journal papers

[2] O. B. Wojuola and S. H. Mneney, "Multiple-access interference of Gold codes in a DS-CDMA system," *SAIEE African Research Journal,* vol. Volume 106, pp. 4-10, 2015.

[3] O. B. Wojuola and S. H. Mneney, "Correlation properties and multiple-access performance of Gold codes," *Iranian Journal of Sci. and Tech, Trans. of Electrical Engineering,* (submitted).

[4] O. B. Wojuola and S. H. Mneney, "The evolution of CDMA - a review," *South African Journal of Science,* (submitted).

[5] O. B. Wojuola and S. H. Mneney, "Loading characteristics of Gold codes in a spread-spectrum system," *IET Journal of Communications,* (submitted).

[6] O. B. Wojuola and S. H. Mneney, "Performance of a space-time coded MC-CDMA system in a Rayleigh fading channel," *IET Journal of Communications,* (submitted).

[7] O. B. Wojuola, "Performance of DS-CDMA and MC-CDMA systems in Gaussian and Rayleigh fading channels," (to be submitted).

1.5 Organisation

The rest of this thesis is organised as follows. Chapter 2 gives a brief presentation of basic concepts as well as a review of literature on the evolution of CDMA. The treatment includes a historical review of CDMA and its emergence over time, from the basic DS-CDMA to multi-carrier CDMA system, as well as space-time-coded multicarrier CDMA systems.

An important element of any CDMA-based system is its spreading sequences or spreading codes. Hence Chapter 3 deals with spreading sequences and code selection process for the proposed communication system. This is followed by an account of software simulations carried for the purpose of testing some sets of codes prior to their use in the system. Gold codes were selected for the development of the proposed system. These codes form the focus of the chapter that follows.

Chapter 4 investigates the performance Gold codes in a multi-user system, ranging from a few users to hundreds of users, the outcome of which shows that odd-degree Gold codes have better performance than their even-degree counterparts.

In Chapter 5, multicarrier transmission is introduced, for the realization of a multicarrier CDMA system. The chapter examines the performance of a multicarrier CDMA system in a frequency-selective Rayleigh channels, and considered the influence of code length on the system performance for a given number of tones and data rate.

Chapter 6 invokes multiple-antenna transmission and space-time coding for the realisation of a space-time coded multicarrier CDMA system. The performance of the space-time coded system is modelled, the outcome of which demonstrates performance improvement resulting from the diversity and the coding gain obtainable from the composite system.

Chapter 7 concludes the thesis with a discussion of the research outcomes and suggestion of likely future work.

Chapter 2

The Evolution of CDMA

2.0 Introduction

The significance of code division multiple-access (CDMA) to wireless telephony and satellite navigation cannot be overemphasized. This chapter gives an overview of the evolution of CDMA. The treatment includes a historical review of CDMA and its emergence over time, from the basic DS-CDMA to multi-carrier CDMA systems, as well as space-time-coded multicarrier CDMA systems. This chapter also gives a treatment of basic principles underlying this research work.

The rest of this chapter is organized as follows. Section 2.1 gives a brief history of CDMA. Section 2.2 examines basic principles of operation of CDMA systems, followed by a consideration of spread-spectrum codes in Section 2.3. Section 2.4 examines orthogonal frequency-division multiplexing, which happens to be an important multi-carrier technique in today's communication systems. This naturally leads to the consideration of multi-carrier CDMA in Section 2.5. Section 2.6 takes a further look at the multi-carrier CDMA in relation to the indoor channel. Section 2.7 deals with space-time coding. This is an important technique for combating the degrading effect of multi-paths propagation on wireless channels. This is followed by a consideration of space-time-coded multi-carrier CDMA systems in section 2.8.

2.1 History and significance of CDMA

The advent of CDMA dates back to the 1940s. It was developed originally for the military as a means of establishing secure, jam-resistant communications [67-72]. Over the years, however, CDMA has found its way into the larger society because of some other properties that makes it attractive for commercial and civil use. These properties include: multiple access capability, enhanced spectrum efficiency, frequency diversity, unity cluster size and simplified frequency planning [2, 67, 68, 73-75]. Today, CDMA has become a significant worldwide communication technique. Statistics [76] show that the number of CDMA subscribers grew from about 7.8 million in 1997, to about 577 million in 2010. Viterbi [70] indicated that as at 2002, over one hundred million consumers would use devices that employ CDMA technology to provide wireless personal communication or position-location or both. Another indication of CDMA's level of significance is the fact that the 3G cell phone system is based on it. Furthermore, CDMA is the mode of communication in the Global Positioning System (GPS) [77].

2.2 Code Division Multiple Access

Code Division Multiple Access (CDMA) is a multi-access technique that relies on coding to achieve its multi-access property. It assigns each user a unique code, and uses this code to transform (encode) the user's signal into a wide-band signal. The receiver, knowing the code sequence of the user, decodes the received signal after reception to recover the original signal. Because the encoding spreads (enlarges) the spectrum of the signal, CDMA is also known as spread-spectrum (SS) modulation. CDMA is therefore sometimes denoted as Spread-Spectrum Multiple Access (SSMA).

CDMA can be classified into four protocol types: Direct Sequence CDMA (DS-CDMA), Frequency-Hopping CDMA (FH-CDMA), Time-Hopping CDMA (TH-CDMA) and hybrid CDMA [2, 67, 73], where the last group (hybrid CDMA) is obtained from any combination of the first three, or CDMA with any other technique.

In digital DS-CDMA, the message signal is multiplied directly by the code signal and the resulting signal modulates a carrier (Figure 2.1a) for onward transmission through a communication channel. The receiver (Figure 2.1b) demodulates the received signal, and also decodes it by correlating the received signal with the code of the user. Because each user's unique code has low cross-correlation with the other codes, the receiver is able to distinguish between users. Correlating the received signal with a code for a certain user de-spreads (decodes) the signal for the user.

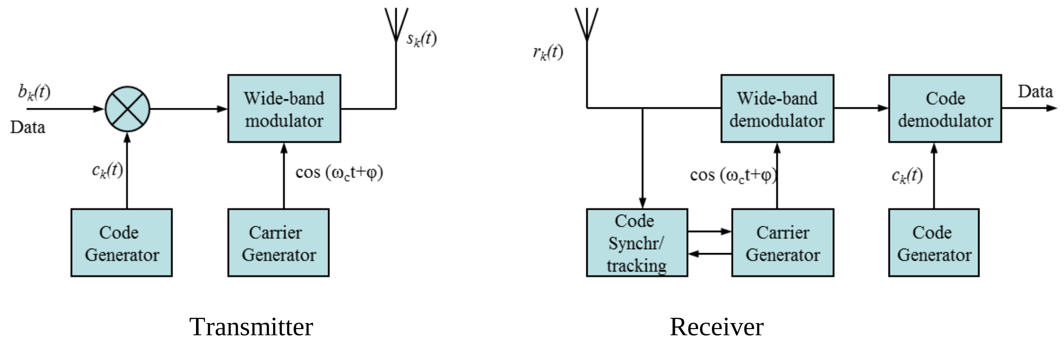

Fig. 2.1 Digital Direct-Sequence CDMA transmitter and receiver

In a wireless channel, due to surrounding objects like walls, buildings and mountains, many reflections of the signal arrive at the antenna of the receiver along different paths and at different times. Depending on the phases of the reflected signals, the reflections add up to cause signal peaks and dips. Hence the channel can be represented by multiple paths having a real positive gain β_l, propagation delay τ_l and phase shift γ_l, where l is path index. The channel impulse response $h_k(t)$ for the k^{th} user for L independent paths can be modelled as

$$h_k(t) = \sum_{l=1}^{L} \beta_{kl} e^{j\gamma_{kl}} \delta(t - \tau_{kl}) \quad (2.1)$$

Here it is assumed that β_{kl}, τ_{kl} and γ_{kl} are independent of time. However, because of motion of people, and other time-varying environmental factors, the parameters β_{kl}, τ_{kl} and γ_{kl} are, in general, randomly-varying functions of time, resulting in variation of the received signal strength - a form of distortion termed *fading*. More generally, the channel impulse response is also position-dependent, so that it may be more correctly expressed as $h_k(t, x)$, where x is the position variable. By implication, the channel variables β_{kl}, τ_{kl} and γ_{kl} are not only time-dependent, but also position-dependent[78].

The pseudo-noise (PN) code $c_k(t)$ for a user k can be denoted as

$$c_k(t) = \sum_{i=1}^{N} c_k^i P_c(t - iT_c), \quad c_k^i \in \{-1, 1\} \quad (2.2)$$

where N is length of the code, and P_c is a rectangular pulse with a duration T_c. If $b_k(t)$ is a binary data, spreading is accomplished by multiplying $c_k(t)$ with $b_k(t)$, after which the resulting signal is used to modulate a carrier, say, $A\cos(\omega_c t + \theta_k)$, having an amplitude A to give the transmitted signal

$$s_k(t) = Ac_k(t)b_k(t)\cos(\omega_c t + \theta_k) \quad \textbf{(2.3)}$$

The multiplication of the code $c_k(t)$ with the data bits $b_k(t)$ results in bandwidth expansion. The bandwidth expansion factor B_c (also called processing gain) is given by

$$B_c = \frac{T_b}{T_c} = N \quad (2.4)$$

where T_b is the data rate, and N is the length of the user's code. It is assumed that $T_b/T_c = N$, so that one code sequence fits into one data bit interval.

At the receiving end, the received signal $r_k(t)$ for the user k is obtained by convolving $s_k(t)$ with $h_k(t)$ and adding noise so that:

$$r_k = \int_{-\infty}^{\infty} s_k(\tau)h_k(t-\tau)d\tau \;+\; n(t) \quad (2.5)$$

where $n(t)$ represents the channel noise. Substituting the expressions for $s_k(t)$ and $h_k(t)$ into this integral, and using relevant properties of the Dirac delta $\delta(t)$ gives

$$r_k(t) = \sum_{l=1}^{L} A\beta_{kl}e^{j\gamma_{kl}}\; c_k(t-\tau_{kl})\, b_k(t-\tau_{kl})\, cos(\omega_c(t-\tau_{kl}) - \theta_{kl}) + \; n(t) \quad (2.6)$$

For a linear multi-user system comprising K users, the received signal $r(t)$ is a linear superposition of the signals for the users, and is given by:

$$r(t) = \sum_{k=1}^{K}\sum_{l=1}^{L} A\beta_{kl}e^{j\gamma_{kl}}\; c_k(t-\tau_{kl})\, b_k(t-\tau_{kl})\, cos(\omega_c(t-\tau_{kl}) - \theta_{kl}) + \; n(t) \quad (2.7)$$

In the absence of a dominant line-of-sight (LOS) signal or a strong received component, gain β_{kl} may be modeled as a Rayleigh random variable; while in the presence of a LOS signal path, it may be modeled as a Rician random variable [4, 79].

2.3 Spread spectrum codes

CDMA codes are pseudo-random numbers, usually referred to as *pseudo-noise* (PN) or *pseudo-random noise* (PRN) codes. The codes are also sometimes called *spreading* or *spread-spectrum* codes. Examples of such codes include maximal linear code sequences, Gold codes, Walsh-Hadamard codes and Kasami codes [2, 77, 80-84].

Spread spectrum codes are known to play a critical role in determining the performance of spread-spectrum systems. Imperfect code properties yield poor system performance. Code properties are known to be a cause of multiple-access interference (MAI), an important limiting factor on the system performance. The significance of spreading codes has made the search for better codes [80, 82, 85-94] and the mitigation of multiple-access interference [95-105] important areas of research.

An aspect of such effort is the search for better orthogonal codes. For example in [104], Chen Hsiao-Hwa, et. al., proposed the generation of perfectly orthogonal complementary codes for the realisation of an interference-free CDMA system. Although orthogonality is a desirable property, it does not in itself solve all the code-associated problems of a spread-spectrum system. Orthogonal codes are excellent in synchronous, but not in asynchronous environment, in which orthogonality is lost.

2.4 Orthogonal Frequency Division Multiplexing

Orthogonal Frequency Division Multiplexing (OFDM) is a multi-carrier modulation technique whose basic principle is to split a high-rate data-stream into a number of low-rate sub-streams that are transmitted simultaneously over a number of subcarriers [3, 5-8, 106, 107]. The following figure illustrates the principle.

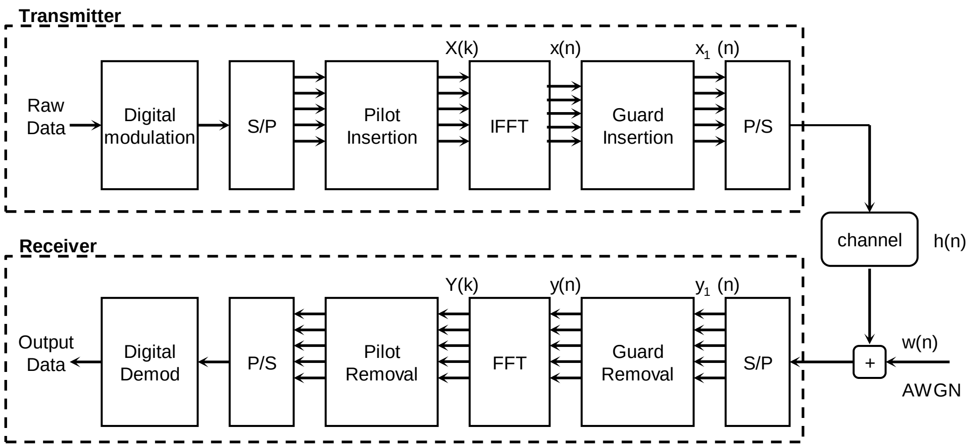

Fig. 2.2 An OFDM transmitter and receiver

Starting from the transmitter, the raw data (binary information) is first grouped and mapped according to some form of digital modulation scheme like the binary phase shift keying

(BPSK), quadrature phase shift keying (QPSK) or quadrature amplitude modulation (QAM). The data is then converted from serial into several parallel sub-streams, typically dozens, hundreds or even thousands. After this, pilot symbols are inserted for the purpose of channel estimation. Inverse Fast Fourier Transform (IFFT) is then used to transform the data sequence $\{X(k)\}$ from frequency domain to give the time domain signal $\{x(n)\}$. Following this, guard time, which is chosen to be larger than the expected delay spread, is inserted to prevent inter-symbol interference (ISI). The guard time allows multipath components to fade away before information is extracted from the next symbol. After inserting the guard time, OFDM signal, which is basically the sum of the subcarrier signals, is obtained. The OFDM signal is transmitted through the channel. The signal convolves with the channel impulse response $h(n)$ and also gets corrupted by noise $w(n)$. As shown by the figure, the receiver carries out an inverse process on the received signal in order to recover the original signal.

OFDM is based on the principle of frequency division multiplexing (FDM). It divides the signal bandwidth into strips of narrowband sub-channels and sends the parallel data sub-streams over the narrowband sub-channels. That is, the wideband frequency-selective channel is divided into a number of parallel narrowband sub-channels, and each of the low-rate data streams is transmitted by a sub-carrier over one sub-channel. As the number of sub-channel increases, the bandwidth corresponding to each sub-channel gets narrower, and the fading on each sub-channel can be considered approximately flat. If the bandwidth of each sub-channel is chosen to be sufficiently smaller than the coherent bandwidth of the channel, then each of the sub-carriers sees the channel as being flat-fading. Effectively, OFDM converts a wideband frequency-selective channel to a flat-fading channel.

2.5 Multicarrier CDMA

Multicarrier CDMA (MC-CDMA), sometimes referred to as multi-tone CDMA (MT-CDMA), is a hybrid CDMA system, comprising orthogonal frequency division multiplexing (OFDM) and CDMA, and was first proposed in the nineties [9, 10, 74, 75, 108-110]. The combination of OFDM and CDMA, as found in the MC-CDMA, provides robustness against channel fading [3, 4, 8-10].

There are different implementations of MC-CDMA technique [4-7, 9, 10, 74, 75, 109-124], but the principles of operation are the same. The following figure illustrates the basic principles.

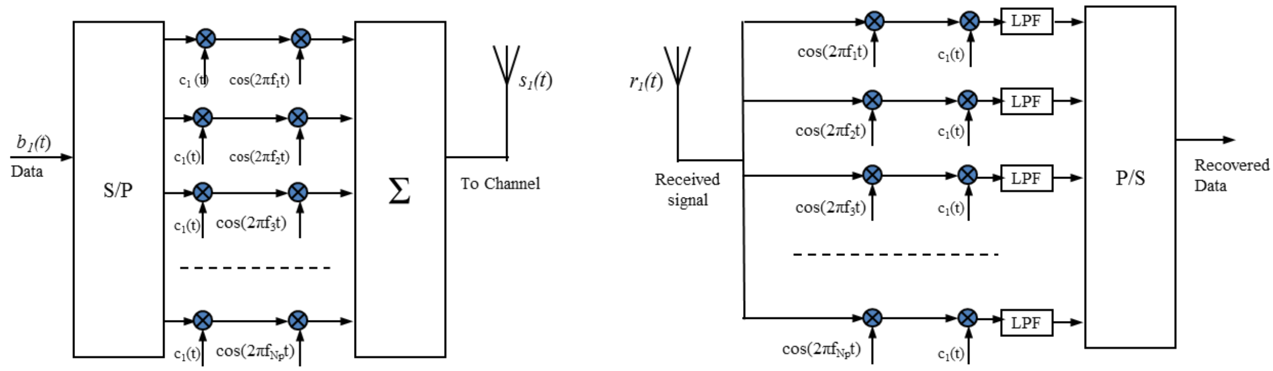

Fig. 2.3 Principles of operation of a multicarrier CDMA system showing the (a) transmitter, and (b) receiver.

In the transmitter, the message or data stream is first converted from serial to, say, N_p parallel symbol streams, having a symbol duration T_s. Each symbol stream is multiplied by the user code *c(t)*, after which the resulting signal for the *p*th symbol stream modulates a subcarrier f_p. The subcarriers are orthogonal on the symbol duration and are given by $f_p = f_o+p/T_s$, where f_o is RF frequency. The multicarrier signal *s(t)* is obtained from addition of the different subcarrier signals. The signal *s(t)* is transmitted through the channel onto the receiver to give a received signal *r(t)*. The received signal *r(t)* is a convolution of *s(t)* and the channel impulse response, corrupted by noise. To recover the original data, the receiver carries out the reverse of what the transmitter does. In actual implementation, fast Fourier transform (FFT) is normally employed for improved system efficiency.

The previous figure (Fig. 2.3) represents an MC-CDMA system for a *single* user. The structure of a multi-user MC-CDMA system will now be examined, as shown by the following figure, briefly described below.

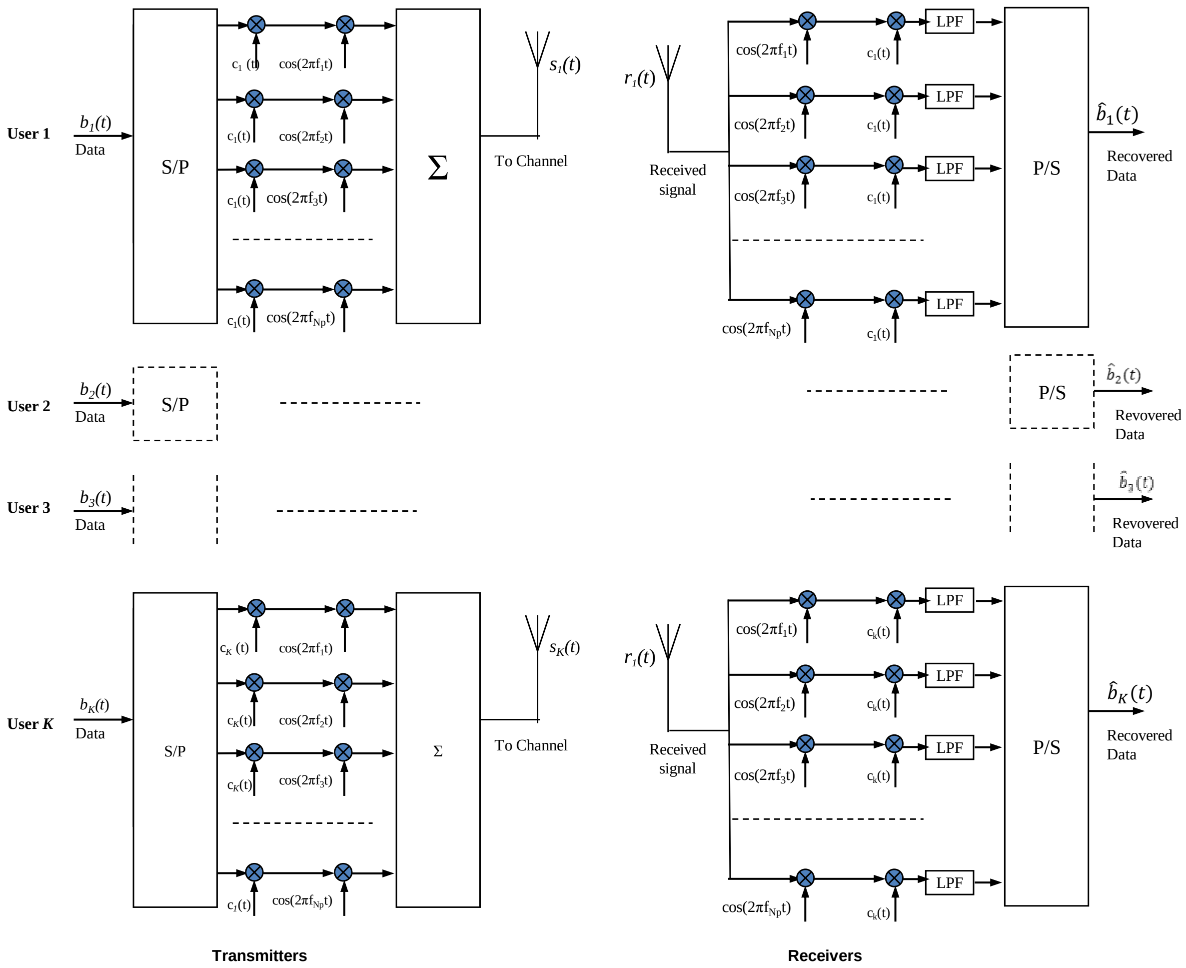

Fig. 2.4 Multi-user MC-CDMA system.

For an MC-CDMA system comprising *K* multiple users, all the users transmit on the same set of OFDM subcarriers but with different *PN*-codes. In general, each user *k* (where *k* = 1, 2, 3,…, *K*) has a transmitter and a corresponding receiver having the MC-CDMA structure presented earlier in Fig. 2.3. The signal reaching each receiver is a superposition of all the signals transmitted by all the users. Since each receiver is interested in recovering one and only one signal (i.e. the signal for a particular user), every other signal constitutes interference. This brings about the concept of *multi-user interference*.

As shown by Fig. 2.4, for *K* multiple users, there are, in general, *K* transmitters and *K* corresponding receivers. However, for a system involving a base station, the situation is somewhat different. This is explained as follows. For uplink transmission (from mobile terminals to the base station), there are multiple transmitters but only one receiver, the base station (Fig. 2.5a). That is, the multi-user system of Fig. 2.4 reduces to that having just one receiver (i.e. a *K*-to-1 system). The converse is the case for downlink transmission: the base station becomes the only transmitter sending signals to multiple receivers - the mobile terminals (Fig. 2.5b). This example is more of an outdoor network, but is used here to illustrate the principles. An example of indoor systems having a similar uplink-downlink topology is a server communicating wirelessly with some other terminals of a local area indoor network.

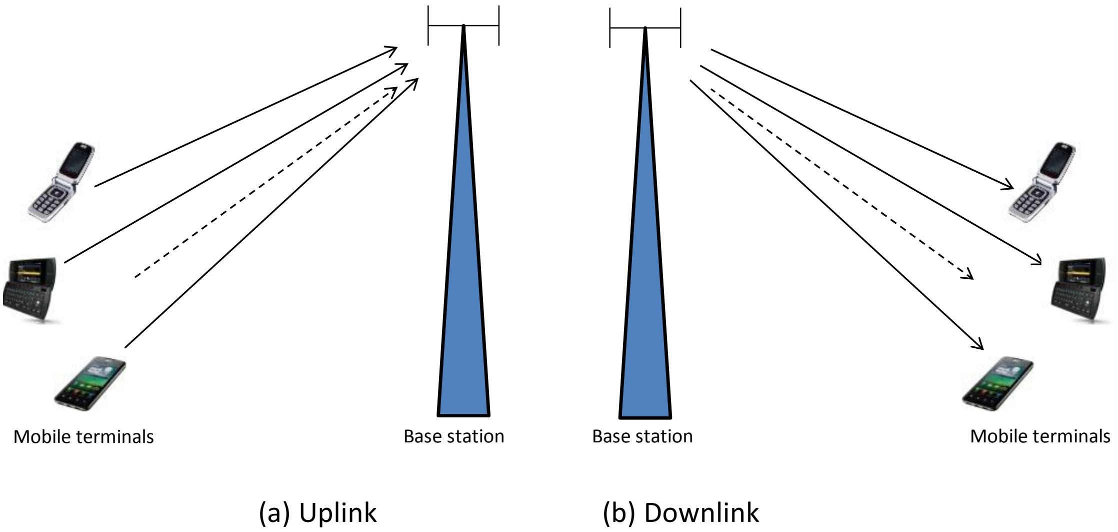

Fig. 2.5. (a) Uplink and (b) downlink signal transmission.

2.6 MC-CDMA in the indoor channel

It is doubtless to say that over the years, much work has been done on MC-CDMA systems. However, literature survey shows that not much of available literature relates to the performance of MC-CDMA in the indoor channel. This is therefore an open research topic. In saying this however, a careful consideration of merits or otherwise of the system in the indoor channel might be useful, in the light of propagation characteristics of the channel.

A useful parameter for evaluating the merits of a MC-CDMA system in an indoor channel is the delay spread. Reported values of the delay spread vary widely, ranging from about 3 – 300 ns [79]. For example, reported values include: less than 22 ns for a line of sight (LOS) measurement in a 10 x12-meter size office, less than 55 ns in a non-LOS measurement with transmitter and receiver separated by 7 - 20 meters, and wall partitions [125]; between 20 and 50 ns for 3 x 4-meter small- and 4 x 8-meter medium-size offices [126], 15 - 300 ns for various factory environments having between 25 000 to 150 000 square meter of factory space [127], under 100 ns at several university buildings, classrooms, small-room offices, an auditorium, a library and a machine room [128], etc. Nowin this thesis we will assume mean rms delay spread of 20, 50 and 150 ns for small, medium and large indoor channels respectively. This translates to coherent bandwidth of 50, 20 and 6.67 MHz for the small, medium and large indoor channel respectively. Consider a wideband CDMA (WCDMA) having a transmission bandwidth of 5 MHz. By comparing this value to the mean rms delay spreads, it is obvious that the transmission bandwidth is less than the least of the channel coherent bandwidths. This implies that with respect to the WCDMA, the indoor channel is flat-fading. Hence, multicarrier modulation may not be of much performance advantage in the indoor channel, except in large indoor environments. Even in such large environments, the frequency diversity inherent in CDMA provides enough compensation that could make multicarrier transmission unnecessary for the indoor channel.

2.7 Space-Time Coding

Space-time coding (STC) is a method for transmitting data in multi-antennae systems. It encodes a data stream across different transmit antennae and time slots, so that multiple redundant copies of the data stream can be transmitted through independent fading channels. By doing so, more reliable detection can be obtained at the receiver. Space-time coding helps in exploiting the diversity or spatial multiplexing gain of Multiple-Input-Multiple-Output (MIMO) systems [3].

2.8 Space-time coded MC-CDMA system

Space-time coding (STC) is known to be an effective diversity technique for combating channel fading without bandwidth penalty. STC combines transmit diversity with coding scheme. In recent years, different types of space-time coding schemes, including space-time block codes (STBC), space-time trellis codes (STTC), concatenated STBC-STTC, and super-orthogonal STTC (SOSTTC) have been studied [129]. STBC, first proposed by Alamouti in 1998 [130], and later generalised by Tarokh [131, 132], provides diversity gain but no coding gain. However, the attractiveness in STBC includes its ability to achieve maximum possible diversity advantage, coupled with the simplicity of its implementation and decoding algorithm [12]. On the other hand, STTC provides both diversity and coding gain, but at the expense of complexity of implementation and decoding.

Space-time coding is designed primarily for flat-fading channels. Consequently, STC schemes cannot be applied as-is to frequency-selective wideband CDMA systems. However, the combination of orthogonal frequency division multiplexing (OFDM) with code-division multiple access (CDMA), as found in multicarrier CDMA (MC-CDMA) removes this barrier, giving the opportunity to use space-time coding schemes in broadband frequency-selective channels. Basic principles of operation of STC MC-CDMA system are briefly described as follows.

Raw data is space-time coded into parallel data sub-streams which are distributed across parallel MC-CDMA modulators (Fig. 2.6). The MC-CDMA modulators process the data sub-streams, and transmit them over OFDM sub-carriers, across different M_T transmit antennae and time slots. The signals propagate through the channel, convolves with the channel impulse response, mix with noise, and are thus picked up by n_R receive antennae. To recover the original data, the receiver carries out an inverse process on the received signal - the MC-CDMA demodulators demodulate the signals and then pass them on to the space-time decoder to recover the original data.

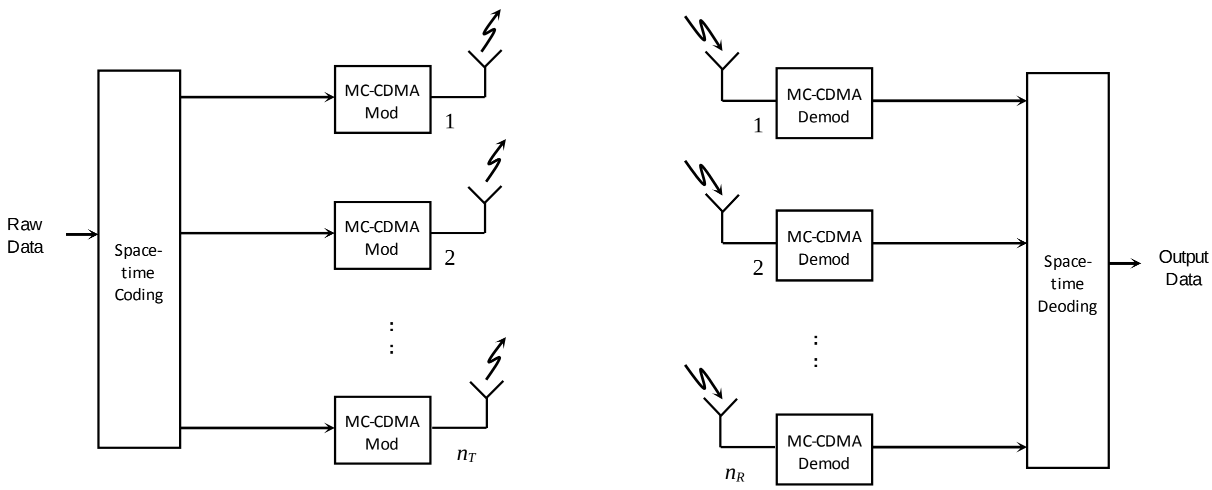

Fig. 2.6 A space-time coded multicarrier CDMA system

In recent years, significant amount of work has been done on space-time-coded MC-CDMA systems, with most of the work being on STBC MC-CDMA systems [11-13, 16, 18, 19, 27, 31, 33, 35, 38-40, 42-45, 53, 58, 133-135], and very limited fraction on STTC MC-CDMA and concatenated STTC-STBC MC-CDMA systems [12, 49, 59, 136], and none on SOSTCC MC-CDMA systems. Literature survey also shows that a larger fraction of existing works involves the use of Walsh-Hadamard codes as spreading sequences [11-62]. Only a few reported works [63-66] involving the use of Gold codes in STC MC-CDMA systems are found in literature. This thesis contributes to this small pool of works by investigating the performance of a series of Gold codes in a STBC CDMA system.

2.9 Chapter summary

This chapter presented a brief review of evolution of CDMA, from its early days of military applications, to present emerging forms of the technology, as well as its significance to worldwide wireless telephony and satellite navigation. This chapter also presented principles of operation of CDMA and associated technology, including OFDM multicarrier signal transmission and space-time coding. Furthermore, this chapter identified certain gaps in research that could be explored, which include the investigation of performance of certain classes of space-time coded multicarrier CDMA systems.

Chapter 3

Correlation properties of *m*-sequences and Gold codes

3.0 Introduction

In the previous chapter, general concepts relating to CDMA-based systems were given. In this chapter, we shall be focusing on an important element of CDMA systems – spreading codes. Doing this is essential because the performance of a CDMA system is affected by the properties of its spreading codes. Successful implementation of a CDMA-based system requires the use of right set of codes having necessary properties for multiple-access applications. This chapter gives an overview of spreading sequences and code selection process for the proposed communication system. This is followed by an account of software simulations carried out for the purpose of testing selected sets of codes prior to their use in the system. In the last section of this chapter, selected codes are used for signal transmission through a noiseless as well as a noisy channel. This prepares the ground for the development of the proposed communication system.

The rest of this chapter is organised as follows. Section 3.1 gives an overview of spread spectrum codes. Section 3.2 gives an account of code generation for the development of the communication system. Sections 3.3 and 3.4 present results of tests carried out on essential properties of the codes. Sections 3.5 and 3.6 give initial results on the use of the codes for signal transmission through a communication channel. This chapter concludes with a summary in Section 3.7.

3.1 Spread spectrum codes

Spread spectrum codes are pseudo-noise (PN) codes, and examples of such codes include maximal linear code sequences, Gold codes, Walsh-Hadamard codes and Kasami codes [80-

84]. Maximal linear code sequences (often abbreviated as *maximal* or *m*-sequences) are commonly implemented using Linear Feedback Shift Register (LFSR). An *m*-sequence represents LFSR sequence with its *maximum* possible period, which is $2^n - 1$, where n is the length of the shift register. *M*-sequences have an excellent autocorrelation function which is given by [2, 137-140]

$$\varphi(j) = \begin{cases} N & j = 0 \\ -1 & 1 \le j \le n-1 \,. \end{cases} \tag{3.1}$$

However, *m*-sequences have poor cross-correlation properties: the cross-correlation function between any pair of *m*-sequences of the same period can have relatively large peaks [138, 141] which make them unsuitable for CDMA applications. Another limitation is that the number of available *m*-sequences is too small for CDMA applications.

Walsh-Hadamard code is another class of spreading sequences commonly found in literature. The codes have excellent performance when synchronisation is perfect, but this condition cannot always be guaranteed in practice. The codes perform well in synchronous but not in asynchronous transmission. Their usefulness is therefore limited to downlink transmission. Apart from this, the number of available Walsh-Hadamard codes is relatively limited.

Gold codes are a type of PN sequences with better periodic cross-correlation properties that make them appropriate for CDMA systems. They are derived from certain pairs of *m*-sequences called *preferred sequences.* Preferred sequences are unique because when they are combined appropriately, any two of them produce a huge number of Gold codes. Gold codes exhibit triple-valued cross-correlation function [2, 137-140] with values {-1, -$t(m)$, $t(m)$-2} where

$$t(m) = \begin{cases} 2^{(m+1)/2} + 1 & m \text{ odd} \\ 2^{(m+2)/2} + 1 & m \text{ even.} \end{cases} \tag{3.2}$$

For example, if $m = 10$, $t(m) = 65$, giving the cross-correlation values as {-1, -65, 63}. This implies for a 10-stage shift register, the maximum value of cross-correlation for any pair of the Gold code is 65. This can be compared to the maximum cross-correlation for *m*-sequences which is 383.

Kasami code is another class of PN-code having properties similar to that of Gold codes. According to Prasad [2], Gold codes are among the most popular codes in use, their favourable correlation properties being a factor. For the current work, Gold codes will be used.

3.2 Generation of the PN codes

The initial stage of the research work involved generation of spread-spectrum codes. The following Table 3.1 shows *m*-sequences that were generated using linear feedback shift registers. Each of the *m*-sequences is 31-chip long, obtained from a 5-stage shift register. Table 3.2 below shows an array of 33 Gold codes, each is also 31-chip long, generated from MATLAB simulations. The 33 Gold codes were obtained by combining the first *m*-sequence with a modulo-2 addition of time-shifted versions of the second *m*-sequence. This shows the huge number of Gold codes that can be generated from a combination of just a pair of *m*-sequences, and it highlights an important advantage of Gold codes over *m*-sequences, because the number of available *m*-sequences is generally too small for CDMA applications.

Table 3.1. Examples of generated 31-chip *m*-sequences

m-sequence1
1 1 1 1 1 0 0 1 1 0 1 0 0 1 0 0 0 0 1 0 1 0 1 1 1 0 1 1 0 0 0

m-sequence2
1 1 1 1 1 0 0 1 0 0 1 1 0 0 0 0 1 0 1 1 0 1 0 1 0 0 0 1 1 1 0

m-sequence3
1 1 1 1 1 0 1 1 0 0 1 1 1 0 0 0 0 1 1 0 1 0 1 0 0 1 0 0 0 1 0

Table 3.2. An array of generated 33-by-31-chip Gold codes

S/N	**Gold Codes**																														
1.	1	1	1	1	1	0	0	1	1	0	1	0	0	1	0	0	0	0	1	0	1	0	1	1	1	0	1	1	0	0	0
2.	1	1	1	1	1	0	0	1	0	0	1	1	0	0	0	0	1	0	1	1	0	1	0	1	0	0	0	1	1	1	0
3.	0	0	0	0	0	0	0	0	1	0	0	1	0	1	0	0	1	0	0	1	1	1	1	0	1	0	1	0	1	1	0
4.	1	0	0	0	0	1	0	1	0	0	1	1	1	1	0	0	0	1	1	1	0	0	0	1	0	0	1	1	1	1	1
5.	0	1	0	0	0	1	1	1	1	1	1	0	1	0	0	0	0	0	0	0	0	1	1	0	1	1	1	1	0	1	1
6.	0	0	1	0	0	1	1	0	1	0	0	0	0	0	1	0	0	0	1	1	1	1	0	1	0	0	0	1	0	0	1
7.	0	0	0	1	0	1	1	0	0	0	1	1	0	1	1	1	0	0	1	0	0	0	0	0	1	1	1	0	0	0	0
8.	1	0	0	0	1	1	1	0	0	1	1	0	1	1	0	1	1	0	1	0	1	1	1	0	0	0	0	1	1	0	0
9.	1	1	0	0	0	0	1	0	0	1	0	0	0	0	0	0	1	1	1	0	1	0	0	1	0	1	1	0	0	1	0
10.	1	1	1	0	0	1	0	0	0	1	0	1	0	1	1	0	0	1	0	0	1	0	1	0	1	1	0	1	1	0	1
11.	0	1	1	1	0	1	1	1	0	1	0	1	1	1	0	1	0	0	0	1	1	0	1	1	0	0	0	0	0	1	0
12.	1	0	1	1	1	1	1	0	1	1	0	1	1	0	0	0	1	0	1	1	0	0	1	1	1	1	1	0	1	0	1
13.	0	1	0	1	1	0	1	0	0	0	0	1	1	0	1	0	0	1	1	0	0	1	1	1	1	0	0	1	1	1	0
14.	1	0	1	0	1	0	0	0	0	1	1	1	1	0	1	1	0	0	0	0	1	1	0	1	1	0	1	0	0	1	1
15.	0	1	0	1	0	0	0	1	0	1	0	0	1	0	1	1	1	0	1	1	1	0	0	0	1	0	1	1	1	0	1
16.	0	0	1	0	1	1	0	1	1	1	0	1	0	0	1	1	1	1	1	0	0	0	1	0	0	0	1	1	0	1	0
17.	1	0	0	1	0	0	1	1	1	0	0	1	1	1	1	1	1	1	0	0	1	1	1	1	0	1	1	1	0	0	1
18.	0	1	0	0	1	1	0	0	1	0	1	1	1	0	0	1	1	1	0	1	1	0	0	1	1	1	0	1	0	0	0
19.	1	0	1	0	0	0	1	1	0	0	1	0	1	0	1	0	1	1	0	1	0	0	1	0	1	0	0	0	0	0	0
20.	1	1	0	1	0	1	0	0	1	1	1	0	0	0	1	1	0	1	0	1	0	1	1	1	0	0	1	0	1	0	0
21.	1	1	1	0	1	1	1	1	0	0	0	0	0	1	1	1	1	0	0	1	0	1	0	1	1	1	1	1	1	1	0
22.	1	1	1	1	0	0	1	0	1	1	1	1	0	1	0	1	1	1	1	1	0	1	0	0	1	0	0	1	0	1	1
23.	0	1	1	1	1	1	0	0	0	0	0	0	1	1	0	0	1	1	0	0	0	1	0	0	0	0	1	0	0	0	1
24.	0	0	1	1	1	0	1	1	0	1	1	1	0	0	0	0	0	1	0	1	1	1	0	0	0	1	1	1	1	0	0
25.	1	0	0	1	1	0	0	0	1	1	0	0	1	1	1	0	0	0	0	1	0	0	0	0	0	1	0	1	0	1	0
26.	1	1	0	0	1	0	0	1	0	0	0	1	0	0	0	1	0	0	1	1	0	1	1	0	0	1	0	0	0	0	1
27.	0	1	1	0	0	0	0	1	1	1	1	1	1	1	1	0	1	0	1	0	0	1	0	1	0	1	0	0	1	0	0

28.	1	0	1	1	0	1	0	1	1	0	0	0	1	0	0	1	0	1	1	0	1	1	0	0	1	1	0	0	1	1	0
29.	1	1	0	1	1	1	1	1	1	0	1	1	0	0	1	0	1	0	0	0	1	0	0	0	0	0	0	0	1	1	1
30.	0	1	1	0	1	0	1	0	1	0	1	0	1	1	1	1	0	1	1	1	1	0	1	0	0	1	1	0	1	1	1
31.	0	0	1	1	0	0	0	0	0	0	1	0	0	0	0	1	1	0	0	0	0	0	1	1	0	1	0	1	1	1	1
32.	0	0	0	1	1	1	0	1	0	1	1	0	0	1	1	0	1	1	1	1	1	1	1	1	1	1	0	0	0	1	1
33.	0	0	0	0	1	0	1	1	1	1	0	0	0	1	0	1	0	1	0	0	0	0	0	1	1	0	0	0	1	0	1

3.3 Experimentation on the correlation properties of the codes

After generating the *m*-sequences and the Gold codes, software simulations were carried out on their autocorrelation and cross-correlation properties. Autocorrelation and cross-correlation of code sequences indicate the number of agreements minus the number of disagreements when the code or codes are compared chip by chip. Mathematically, periodic cross-correlation function for sequences x_n and y_n can be represented as [142, 143]

$$r_{x,y}(l) = \sum_{n=0}^{N-1} x_n y_{n+l}. \tag{3.3}$$

Hence, autocorrelation function may be expressed as:

$$r_{x,x}(l) = \sum_{n=0}^{N-1} x_n x_{n+l}. \tag{3.4}$$

Auto-correlation plot for *m*-sequences is double-valued, with a peak only at zero shift point. This is an invaluable property because it allows a receiver to discriminate between signals on a yes-no basis. Because of the well-defined autocorrelation function of *m*-sequences, a system may use the same code for modulation by treating its phase-shifted version as a different code. An example of a typical system employing this technique is the global positioning system. Unfortunately however, cross-correlation of *m*-sequences is not so well-behaved as their autocorrelation, and this limits their use in multi-access communication systems.

Figure 3.1(a) shows the graph of autocorrelation of each of the *m*-sequences, while Figure 3.1(b) shows the results of cross-correlating one *m*-sequence with another. Figure 3.1(a) confirms the autocorrelation property of *m*-sequences, as predicted by equation 3.1.

However, the cross-correlation graphs, Fig. 3.1(b), deserve a close look. The cross-correlation of *m*-sequences is generally believed to be random-valued. In contrast, Fig. 3.1(b) indicates that it is not random but triple-valued. A close look at the graphs shows that the cross-correlation values correspond to those predicted by Equation (3.2) for Gold codes. This observation implies that the *m*-sequences have the same cross-correlation property as Gold codes.

In general, cross-correlation of *m*-sequences is random-valued. In contrast, cross-correlation of preferred pairs is triple-valued. When such preferred pairs are combined appropriately, they generate a huge number of Gold codes. These are unique properties of preferred pairs.

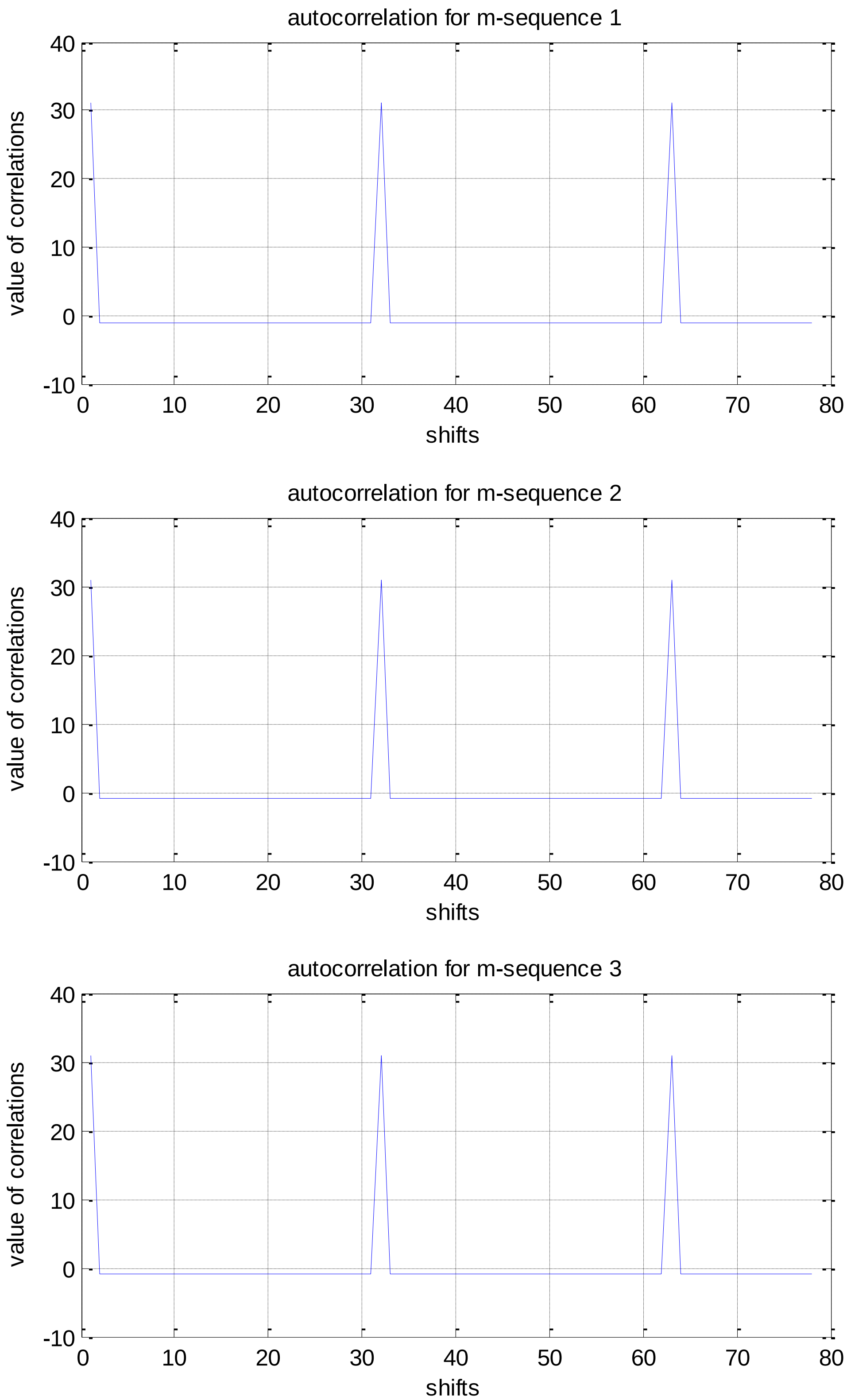

Fig. 3.1 (a) Autocorrelation of three *m*-sequences.

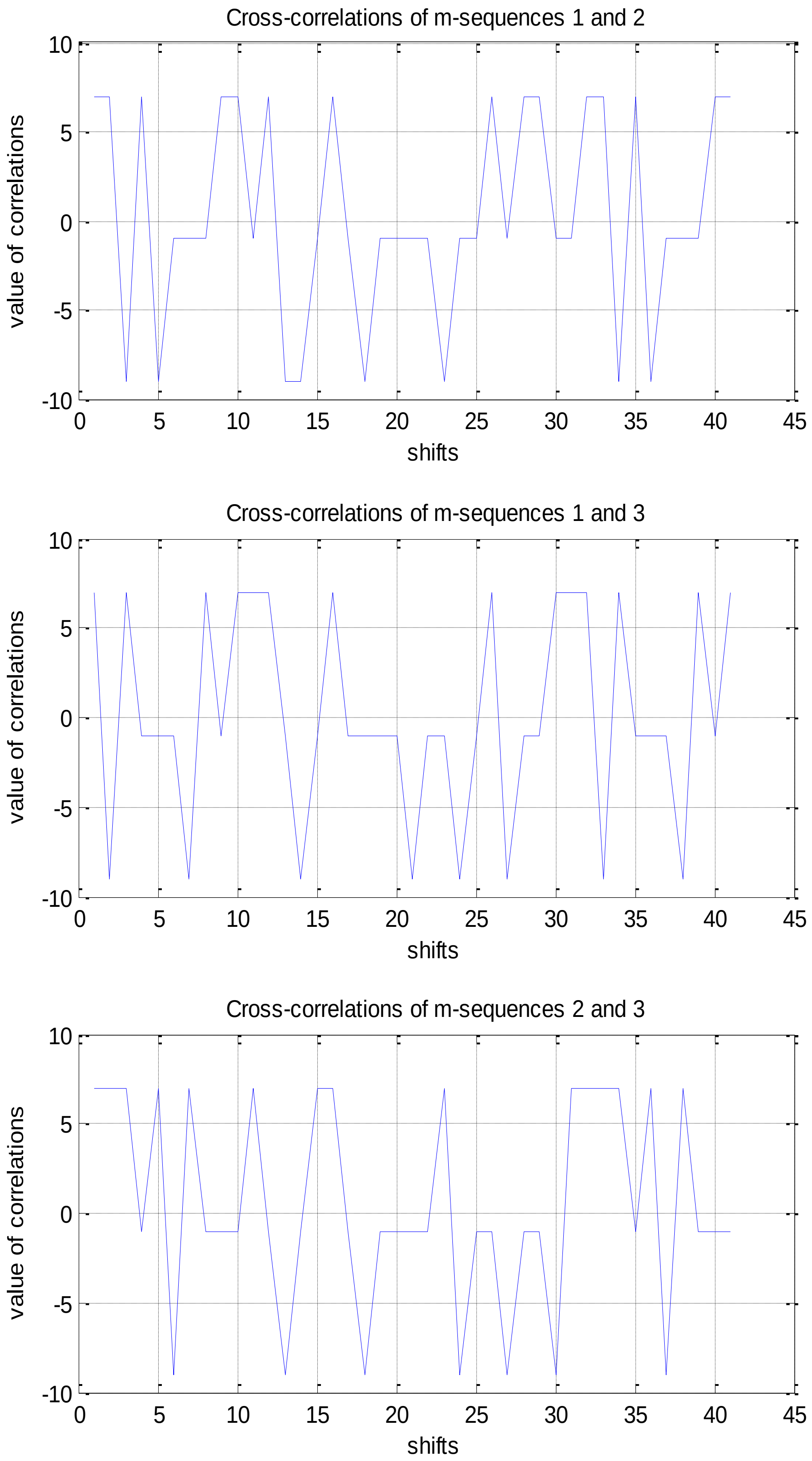

Fig. 3-1(b) Cross-correlation of the three *m*-sequences.

Figs. 3.2 and 3.3 show some other results for 31-chip codes. In every case, the autocorrelation plots show that all the codes are *m*-sequences. In addition, the cross-correlation plots show that the pairs of codes are all preferred sequences.

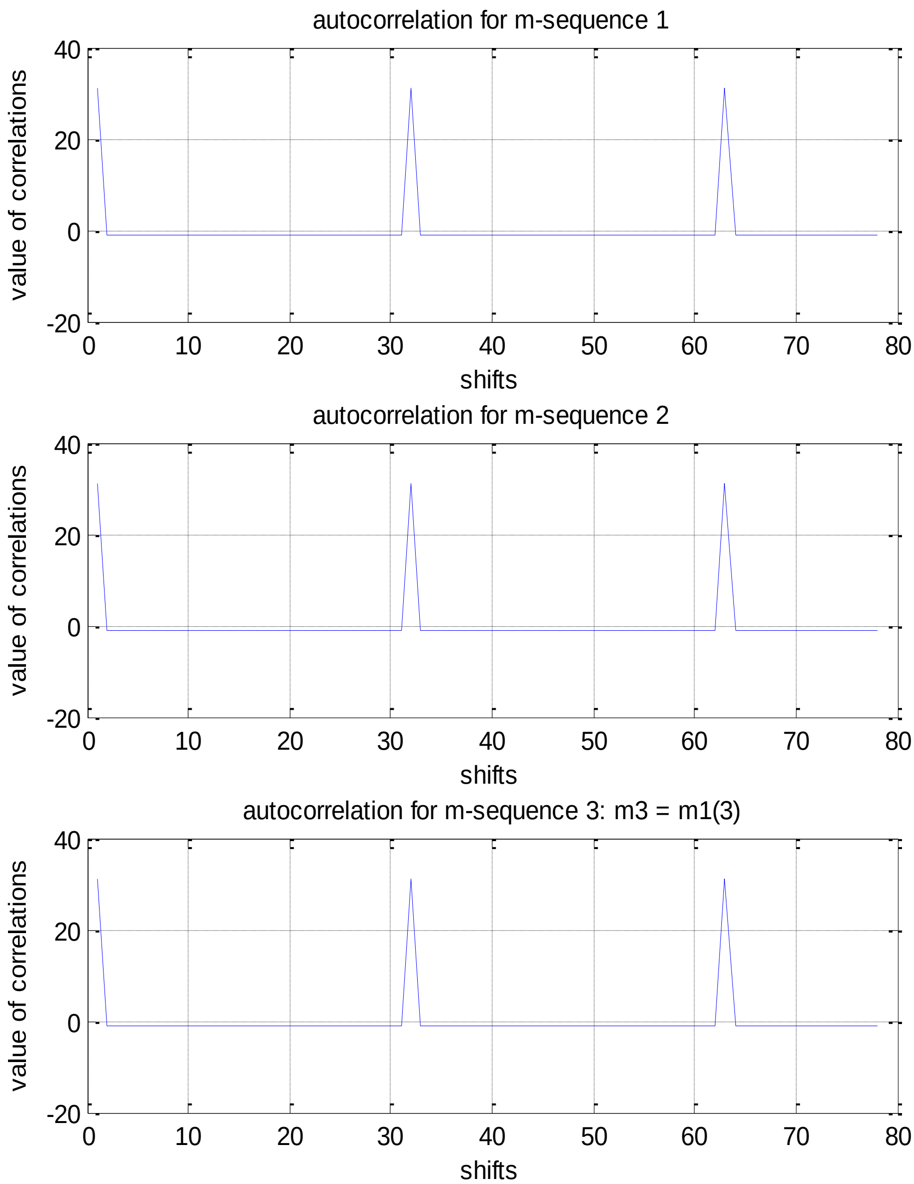

Fig. 3.2 (a) Graphs of autocorrelation of other 31-chip m-sequences

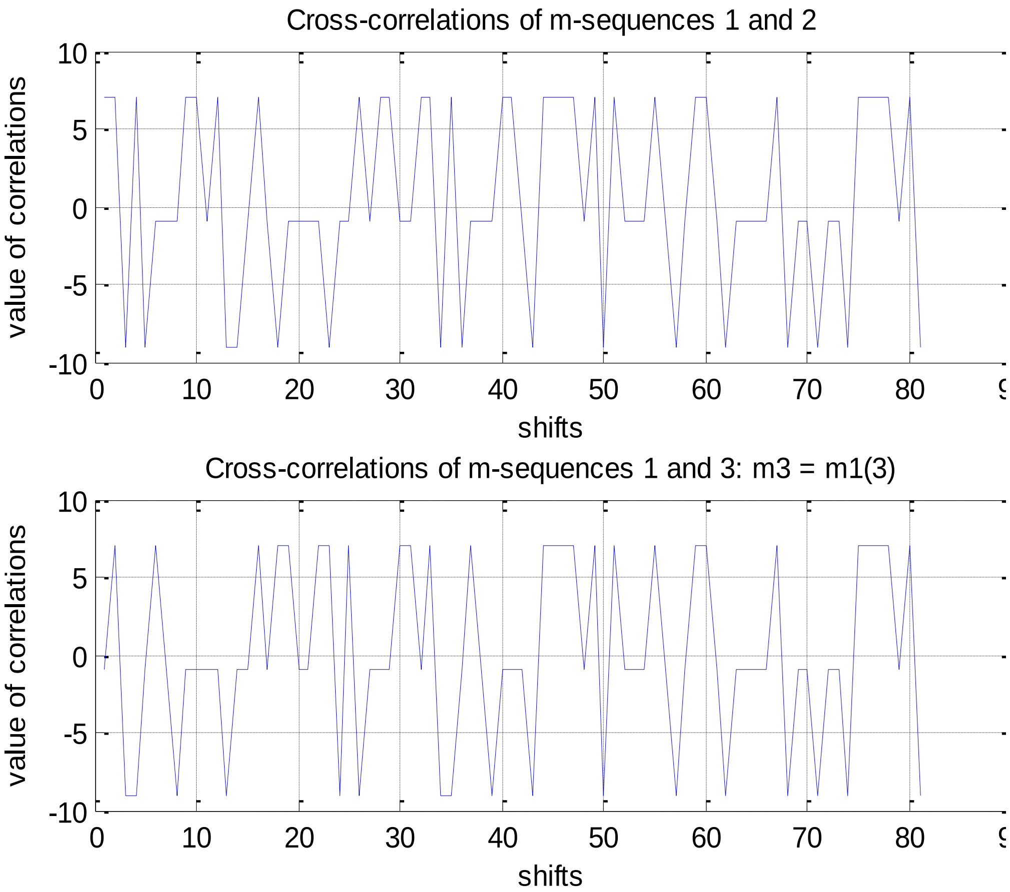

Fig. 3.2 (b) Graphs of cross-correlation of the 31-chip m-sequences of Fig. 3-2(a)

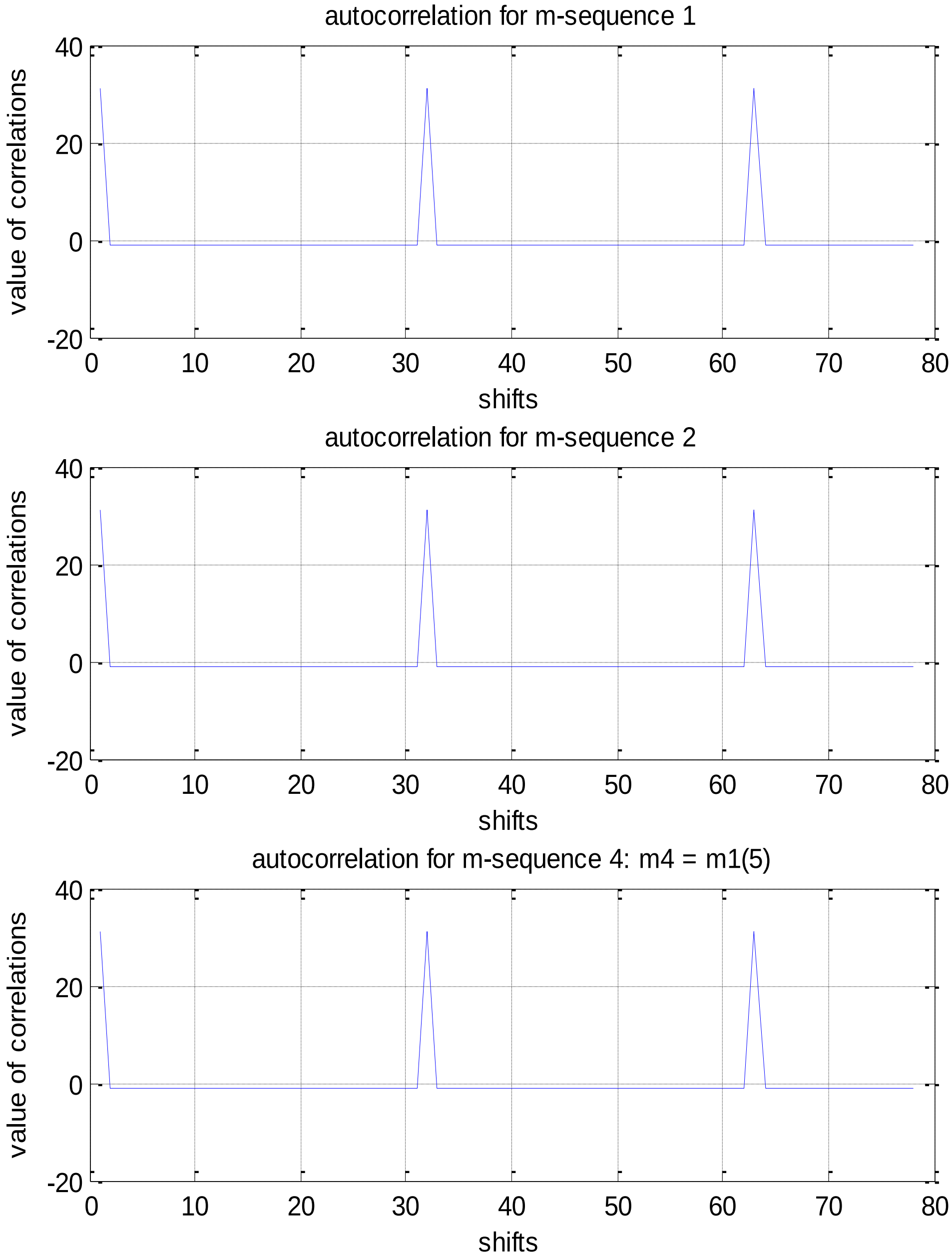

Fig. 3.3 (a) Graphs of autocorrelation of some other 31-chip *m*-sequences

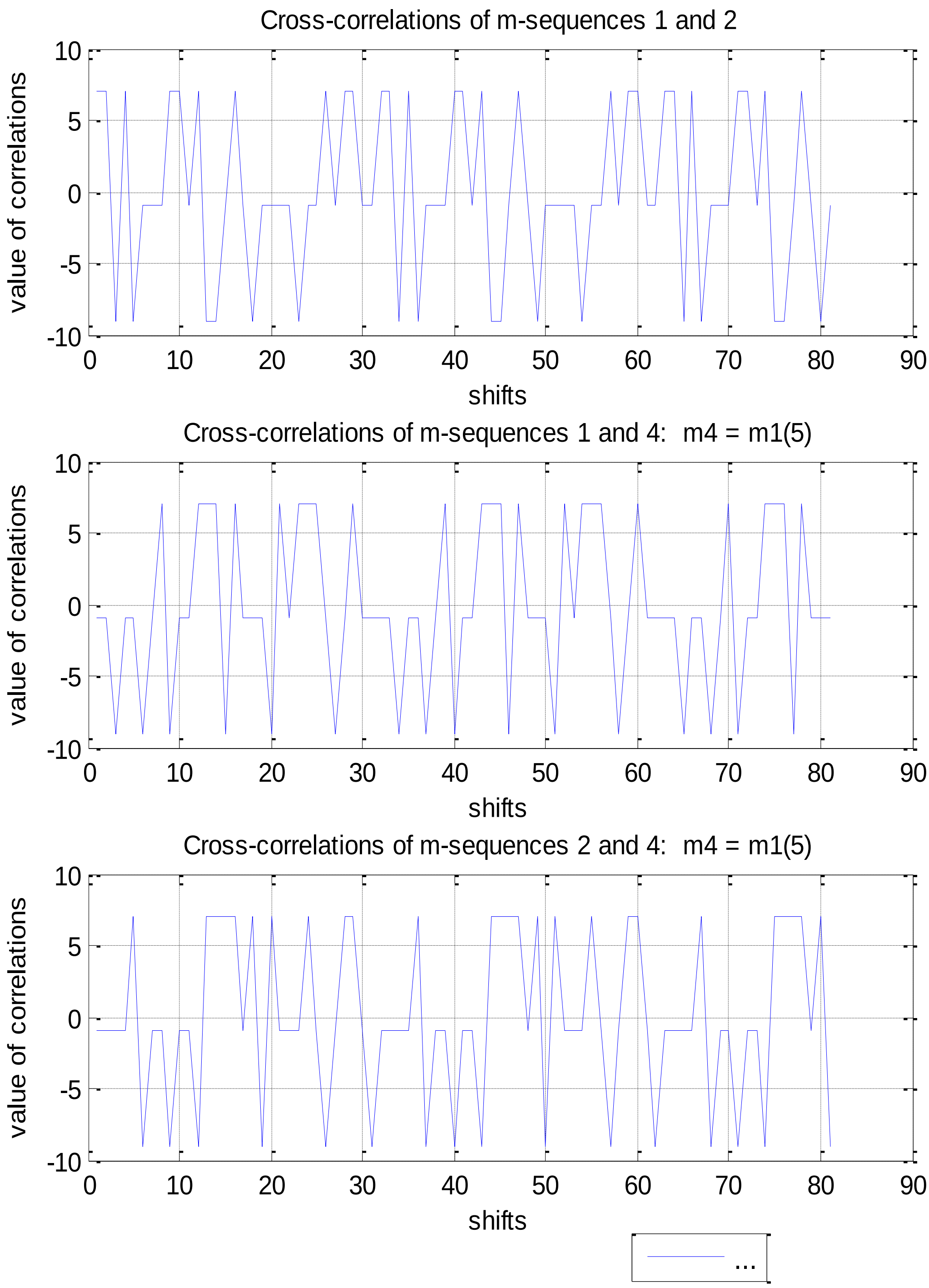

Fig. 3-3(b) Graphs of cross-correlation of 31-chip the *m*-sequences of Fig. 3-3(a)

Figure 3.4(a) shows the autocorrelation of one of the Gold codes, selected from the family of Gold codes of Table 3.2. Figure 3.4(b) shows the cross-correlation graph for two of the Gold codes. These graphs agree with the theoretical predictions for Gold codes.

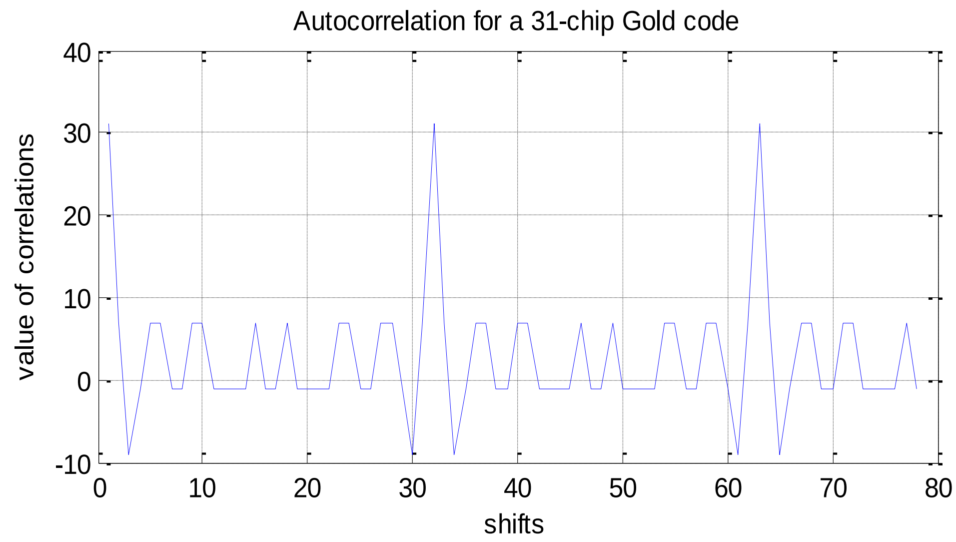

(a)

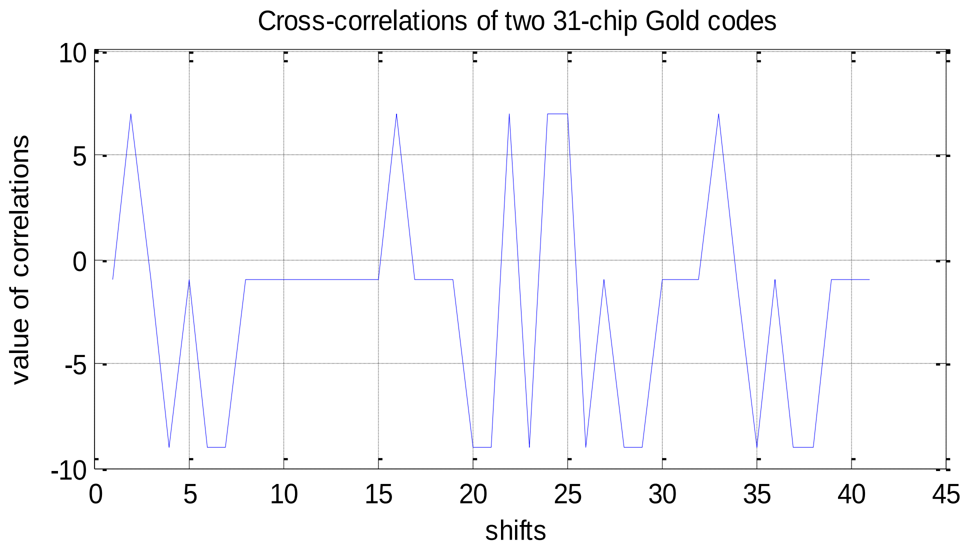

(b)

Fig. 3.4. Graph of (a) autocorrelation for a 31-chip Gold code (b) cross-correlation function for two Gold codes.

Although the 31-chip codes that have just been presented provide useful models, they are not suitable as spreading elements for practical spread-spectrum systems because of their short length. The 31-chip codes may only support a few simultaneous users at their best. Practical applications require longer codes [141]. In the next section, simulations involving longer codes will be presented.

3.4 Generation of longer codes

Longer codes, including 127-, 511- and 2047-chip codes were also generated and investigated. Fig. 3.5 shows the results for 127-chip *m*-sequences. This figure involves four different *m*-sequences, numbered 1 to 4. On this figure, the first four graphs are autocorrelation plots, while the rest are cross-correlation plots. The autocorrelation plots confirm that the codes are indeed *m*-sequences, while the cross-correlation plots show that any pair of the *m*-sequences constitutes a preferred pair.

Fig. 3.6 shows results for 511-chip *m*-sequences. On this figure, the autocorrelation plots (the first four plots) confirm that the sequences are *m*-sequences. The cross-correlation plots between *m*-sequence pairs 1 and 3 as well as 1 and 4 are triple-valued, confirming that the pairs are preferred sequences. The cross-correlation plots between *m*-sequence pairs 2 and 4 are also triple-valued, which indicate that they are preferred pairs with respect to one another. That is, *m*-sequence 4 is a preferred pair of both *m*-sequence 1 and 2. The cross-correlation plot between sequence 1 and sequence 2 confirms that they are not preferred pairs. The same applies to pairs 2 and 3, as well as 3 and 4.

Fig. 3.7 shows results for 2047-chip codes. Among other things, the cross-correlation graphs between *m*-sequence pairs 1 and 3 as well as 1 and 4 are triple-valued, confirming that these pairs are preferred sequences. The cross-correlation plots of the remaining parings confirm that they are not preferred pairs.

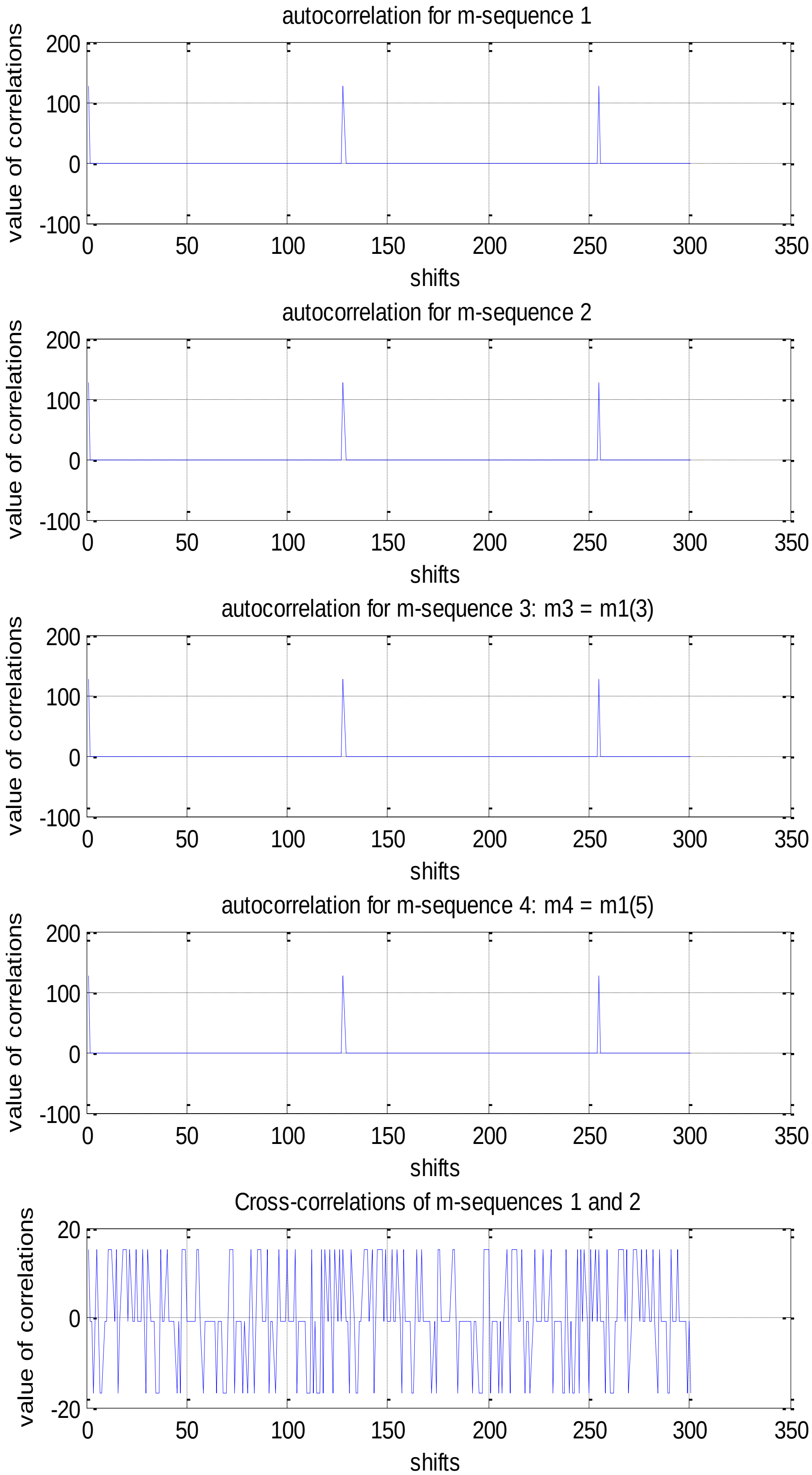

Fig. 3.5. Graphs of autocorrelation and cross-correlation of 127-chip m-sequences

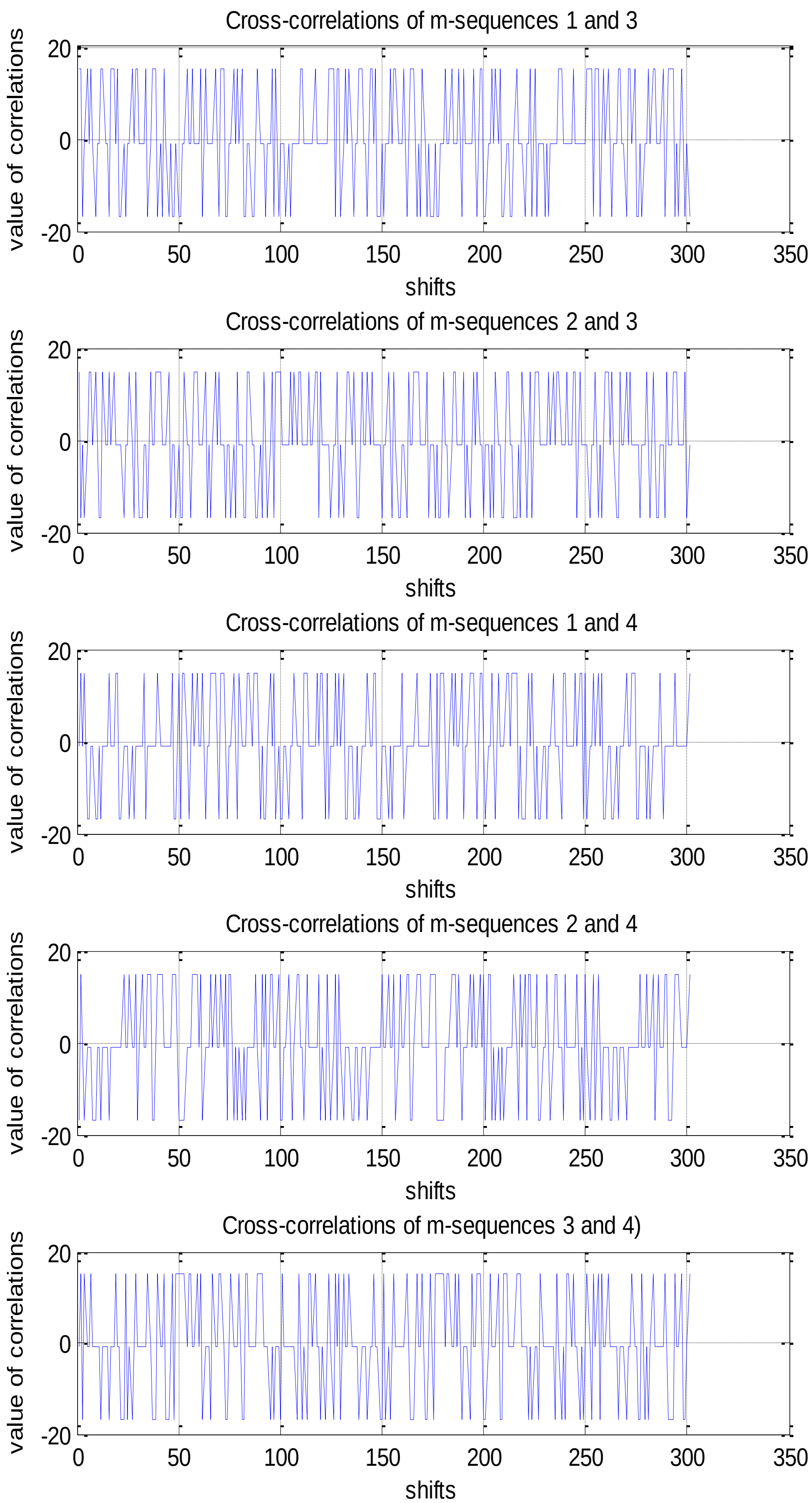

Fig.3.5 contd. Graphs of autocorrelation and cross-correlation of 127-chip *m*-sequences

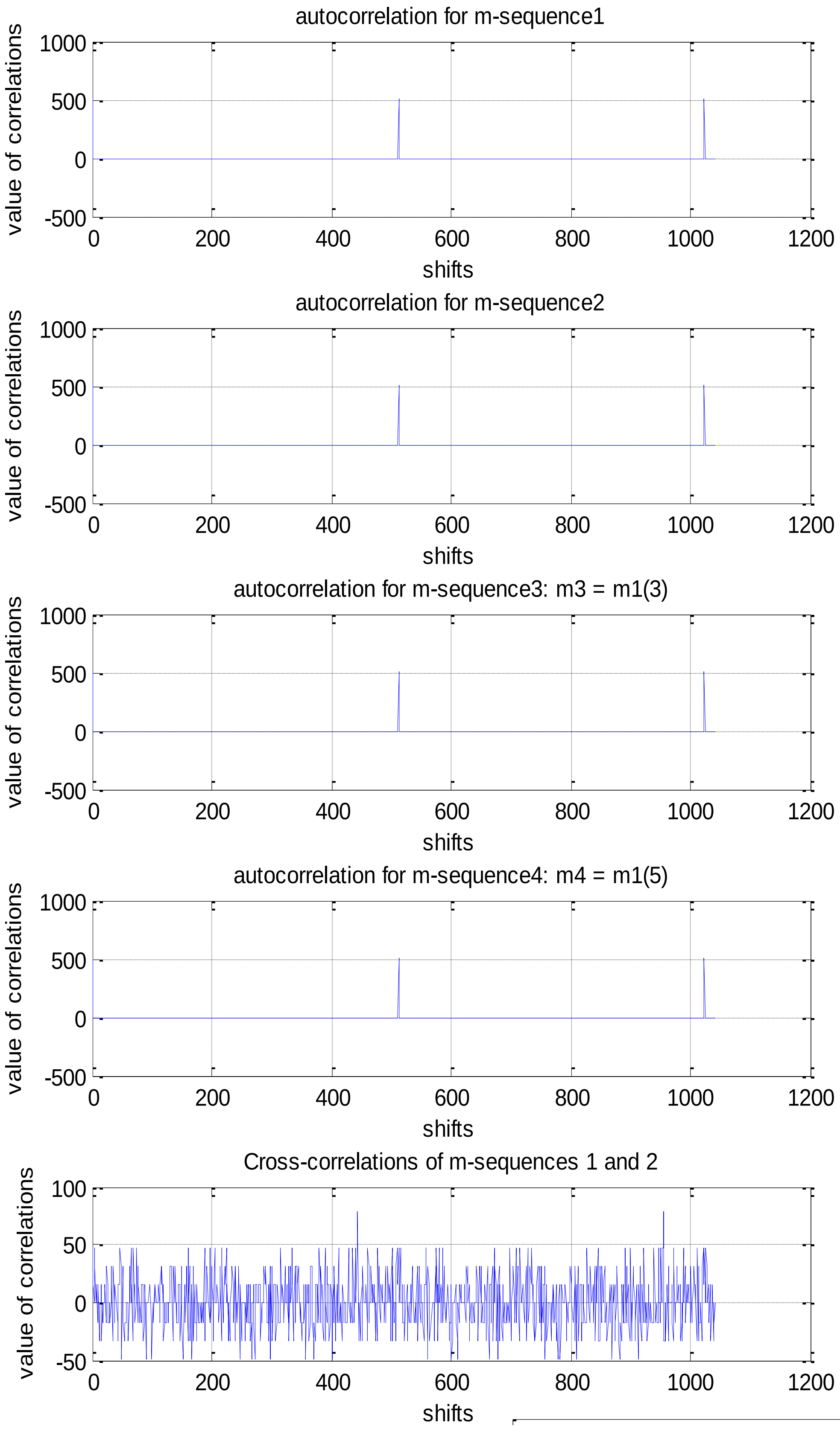

Fig. 3.6. Graphs of autocorrelation and cross-correlation of 511-chip m-sequences

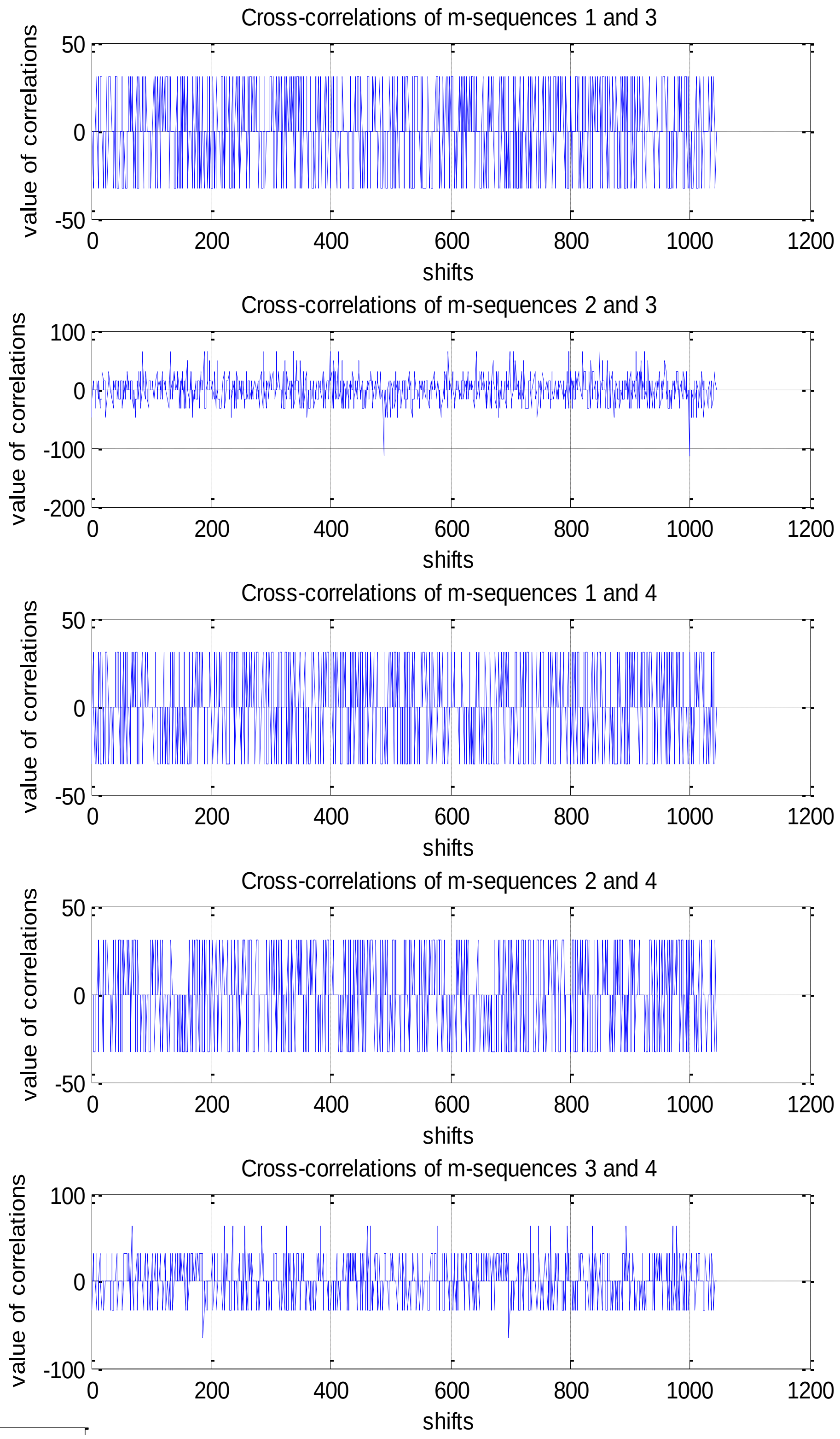

Fig. 3-6 contd. Graphs of autocorrelation and cross-correlation of 511-chip *m*-sequences

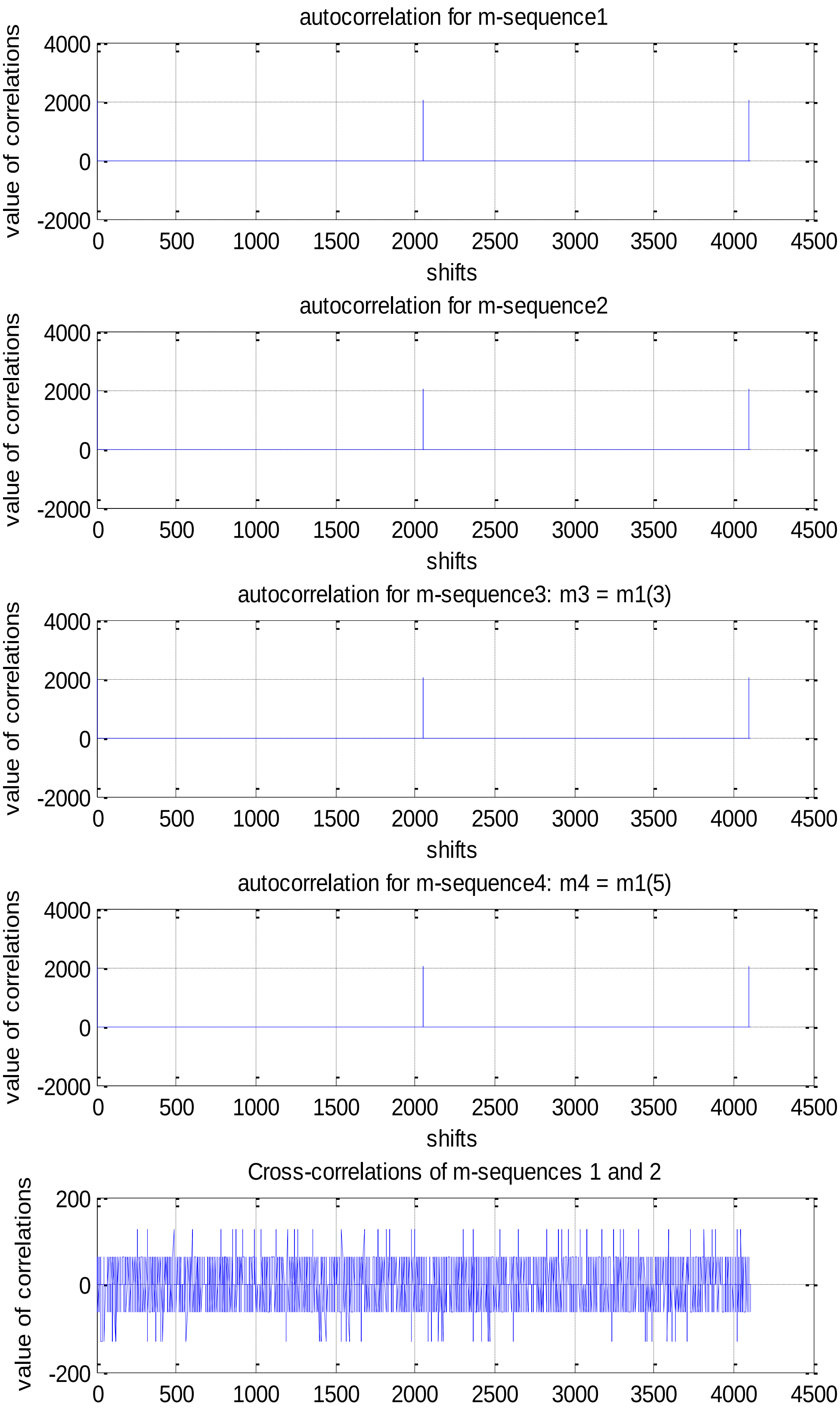

Fig. 3.7 Graphs of autocorrelation and cross-correlation of 2047-chip m-sequences

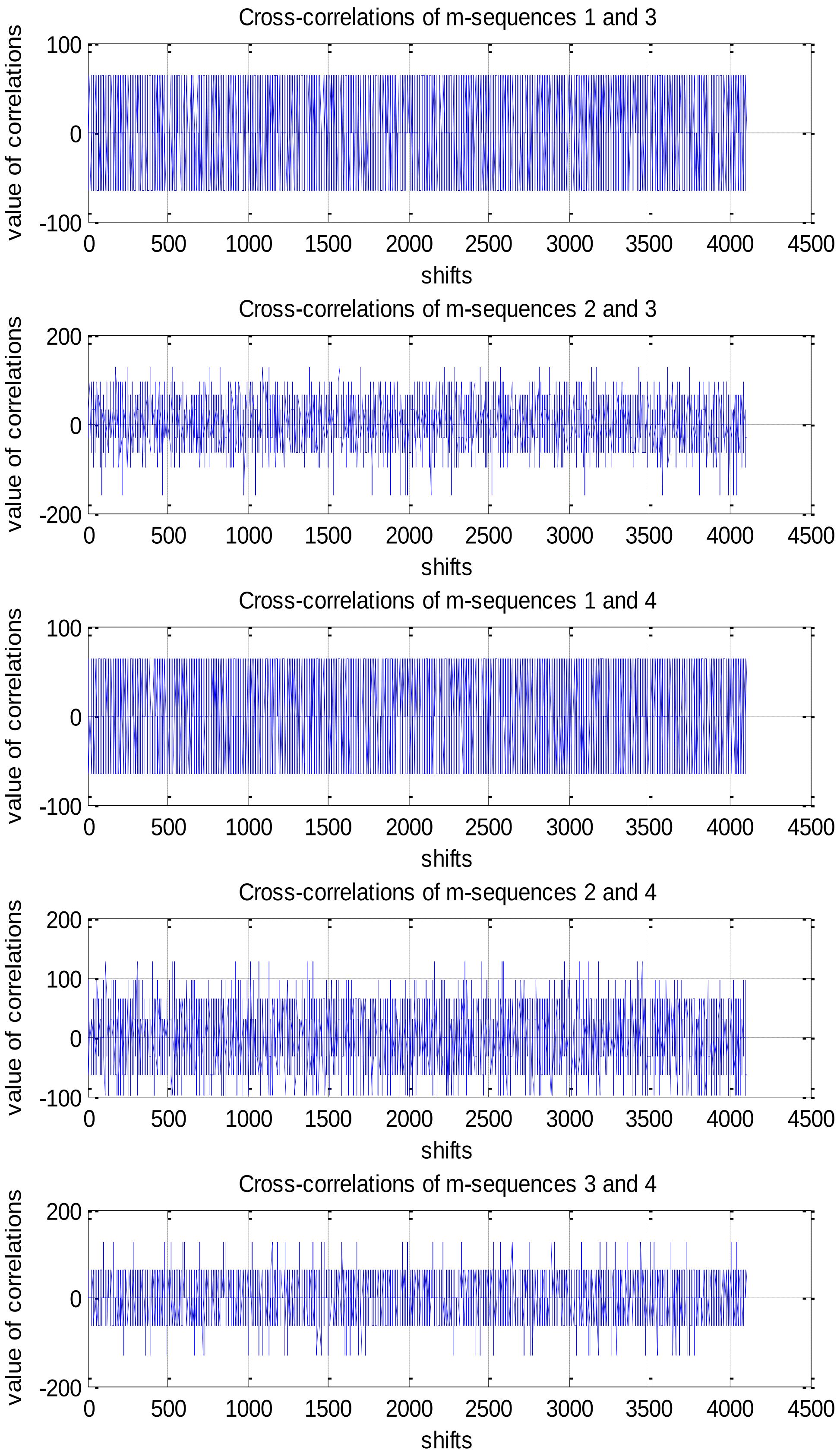

Fig. 3-7 contd. Graphs of autocorrelation and cross-correlation of 2047-chip *m*-sequences

3.5 Signal transmission through a noiseless channel

In this section, we shall start developing and testing software models for the proposed communication system. The development process begins with the simulation of a baseband CDMA for signal transmission through a noiseless, non-fading channel, Fig. 3.8. Basically, this model involves PN-encoding-decoding. Since the transmission is through a noiseless channel, it is expected that every transmitted signal should be received without any errors. That is, the bit-error-rate (BER) should be zero, regardless of the length of the data stream being transmitted. Simulation results that were obtained confirmed this to be the case. The model was simulated for 4-bit, 8-bit, 13-bit as well as one million-bit random data streams, and in every case, the signal reception was without errors. The outcome of the simulation helped in further validating the Gold codes. Were the transmitted bits recovered with errors, it would mean that the Gold codes are faulty codes.

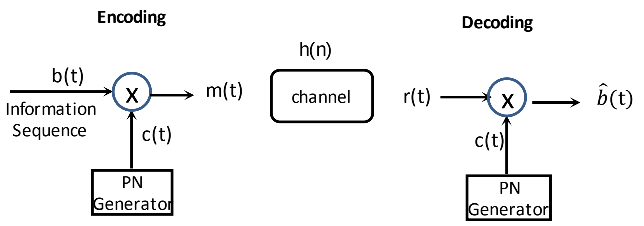

Fig. 3.8. Signal transmission through a noiseless channel

3.6 Signal transmission through a noisy channel

As part of initial phase of the system development process, models were simulated for signal transmission through a noisy channel. We shall begin with a brief treatment of the underlying theory, as illustrated by Fig. 3.9. As shown by this figure, binary information stream *b(t)* is first digitally modulated to give a modulated signal *m(t)*. The modulated signal is then encoded with a PN-code *c(t)*, after which the signal convolves with channel impulse response *h(n)*, and then becomes corrupted by noise *n(t)*. To recover the original information stream, the receiver carries out the reverse process. The recovered output $\hat{b}(t)$ is then compared with the original information stream *b(t)* to determine the number of errors, for bit-error-rate (BER) analysis.

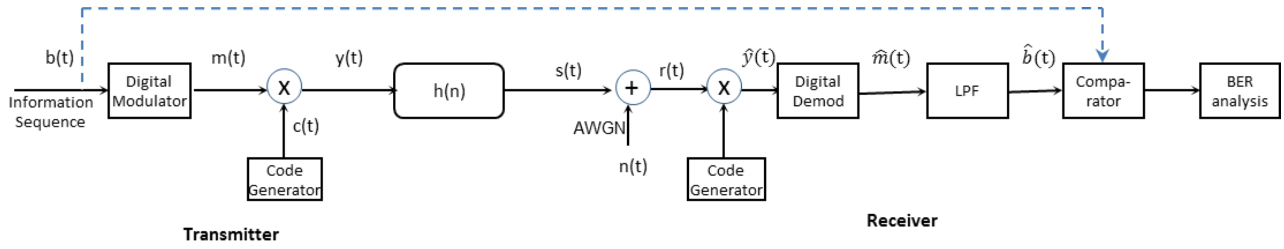

Fig. 3.9. Baseband CDMA model showing signal transmission through a noisy channel

For binary phase-shift-keying (BPSK), the modulated signal *m(t)* can be expressed as

$$m(t) = b(t)\cos\omega t, \tag{3.5}$$

where $b(t) = \pm 1$, and ω is carrier frequency. Applying the PN code to this expression gives

$$y(t) = c(t)b(t)\cos\omega t \tag{3.6}$$

This signal is transmitted through the channel, where it convolves with the channel impulse response, and then become corrupted by the additive white Gaussian noise (AWGN) *n(t)* to give

$$r(t) = y(t) * h(t) + n(t) \tag{3.7}$$

For the case a Gaussian channel, if we assume an infinite bandwidth channel, then $h(t) = \delta(t)$. Therefore,

$$r(t) = c(t)b(t)\cos\omega t + n(t) \tag{3.8}$$

At the receiver, assuming perfect synchronisation, multiplying the received signal with the same PN code gives the decoded signal

$$\begin{aligned}\hat{y}(t) &= r(t)c(t)\\ &= c^2(t)b(t)\cos\omega t + c(t)n(t)\end{aligned} \tag{3.9}$$

So with coherent demodulation, we have that

$$\hat{m}(t) = \frac{c^2(t)}{2}b(t)[1 + \cos 2\omega t] + n(t)c(t)cos\omega t \tag{3.10}$$

Assuming *c(t)* is an antipodal signal (i.e. $c(t) = \pm 1$), and applying a low-pass filter to remove the double frequency *(2ω)* reduces the last expression to give

$$\hat{b}(t) = \frac{b(t)}{2} \pm n(t)cos\omega t \quad \textbf{(3.11)}$$

Since *n(t)* is a random noise, passing this signal through an integrator will help in suppressing the second term for a recovery of the original data.

For initial testing, a few random bits were BPSK-modulated, encoded with Gold codes and then transmitted through the noisy channel at a signal-to-noise ratio (SNR) of 10 dB. Recovered output bit streams were then examined visually for errors. In addition, scatter plots (Fig. 3.10) of received data bits were generated. Because of noise, it is expected that the received data bits should scatter (cluster) around ideal BPSK constellation points. Fig. 3.10 confirmed this to be the case. In addition, because of the value of the SNR (10 dB) used for the simulation, it is expected that data bits should be recovered without errors. Simulation results confirmed this to be the case: in every case, all the data bits were recovered without errors.

Following the initial testing with a few random bits, the binary information stream was increased to a hundred bits, after which the transmission process was repeated for different values of SNR. Fig. 3.11 shows the scatter plots of received data for SNR values of 20, 10, 0, -10 and -20 dB. It is expected that as SNR decreases, the received data bits should scatter further away from ideal BPSK constellation points (±1). These results confirm this. In addition, it is expected that as SNR goes down, errors should creep into the recovered bit streams. Simulation results confirmed this to be the case, as shown by Table 3.3. This table shows that as SNR decreases, BER worsens.

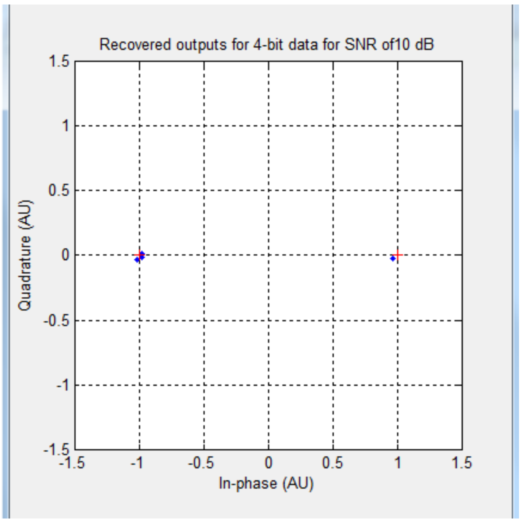

(a)

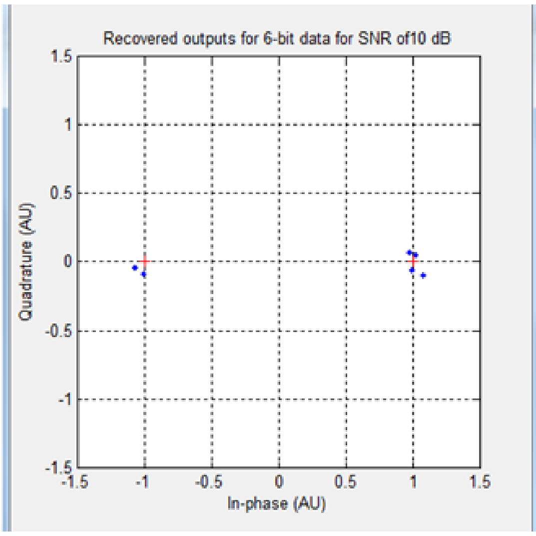

(b)

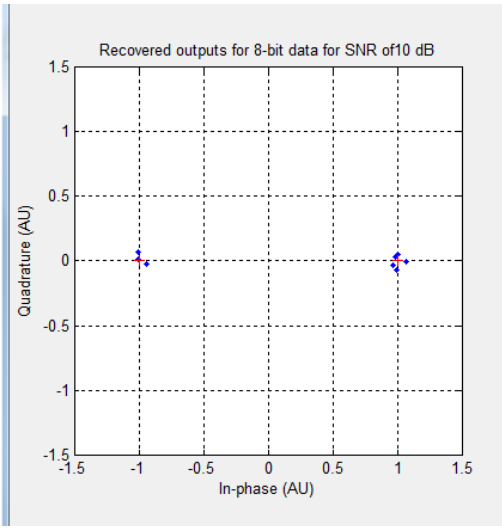

(c)

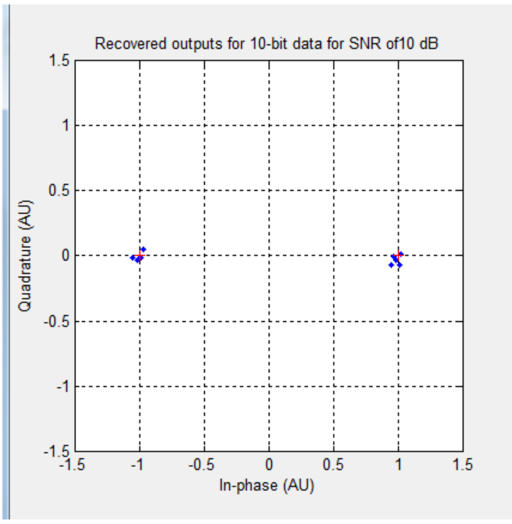

(d)

Fig. 3.10. Scatter plots for signal transmission through a noisy Gaussian channel at an SNR of 10 dB for (a) 4-bit (b) 6-bit (c) 8-bit and 10-bit data.

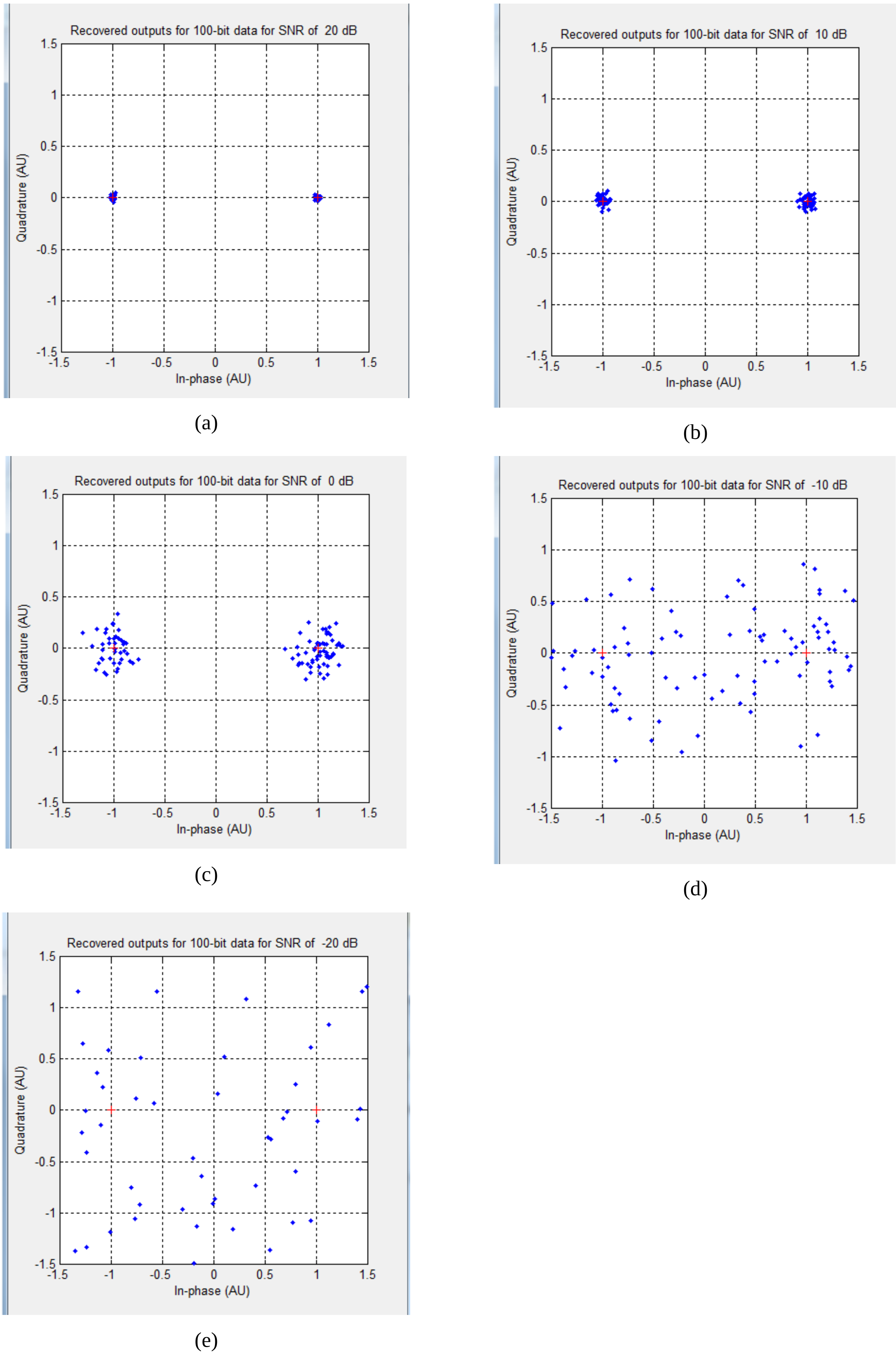

Fig. 3.11. Scatter plots for a 100-bit data transmitted through the noisy Gaussian channel at an SNR of (a) 20 dB (b) 10 dB (c) 0 dB (d) -10 dB and (e) -20 dB.

Table 3.3. Measured bit-error rate for transmission of 100 bits through the noisy channel

SNR (dB)	Bits received in error	BER
20	0	0
10	0	0
0	0	0
-10	2	0.0200
-20	27	0.2700

3.7 Chapter summary

This chapter began with an overview of spreading sequences and code selection process for the proposed communication system. This was followed by an account of software simulations carried on *m*-sequences and Gold codes. The simulations involved generation of the codes, and experimentation on their correlation properties. Gold codes were selected in preference to other spreading sequences because of their favourable correlation properties. Added to this is the fact that large number of Gold codes can easily be generated for multiple-access applications. This chapter also initiated the development and testing of the proposed communication system. Signal transmission through a noisy channel for a baseband CDMA system using the Gold codes as spreading sequences was modelled and tested. The work reported in this chapter provides a foundation for the rest of this research work.

Chapter 4

Multiple-access performance of Gold codes in a DS-CDMA system

4.0 Introduction

In the previous chapter, an account of code selection process was given. The current chapter investigated multiple-access performance of the class of code, the Gold codes, selected for the development of the proposed communication system.

Spreading codes play critical role in determining the performance of spread-spectrum systems. Code properties are known to be a cause of multiple-access interference (MAI), an important limiting factor on the system performance. The significance of spreading codes has made the search for better codes [80, 82, 85-94] and the mitigation of multiple-access interference [95-105] important areas of research.

An aspect of such effort is the search for better orthogonal codes. For example in [104], Chen Hsiao-Hwa, et al proposed the generation of perfectly orthogonal complementary codes for the realisation of an interference-free code division multiple access (CDMA) system. Although orthogonality is a desirable property, it does not in itself solve all the code-associated problems of a spread-spectrum system. Orthogonal codes are excellent in synchronous, but not in asynchronous environment, in which orthogonality is lost.

This chapter investigates the performance of an important class of code, the Gold codes, to provide new insights on their properties for better system performance. The codes are significant today not only in mobile wireless communication but also in satellite navigation. They are used as spreading codes in Wideband code-division multiple-access (WCDMA) system and as access codes in the global positioning system (GPS). They are also potential candidates for emerging technologies like the space-time coded multicarrier CDMA system. In this chapter, we investigate the performance of odd-degree and even-degree Gold codes in a multi-user system, ranging from a few users to hundreds of users. The outcome of this investigation shows that the odd-degree Gold codes are more resistant to multiple-access-interference, thereby making them better suited than their even-degree counterparts for use in multi-user systems.

A conference paper [144] based on research results of this chapter was presented by the writer at the Global Wireless Summit Conference 2014, Aalborg, Denmark. A journal paper [145] on the results has also been published in South-African Institute of Electrical Engineers African Research Journal.

The rest of this chapter is organised as follows. In Section 4.1, the system model is presented. Sections 4.2 - 4.4 give results of simulations of bit-error-rate performance of even- and odd-degree Gold codes. Sections 4.5 – 4.7 deal with loading characteristics of the codes, as a further test on their multiple-access performance. Section 4.8 concludes this chapter with a summary.

4.1 System model

Consider a multi-user DS-CDMA system comprising *K* users, Fig. 4.1.

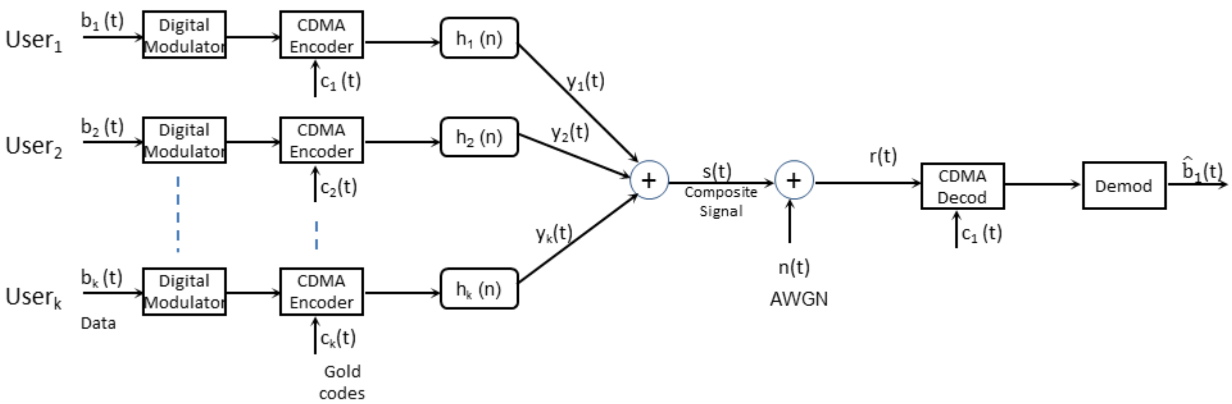

Fig. 4.1. Model of a multi-user DS-CDMA system

For this system, the received signal *r(t)* is a linear superposition of the signals for the users, and is given by

$$r(t) = \sum_{k=1}^{K}\sum_{l=1}^{L} A\beta_{kl}e^{j\gamma_{kl}}\ c_k(t-\tau_{kl})\, b_k(t-\tau_{kl})\, cos(\omega_c(t-\tau_{kl})-\theta_{kl}) + n(t) \qquad (4.1)$$

where k is user index, l is path index, L is number of paths, β_{kl} is path gain for user k and path l, τ_{kl} is propagation delay, γ_{kl} is phase shift, c_k is spreading code for user k, b_k is binary data,

ω_c is carrier frequency, t is time and $n(t)$ is channel noise. Let user-1 be the reference user. Assuming coherent demodulation, the receiver output $z(m)$ for m^{th} bit during the bit duration T_b of the user is given by

$$z_1(m) = \int_{mT_b}^{(m+1)T_b} r(t)c_1(\text{t}) \cos \omega_c t \, dt$$

$$= \int_{mT_b}^{(m+1)T_b} \left\{ \sum_{k=1}^{K} \sum_{l=1}^{L} A\beta_{kl} e^{j\gamma_{kl}} \; c_k(t-\tau_{kl}) \, b_k(t-\tau_{kl}) \, cos(\omega_c(t-\tau_{kl}) - \theta_{kl}) + n(t) \right\} c_1(\text{t})\text{cos}\omega_c t \, dt$$

$$= \int_{mT_b}^{(m+1)T_b} \left\{ \sum_{l=1}^{L} A\beta_{1l} e^{j\gamma_{1l}} c_1(t-\tau_{1l}) b_1(t-\tau_{1l}) cos(\omega_c(t-\tau_{1l}) - \theta_{1l}) \right\} c_1(\text{t}) \cos \omega_c t \, dt$$

$$+ \int_{mT_b}^{(m+1)T_b} \left\{ \sum_{k=2}^{K} \sum_{l=1}^{L} A\beta_{kl} e^{j\gamma_{kl}} \; c_k(t-\tau_{kl}) \, b_k(t-\tau_{kl}) \, cos(\omega_c(t-\tau_{kl}) - \theta_{kl}) \right\} c_1(\text{t}) \cos \omega_c t \, dt$$

$$+ \int_{mT_b}^{(m+1)T_b} n(t)c_1(\text{t})\text{cos}\,\omega_c t \, dt$$

$$= z_{11} + z_{12} + z_{13} \tag{4.2}$$

where

$$z_{11} = \int_{mT_b}^{(m+1)T_b} \left\{ \sum_{l=1}^{L} A\beta_{1l} e^{j\gamma_{1l}} c_1(t-\tau_{1l}) b_1(t-\tau_{1l}) cos(\omega_c(t-\tau_{1l}) - \theta_{1l}) \right\} c_1(\text{t}) \cos \omega_c t \, dt,$$

$$z_{12} = \int_{mT_b}^{(m+1)T_b} \left\{ \sum_{k=2}^{K} \sum_{l=1}^{L} A\beta_{kl} e^{j\gamma_{kl}} \; c_k(t-\tau_{kl}) \, b_k(t-\tau_{kl}) \, cos(\omega_c(t-\tau_{kl}) - \theta_{kl}) \right\} c_1(\text{t}) \cos \omega_c t \, dt$$

and

$$z_{13} = \int_{mT_b}^{(m+1)T_b} n(t)c_1(\text{t})\text{cos}\,\omega_c t \, dt \tag{4.3}$$

z_{11} represents the desired signal for the reference user, z_{12} is interference term, and z_{13} is noise term.

<u>Definition</u>

Let the code length $N = 2^n - 1$. Gold code is said to be an *odd-degree* code if n is odd; and an *even-degree* code if n is even. For example,

if $n = 5$, the code is odd-degree, and $N = 2^5 - 1 = 31$;

if $n = 6$, the code is even-degree, and $N = 2^6 - 1 = 63$.

4.2 Software simulations

For the present investigation, Gold codes were generated for degree n = 5, 6, …,12, corresponding to the code length N = 31, 63, 127, 255, 511, 1023, 2047 and 4095 respectively. The codes were obtained from appropriate combinations of preferred pairs of *m*-sequences (Table 4.1).

Table 4.1. Generator polynomials for the Gold codes

n	$P_i^n(x)$	*Generator polynomial	*N*
5	$P_1^5(x)$	x^5+x^2+1	31
	$P_2^5(x)$	$x^5+x^4+x^3+x^2+1$	
6	$P_1^6(x)$	x^6+x^5+1	63
	$P_2^6(x)$	$x^6+x^5+x^4+x+1$	
7	$P_1^7(x)$	x^7+x^6+1	127
	$P_2^7(x)$	x^7+x^4+1	
8	$P_1^8(x)$	$x^8+x^7+x^6+x+1$	255
	$P_2^8(x)$	$x^8+x^7+x^5+x^3+1$	
9	$P_1^9(x)$	x^9+x^5+1	511
	$P_2^9(x)$	$x^9+x^8+x^7+x^2+1$	
10	$P_1^{10}(x)$	$x^{10}+x^7+1$	1023
	$P_2^{10}(x)$	$x^{10}+x^9+x^8+x^5+1$	
11	$P_1^{11}(x)$	$x^{11}+x^9+1$	2047
	$P_2^{11}(x)$	$x^{11}+x^{10}+x^9+x^7+1$	
12	$P_1^{12}(x)$	$x^{12}+x^{11}+x^{10}+x^4+1$	4095
	$P_2^{12}(x)$	$x^{12}+x^{11}+x^{10}+x^2+1$	

*$P_1^n(x)$ and $P_2^n(x)$ are the generator polynomials of the preferred pair used for obtaining corresponding set of Gold codes of degree *n*.

Software simulations were carried out for the transmission of random QPSK symbols for uncoded as well as coded data transmission, through a Gaussian channel of zero mean and unit variance Gaussian noise. The deployment of a Gaussian channel, as opposed to the use of a fading channel, is beneficial to prevent channel fading from obscuring certain important deductions. Following signal recovery, original transmitted data was compared with recovered data for the determination of system bit-error-rate for the various sets of codes. The simulations for the various code lengths were carried out simultaneously during the same simulation session, thereby ensuring consistency of simulation conditions. Results of the simulations will now be examined, starting with odd-degree Gold codes.

4.3 Performance of odd-degree Gold codes

This section presents results of simulations that were carried out for a single as well as multiple users.

4.3.1 Performance for a single user

Here we consider simulation results for a single user, Fig. 4.2. The right-most curve on this figure is that of uncoded data transmission for a single user. The figure shows close agreement between analytic and simulation results for the uncoded data transmission. An analytic result is obtained by direct implementation of an analytic expression; simulation result is obtained by sending random data through the channel, and then counting the number of bits in error at the receiving end. For the uncoded data transmission, the analytic equation for the BER is: $BER = Q\left(\sqrt{2\left(\frac{E_b}{N_0}\right)}\right)$, where Q is q-function, and E_b/N_0 is bit-energy-per-noise ratio. For reference purposes, this curve will be retained on all results to be presented in this thesis. The rest of the curves on Fig. 4.2 show the performance for coded data transmission for different code lengths.

Clearly, Fig. 4.2 shows that longer Gold codes give better error-rate performance. The figure also shows that the use of Gold codes brings about some coding gain. With reference to uncoded data transmission, at a BER of 10^{-4}, the Gold codes provide coding gain of about 15.6, 21.7, 27.8 and 33.9 dB when $N = 31$, 127, 511 and 2047, respectively. From this we see that there is a constant 6.1-dB-step in coding gain between adjacent code lengths, which can be explained in terms of the ratio of the process gain of the codes.

It should be noted that the penalty for the coding gain obtained from the use of Gold codes is increase in bandwidth requirements. Each 6-dB improvement in coding gain corresponds to quadrupling of the bandwidth.

4.3.2 Performance for two to five users

Next, we shall consider the results for a few multiple users. Figs. 4.3 to 4.5 show BER for two, three and five users respectively. A look at these figures shows that increase in number of interferers worsens the system BER. That is, MAI worsens with increasing system load. The results show, for example, that for the code length $N = 31$ chips, at an SNR of -5 dB, BER is 1.1×10^{-3} for a single user, 2.1×10^{-2} for two users, 4.9×10^{-2} for three users and 1.1×10^{-1} for five users. The BERs for the other code lengths (N = 127, 511 and 2047) show a similar trend.

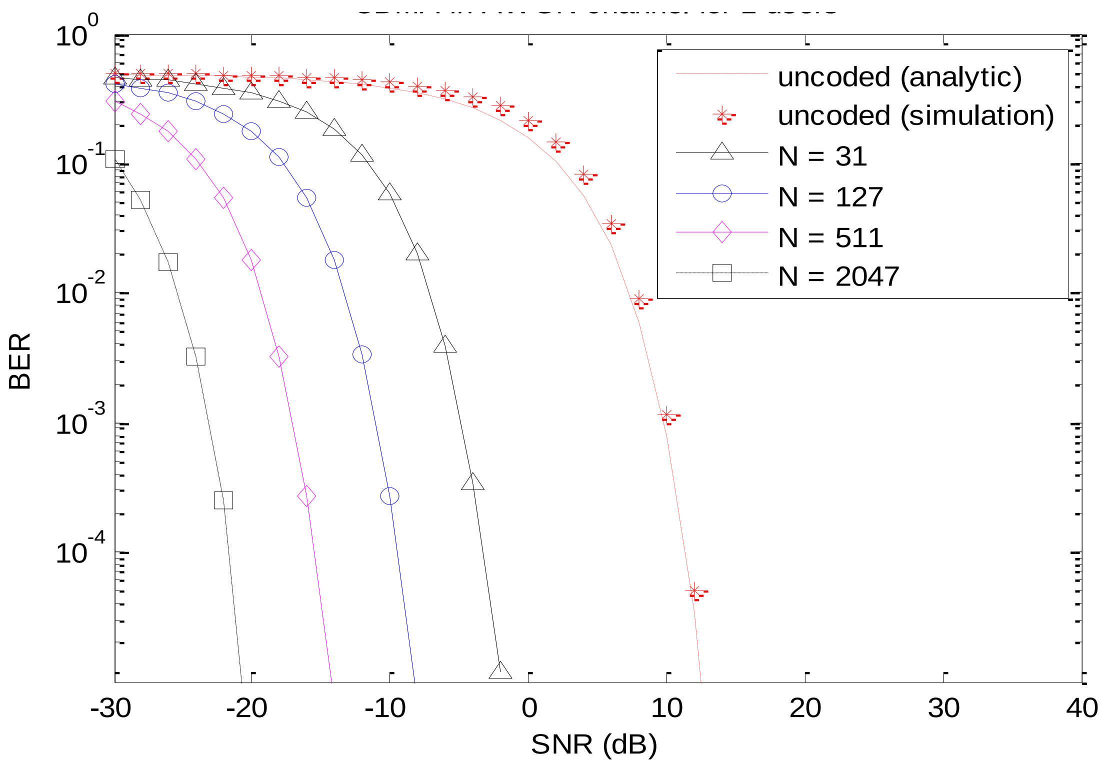

Fig. 4.2. Bit-error-rate for a single user

4.3.3 Performance for higher number of users

We shall now consider simulation results for higher numbers of users. Figs. 4.6 to 4.11 show the BER for 10, 15, 20, 25, 30 and 33 users respectively. As with the previous results, these figures show that as the number of users increase, the system BER becomes worse, resulting from increasing MAI. For the code length N = 31 chips, for example, the results show that at an SNR of 8 dB, BER is 3.13 x 10^{-4} for a ten users, 6.98 x 10^{-4} for 15 users, 2.94 x 10^{-3} for 20 users, 7.71 x 10^{-3} for 25 users,1.45 x 10^{-2} for 30 users and 1.92 x 10^{-2} for 33 users. Because of the MAI, obtaining the same BER for a system involving a higher number of simultaneous users requires higher SNR. For example for the 31-chip code, obtaining a BER of 10^{-4} requires an SNR of about -3.27 dB for a single user (Fig.4.2), 4.01 dB for five users (Fig. 4.3c), 7.28 dB for 10 users, 11.07 dB for 20 users and 14.32 dB for 30 users (Figs 4.4a, c & e).

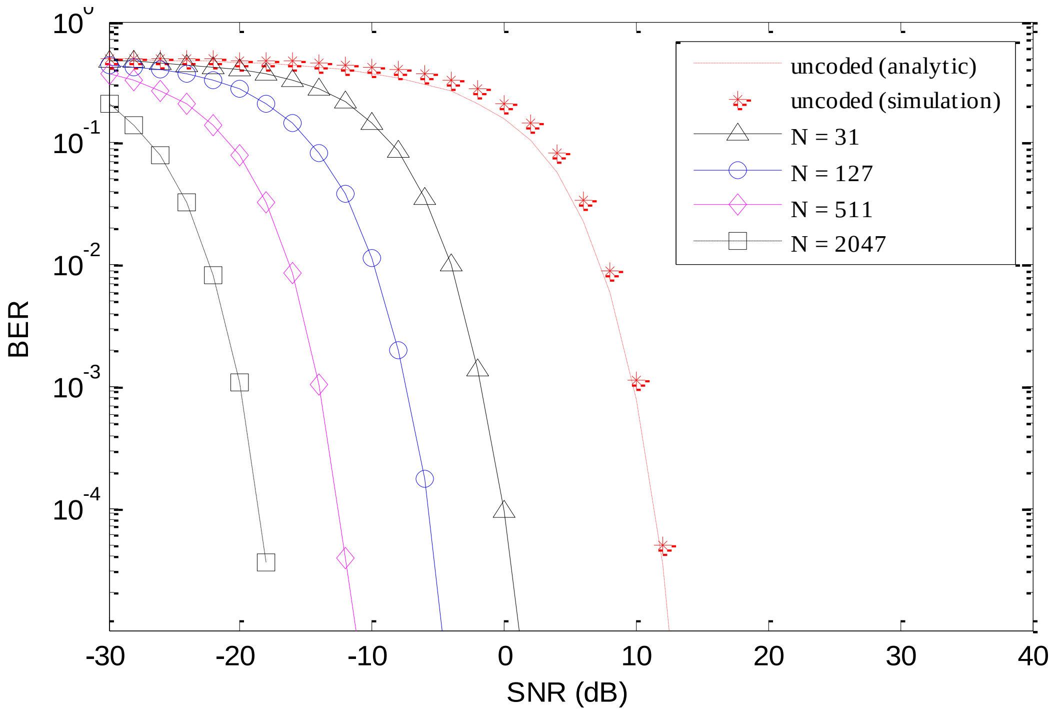

Fig. 4.3. Bit-error-rate for two users

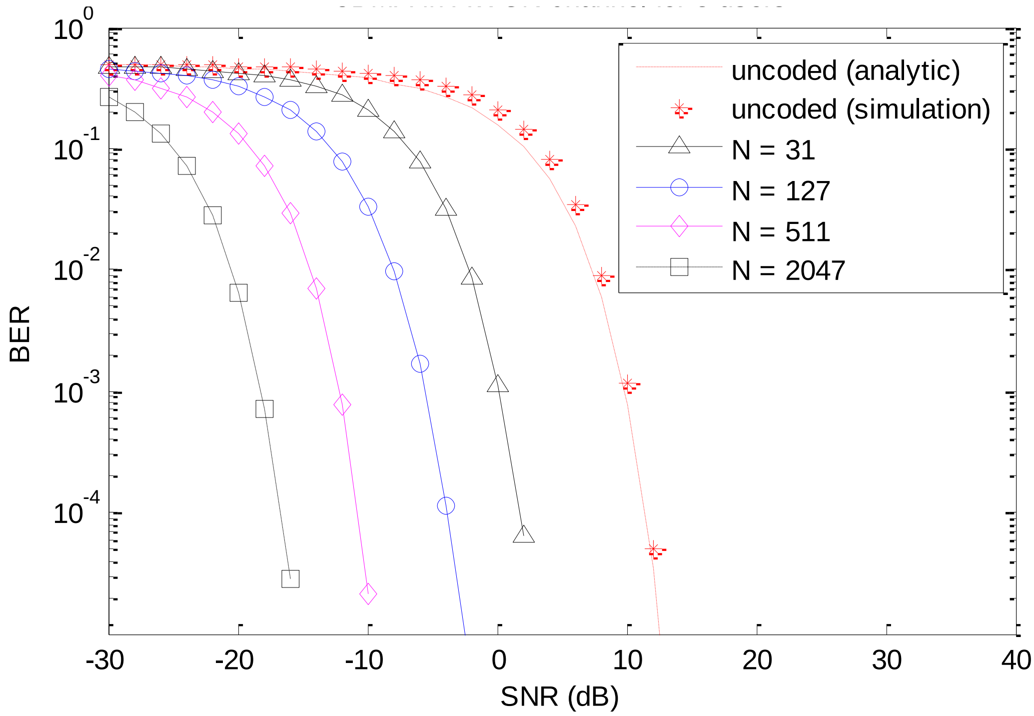

Fig. 4.4 Bit-error-rate for three users

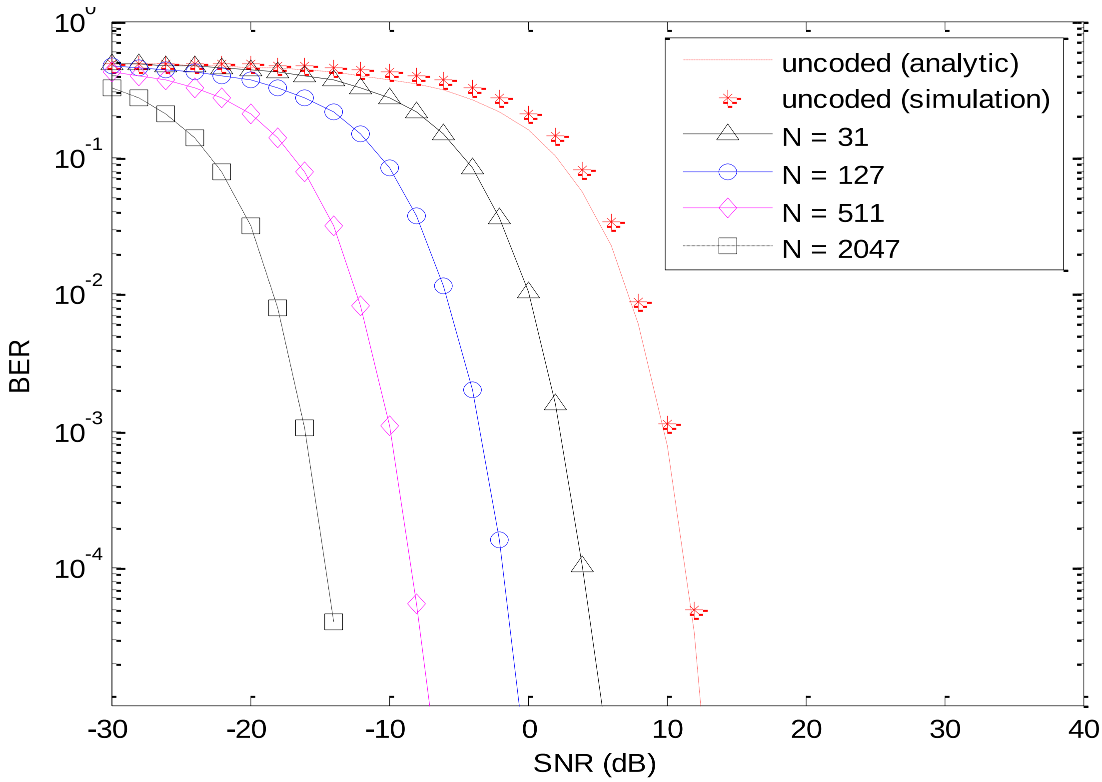

Fig. 4.5 Bit-error-rate for five users.

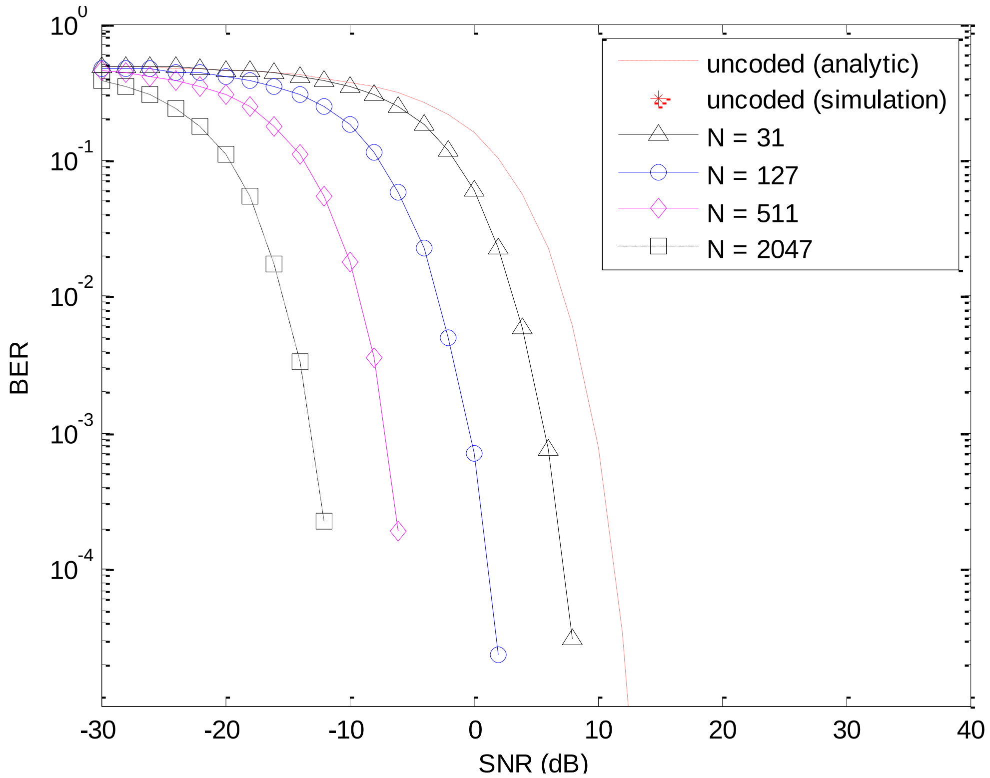

Fig. 4.6 Bit-error-rate for ten users

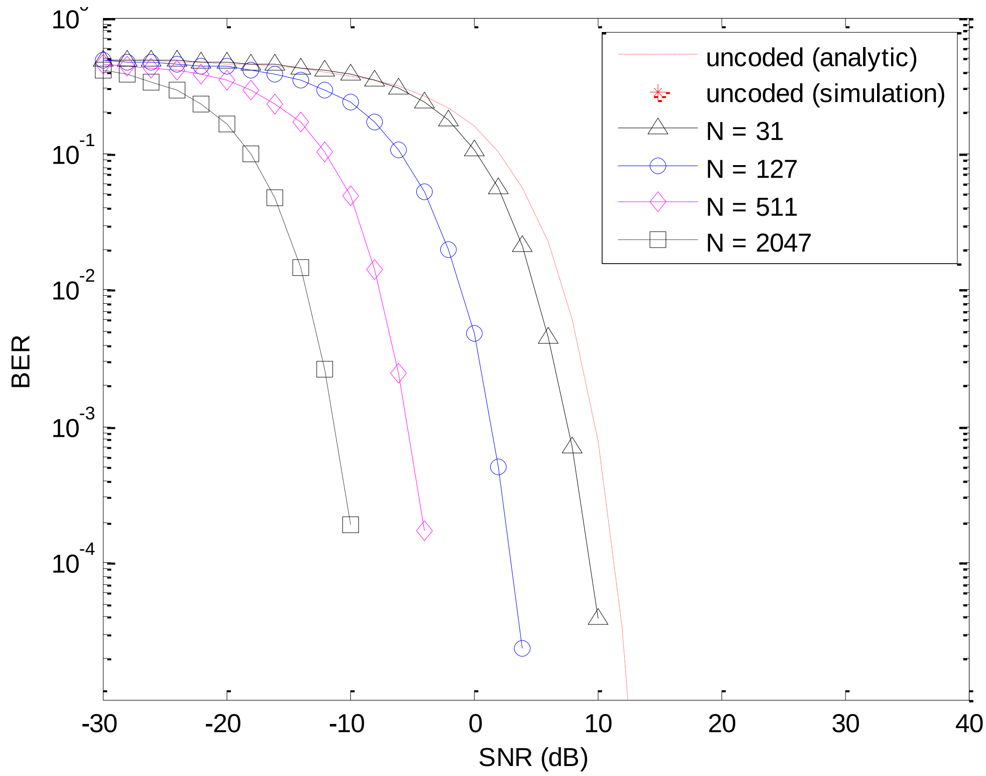

Fig. 4.7 Bit-error rate for 15 users.

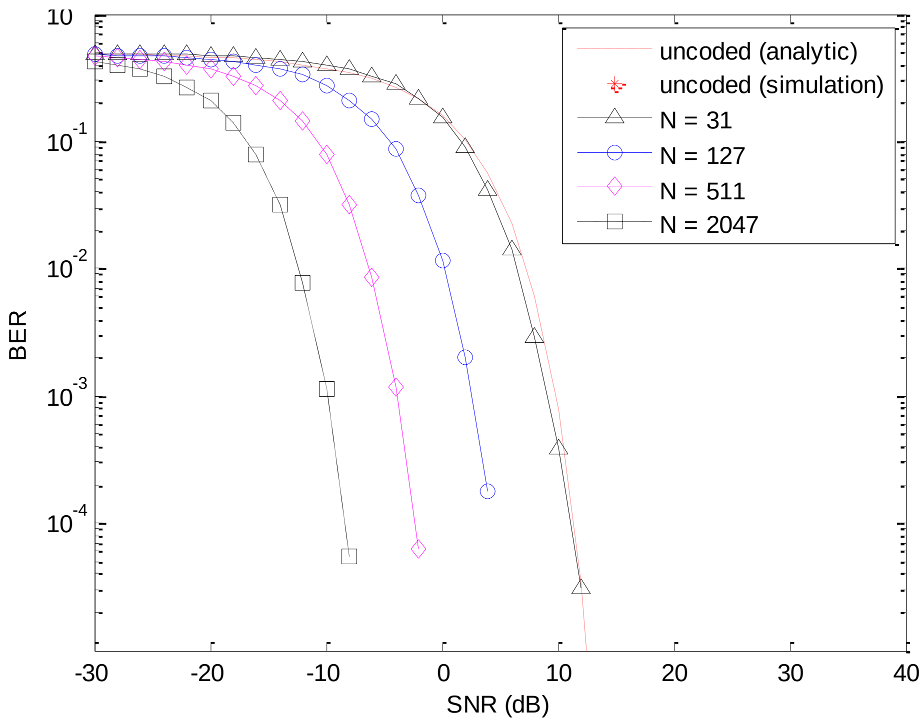

Fig. 4.8. Bit-error-rate for 20 users

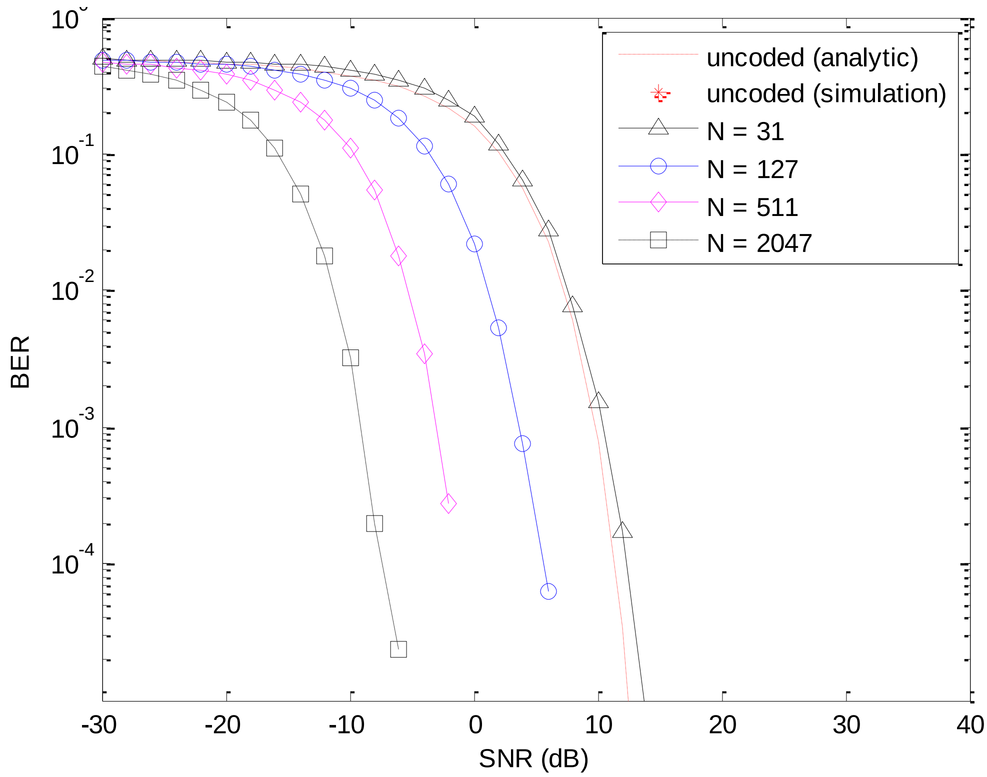

Fig. 4.9 Bit-error-rate for 25 users

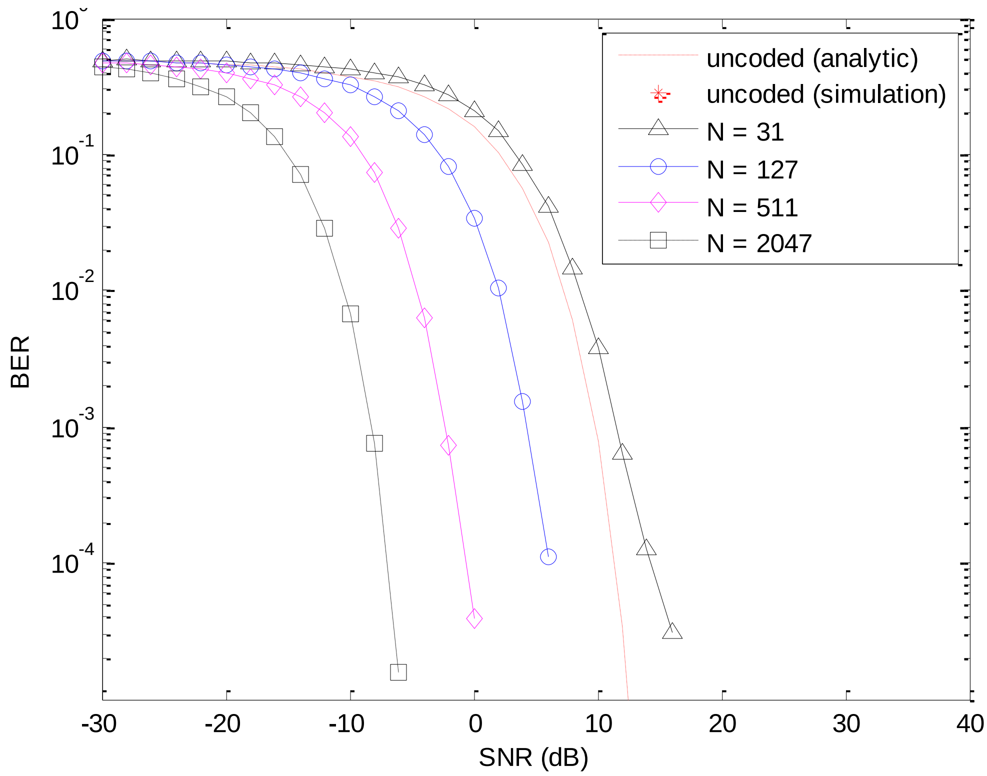

Fig. 4.10. Bit-error-rate for 30 users

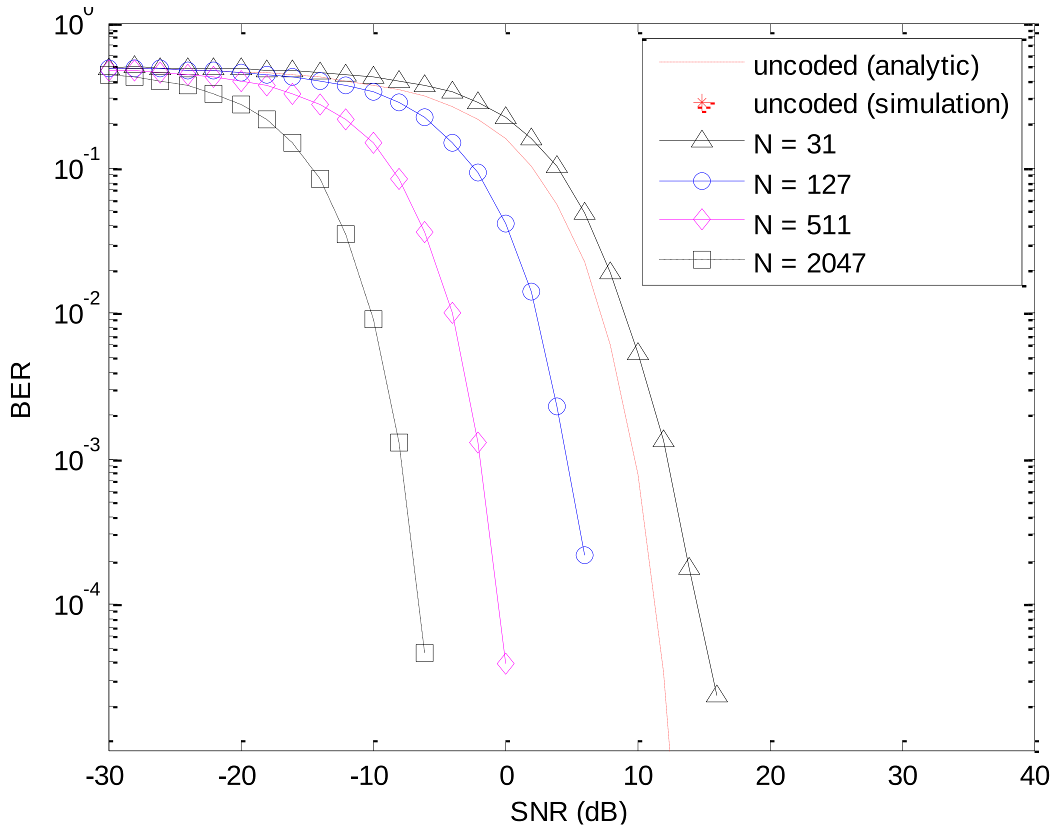

Fig. 4.11 Bit-error-rate for 33 users

4.3.4 Observations

The simulation results that have just been presented confirm that as the number of users increases, the system BER becomes worse. This is consistent with expectation because increasing the number of simultaneous users implies higher MAI. However, a closer look at the results reveals that the simulation results have some surprises, explained as follows.

As the number of users increase, system BER is expected to degrade faster for shorter Gold codes. A reason for this is that shorter codes have higher peak cross-correlation coefficients, Table 4.2. Also, by the virtue of their length, shorter codes approach full-load condition earlier than longer codes.

Table 4.2. Peak cross-correlation of Gold codes*

n	N	t(n)	t(n)/φ(0)
3	7	5	0.7143
4	15	9	0.6000
5	31	9	0.2903
6	63	17	0.2698
7	127	17	0.1339
8	255	33	0.1294
9	511	33	0.0646
10	1023	65	0.0635
11	2047	65	0.0318
12	4095	129	0.0315

*In the last column, peak cross-correlation function, *t(n)*, for Gold code sequence is normalised by peak autocorrelation function *φ(0)*.

Apart from this, for any given code length, BER is expected to increase rapidly as full-load is approached. For example, the BER for a 31-chip Gold code is expected to increase rapidly, to flatten out horizontally, and to exhibit an error floor as the number of users approaches 31. In connection with this, the slopes of the BER curves for different code lengths are expected to become increasingly different when the number of users increases. In contrast, the simulation results give no indication of this: even under full load, the 31-chip Gold code does not show any error floor or system saturation.

As a consequence of the difference in rate of degradation of BER with increasing number users, coding gains between BER curves of adjacent code lengths are expected to become increasingly unequal, as opposed to a single-user case, where the coding gain is constant. In contrast to this, the simulation results show no significant difference in coding gain between BERs of adjacent code lengths. The set of curves appear to maintain similar slopes at high SNR, with no visible difference in their coding gain.

The following are likely explanations for these surprising results:

- **Selected reference user.** Any set of Gold codes comprises *N*+2 members. Two of these represent the preferred pair of *m*-sequences from which the remaining members are derived. In every instance of the current investigation, one of the preferred pairs was used for the encoding (and the decoding) of the data stream of the reference user. Hence, the outcome of the simulation indicates that the preferred pair has low cross-correlation with the rest of the code set.

- **Peak correlation coefficient.** Peak correlation coefficient (Table 4.2) only gives the peak value that the correlation function of a Gold code could have, but not the frequency of occurrence or the distribution of the peaks. If the peak value happens to be few and sparsely distributed for a particular code set, its degrading effect on MAI may not be very significant.

- **Bipolarity of Gold codes.** Gold codes are bipolar codes, being +1 at one instant, and -1 at another. The same fact applies to the cross-correlation coefficients of the codes. As a result, there is the possibility of interference from one user cancelling out that of another. If a code set happens to be well-behaved, the mutual cancelling of the interference from offending users might turn out to enhance the system BER performance.

- **Synchronisation.** For this simulation, perfect synchronisation was assumed, and this might be a factor.

At first sight, the absence of error floor even when the system was heavily loaded raises a question on the validity of the simulation results. Regarding this, further investigation reveals that the outstanding performance is peculiar to the sets of Gold codes that have just been considered. Additional results show that some other sets of Gold codes lack such excellent performance. Fig. 4.12 and 4.13 shows examples of these. These codes exhibited error floor and system saturation when the system was significantly loaded The inferior performance of this set of codes forms our next point of consideration.

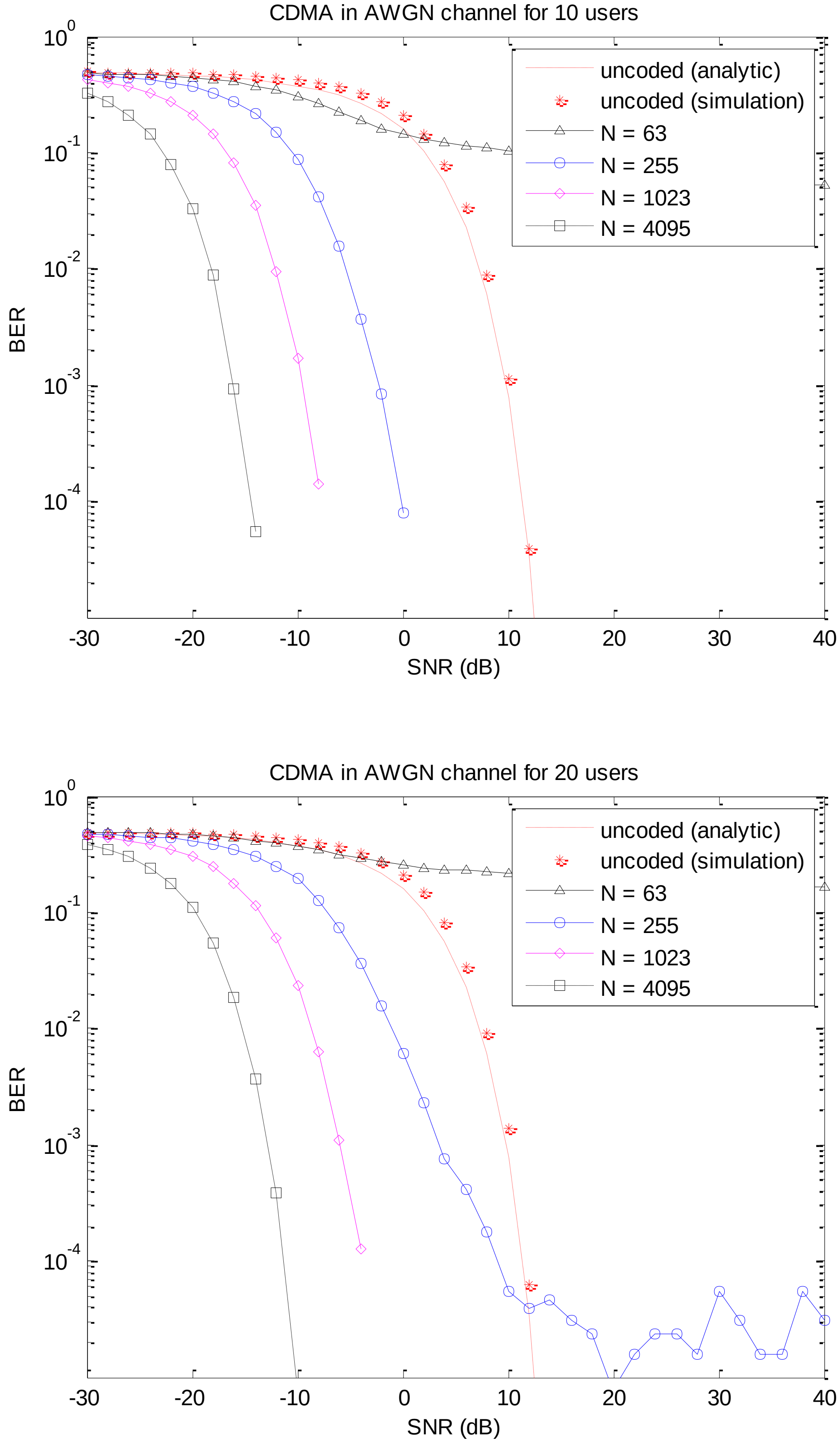

Fig. 4.12. Samples of results showing inferior performance of some other sets of Gold codes.

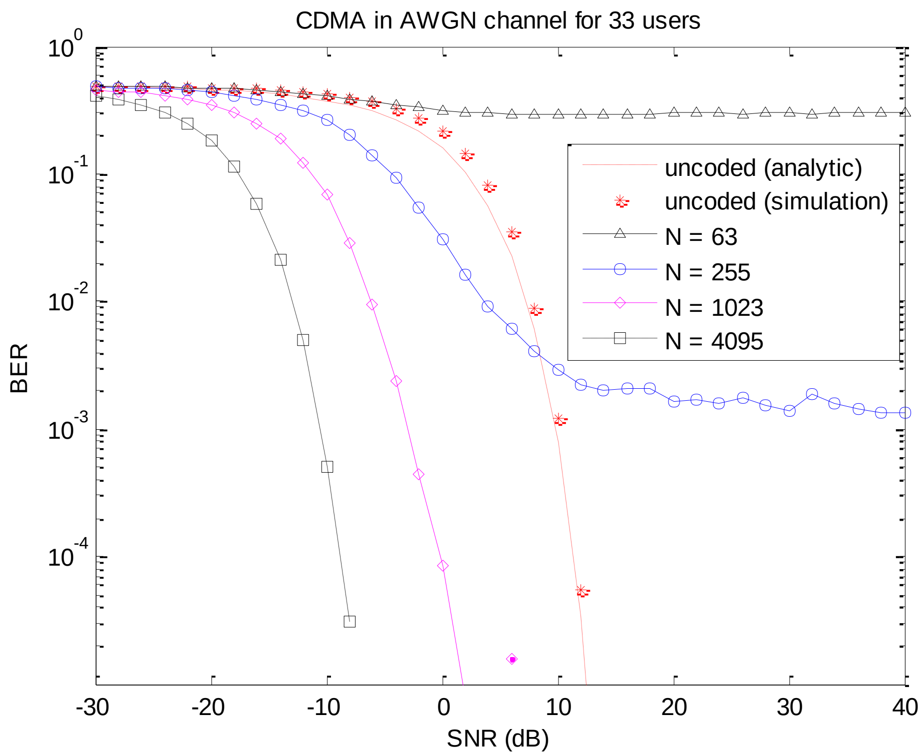

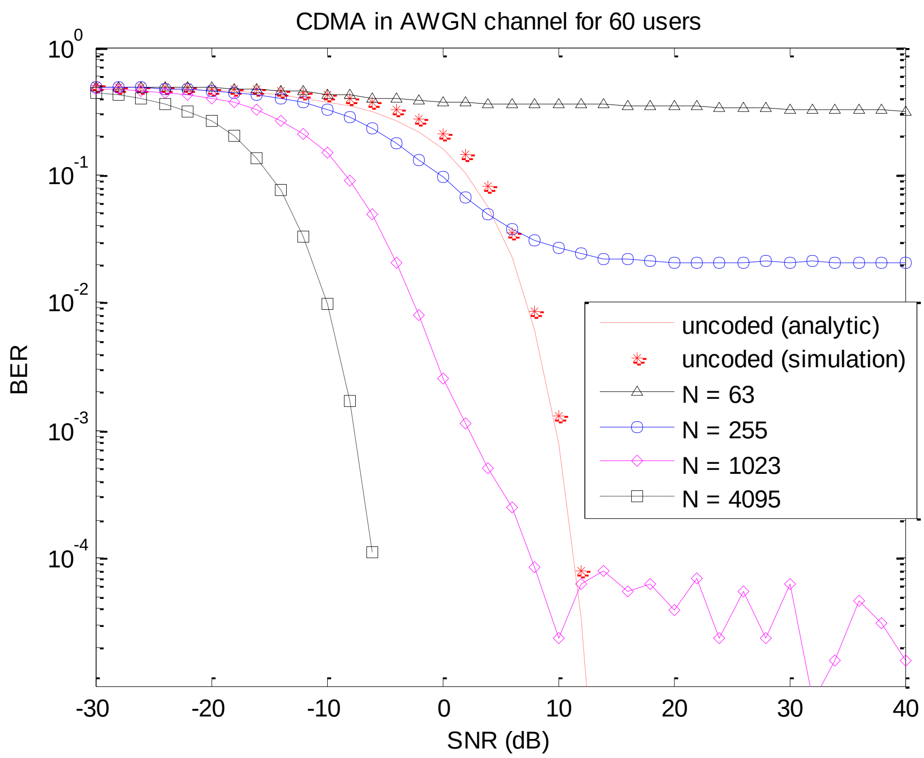

Fig. 4.13 Other samples of results showing inferior performance of some other sets of Gold codes.

4.4 Performance of even- versus odd-degree codes

Here we consider results of further investigation relating to the performance of the codes, for simulations involving both even- and odd-degree codes. We shall adopt a treatment similar to that used in section 4.3, beginning with e results for a single user.

4.4.1 Performance for a single user

Fig. 4.14 shows performance for a single user. Clearly as expected, this figure shows that longer Gold codes give better error-rate performance. The figure also shows that with reference to the uncoded data transmission, at a BER of 10^{-4}, the codes provide coding gain of about 14.8, 17.4, 20.6, 23.8, 26.9 and 29.9 dB when N = 31, 63, 127, 255, 511 and 1023 respectively. This gives a constant coding gain of about 3.03 dB-step between adjacent code lengths, which is in line with the spreading factors of the codes.

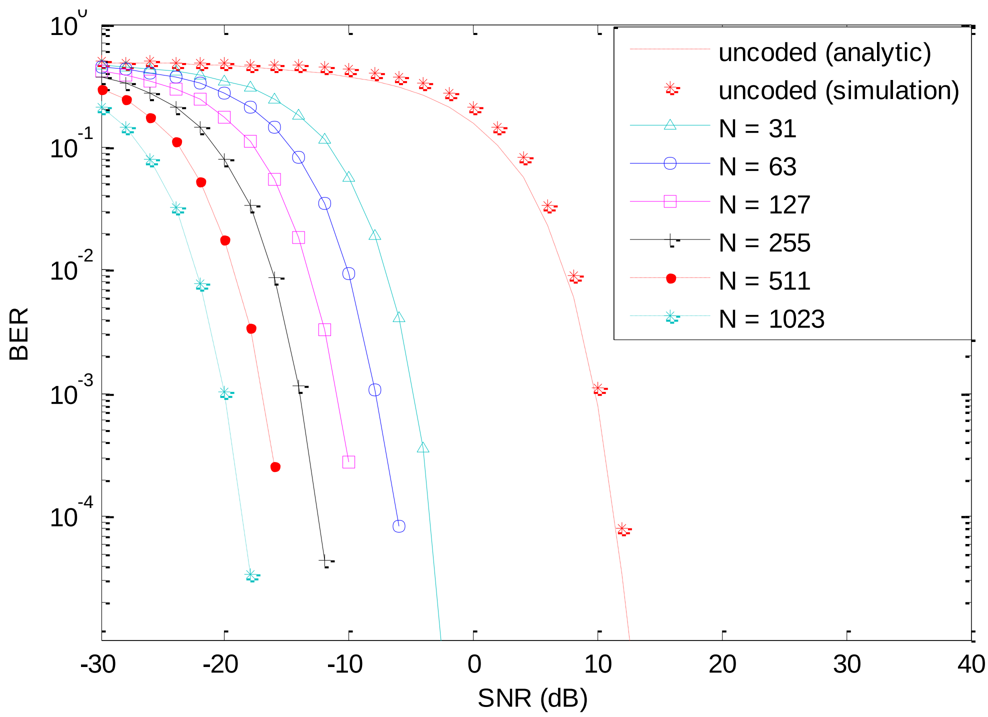

Fig. 4.14. Performance for a single user

4.4.2 Performance for a few multiple users

We shall now consider the results for multiple users. Figs. 4.15 to 4.18 show BER for two to five users respectively. A look at these figures shows that for all the code lengths, increase in number of users results in decibel loss. For example, the figures show that for N = 31, maintaining a BER of 10^{-4} requires an SNR of -0.25, 1.60, 2.95 and 3.94 dB for two, three, four and five users respectively. With reference to a single user (Fig. 4.14), this is equivalent to a decibel loss of 3.24, 5.09, 6.44 and 7.43 dB respectively. This performance loss is expected, in connection with elevated multiple-access interference (MAI) resulting from increase in number of interferers.

In addition to the general trend, a close look at the figures show that the rate of performance degradation is higher for the code length N = 63. This is noticeable on Figs. 4.16 to 4.18 for three to five users respectively, which shows the curve for $N = 63$ suffering higher decibel losses than those of other code lengths. Its graph for four users is seen to cross over that of N = 31, and worse still for five users. This behaviour was initially not expected. The significance of this seeming artefact will become obvious as we consider the system performance for higher number of users.

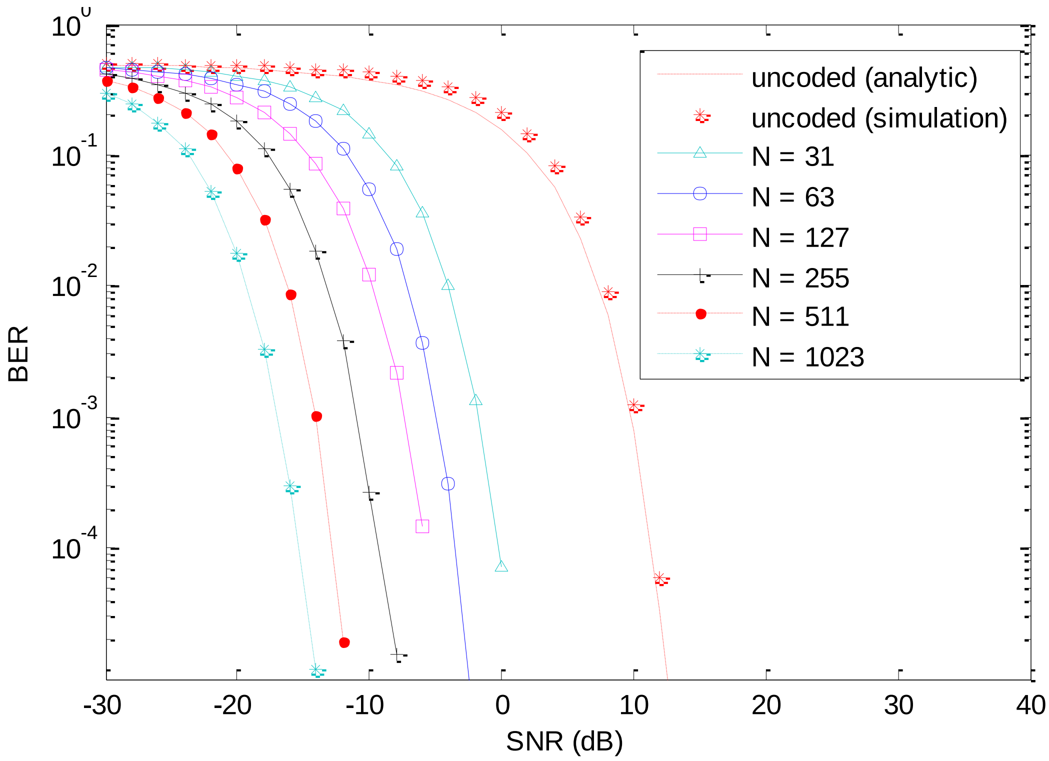

Fig. 4.15. Bit-error-rate for two users

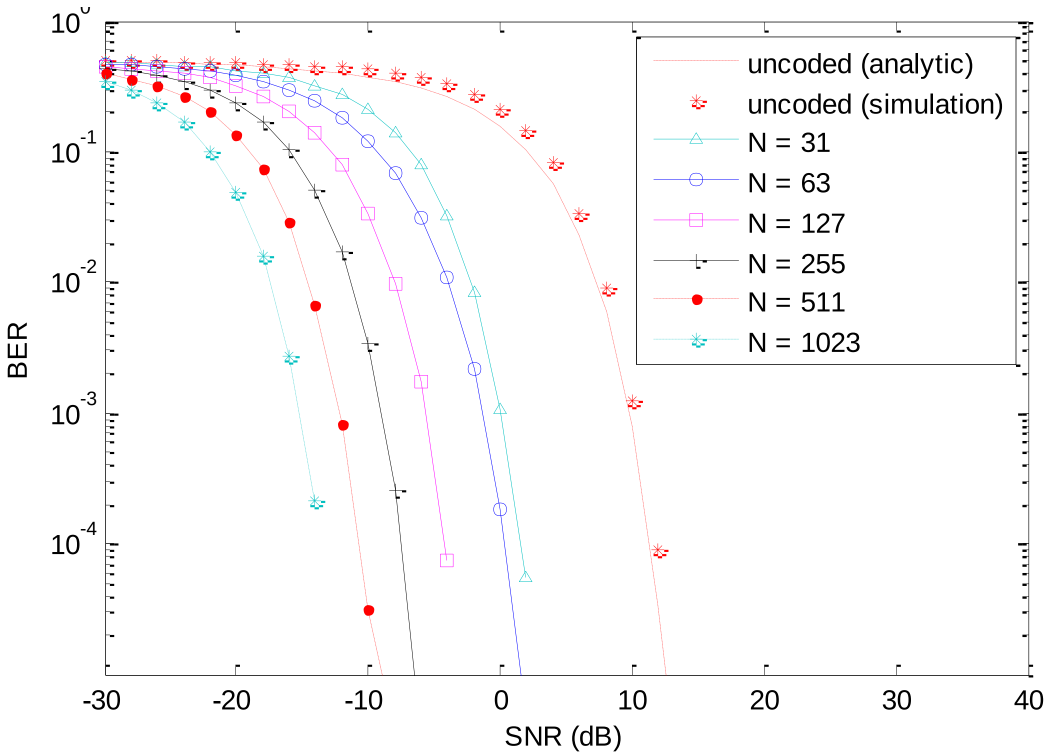

Fig. 4.16. Bit-error-rate for three users

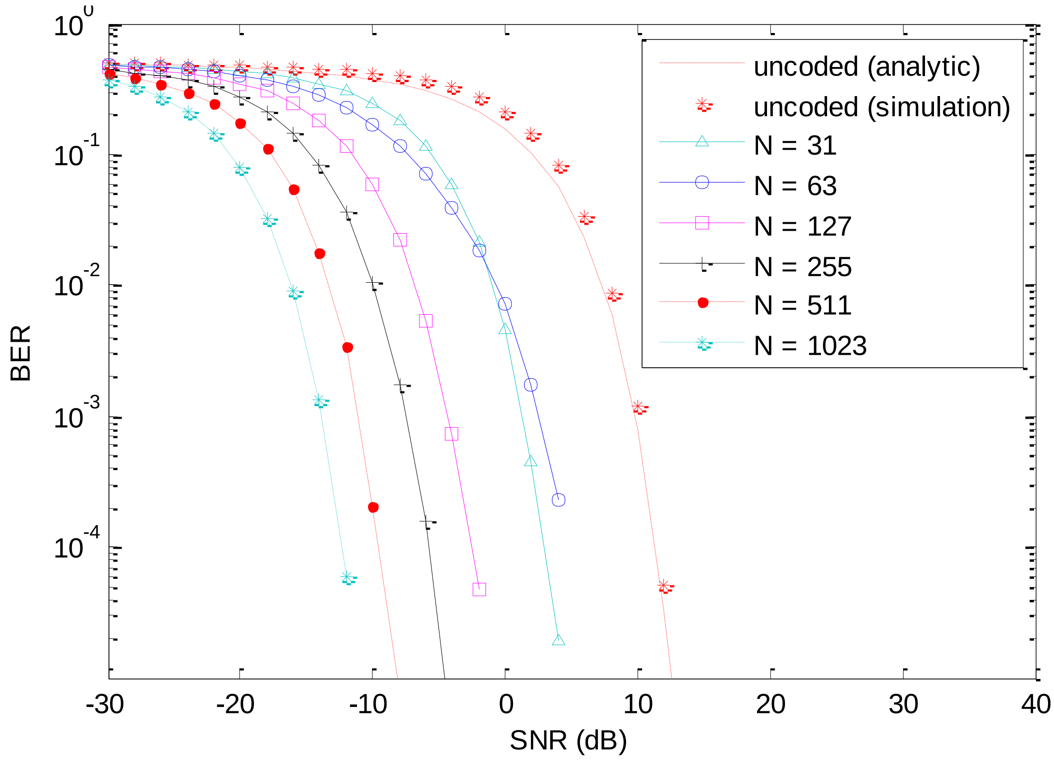

Fig. 4.17. Bit-error-rate for four users

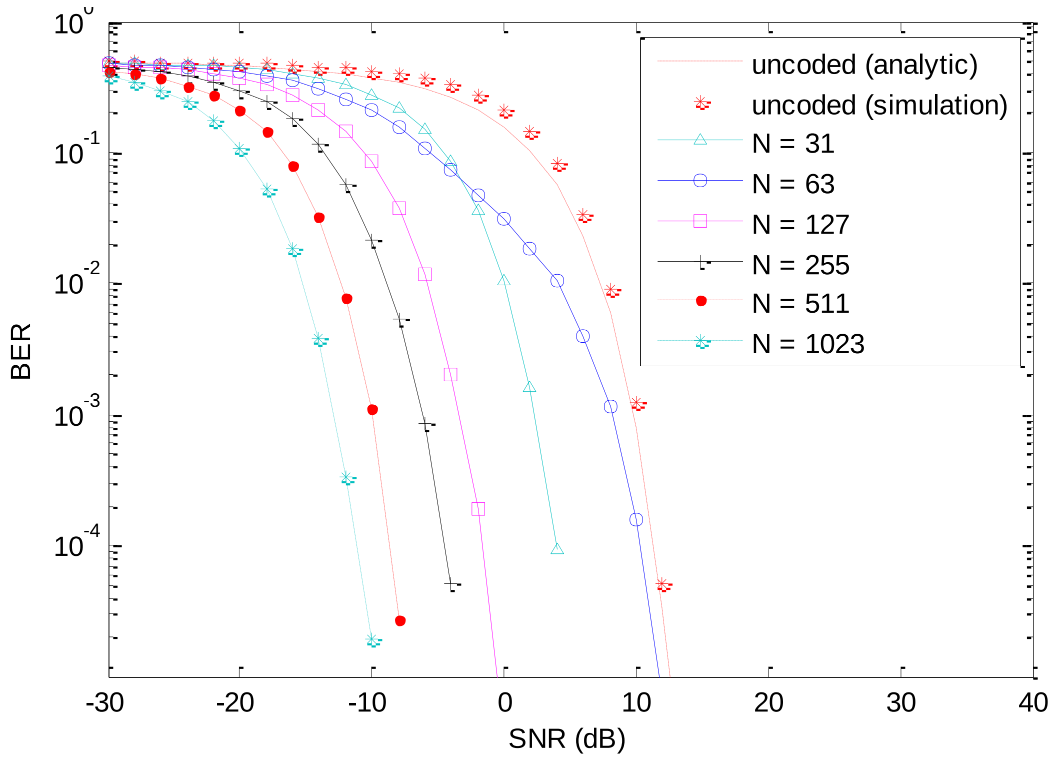

Fig. 4.18 Bit-error-rate for five users

We shall now consider simulation results for higher numbers of users. Figs. 4.19 to 4.22 show the BER for six to nine users. As with the previous results, a look at these figures shows degradation in performance when the number of users increases: the BER curves for all the code lengths shifts to the right, implying decibel loss, which in turn indicates worsening BER.

However, another look at Figs. 4.19 to 4.22 shows that as the number of users increases, the performance for N = 63 degrade quite rapidly if compared with other code lengths. The graph (for N = 63) is seen to continue its crossing-over behaviour, culminating in the emergence of an error floor. The results show that the 63-chip code has a worse performance than its shorter 31-chip counterpart, which is not expected. More will be said about this later.

Another look at Figs. 4.19 to 4.22 shows that the performance for N = 255 is following the trend observed for N = 63. This will become more obvious as we consider the results for higher number of users.

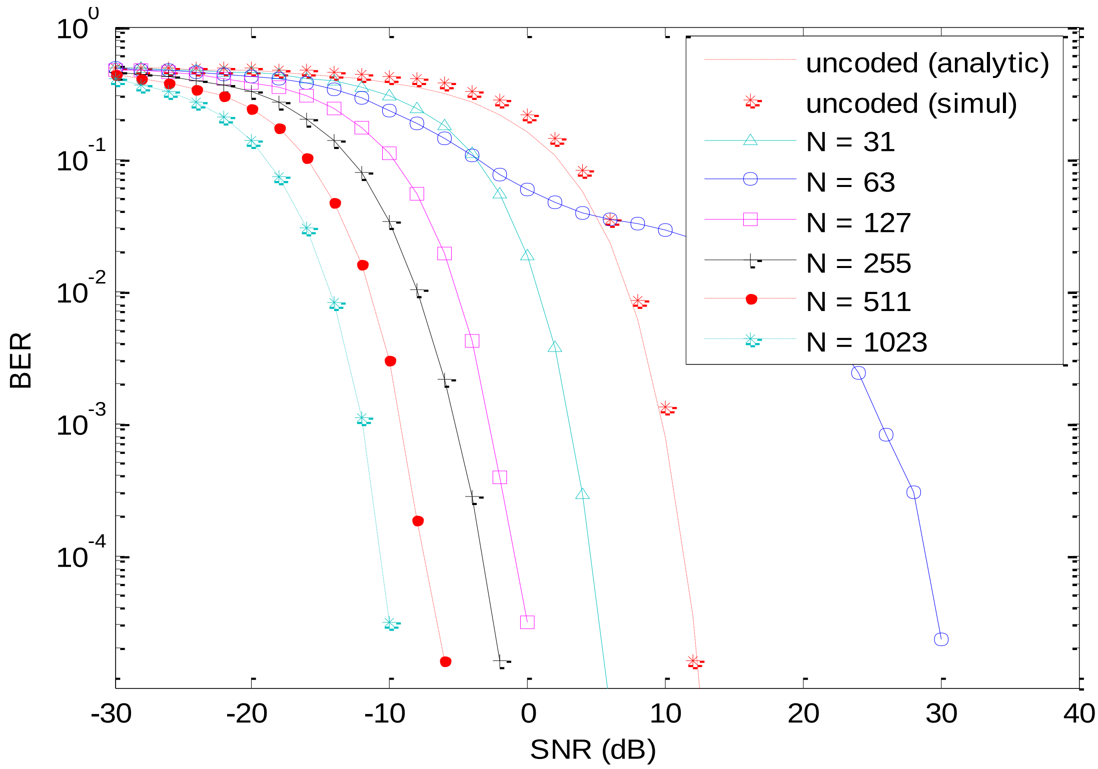

Fig. 4.19 Bit-error-rate for six users

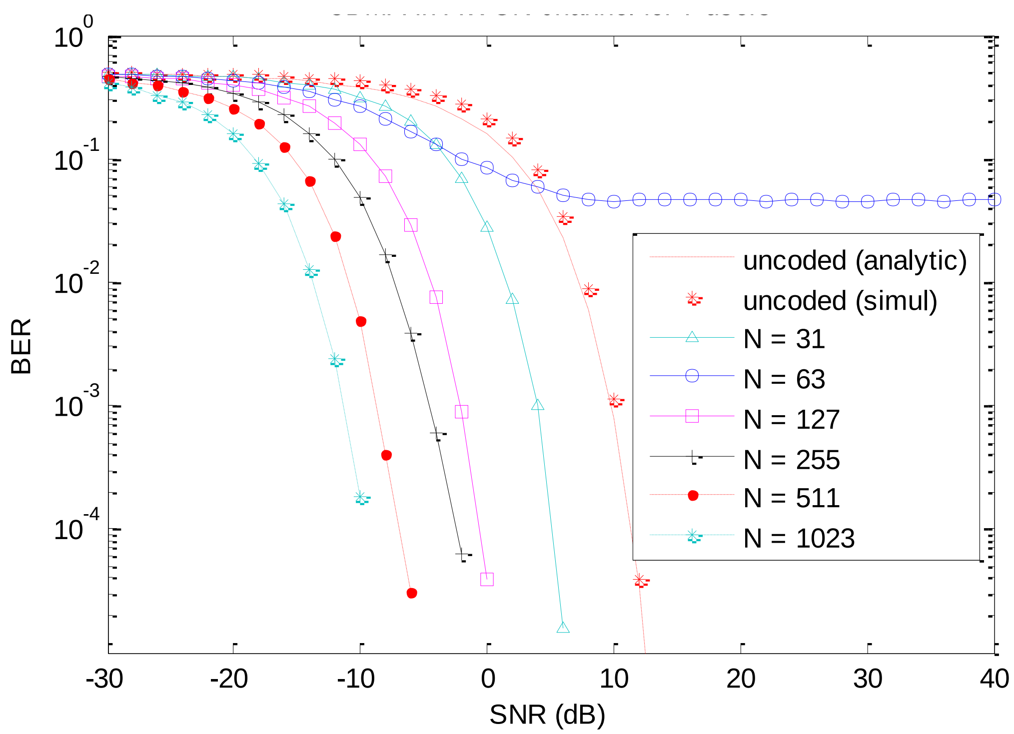

Fig. 4.20 Bit-error-rate for seven users

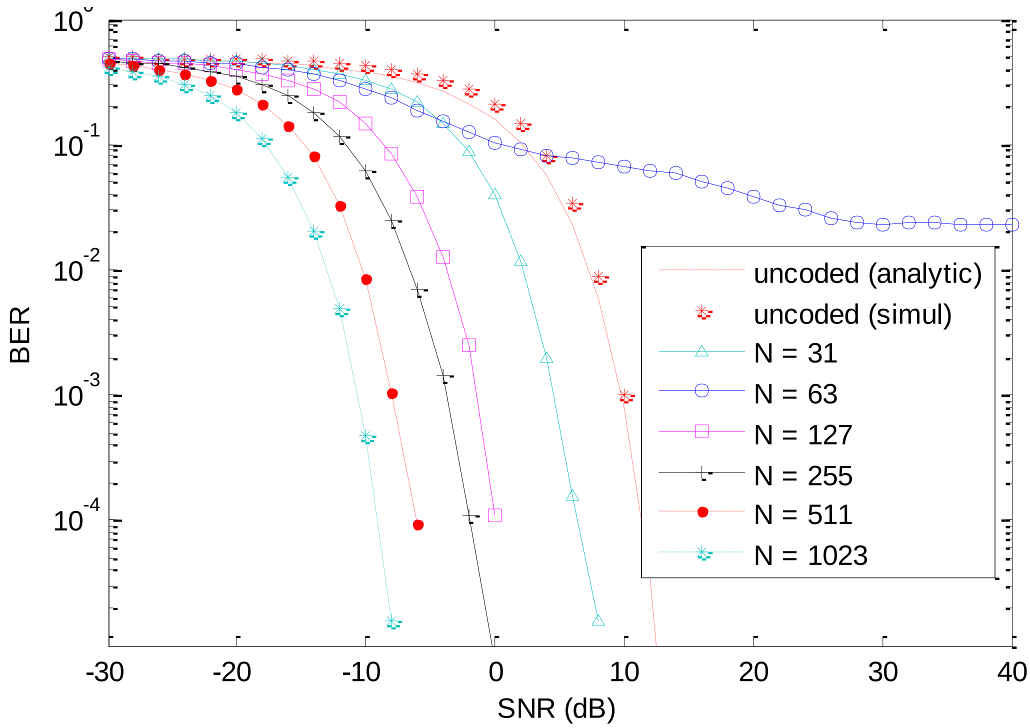

Fig. 4.21 Bit-error-rate for eight users

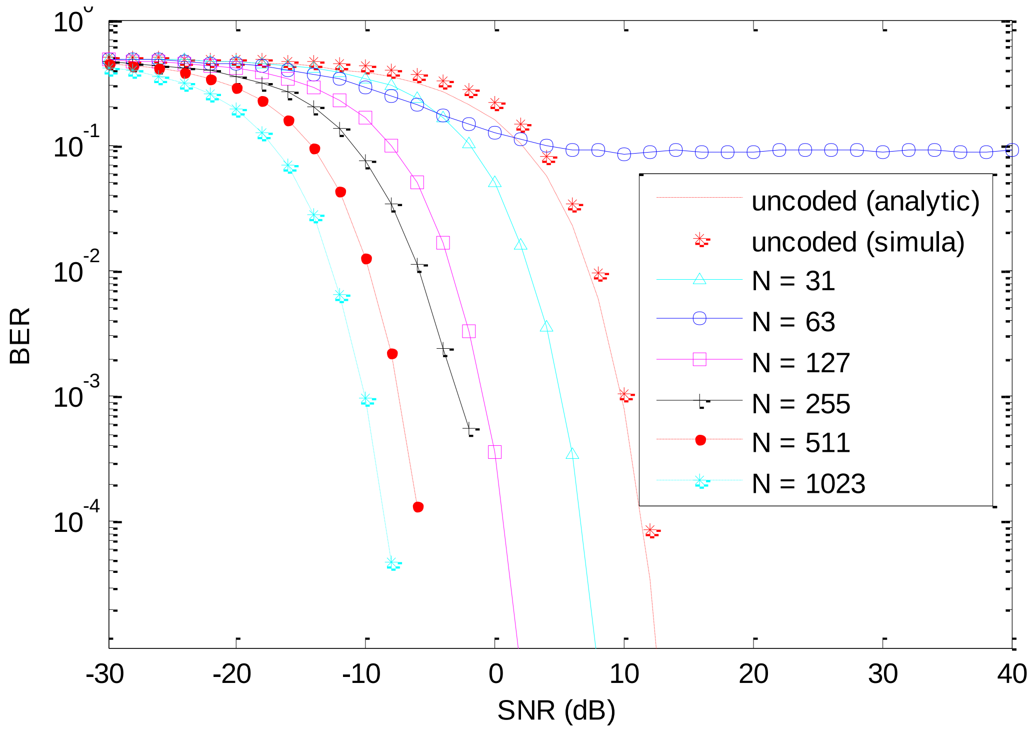

Fig. 4.22 Bit-error-rate for nine users

4.4.3 Performance for higher number of users

We shall now consider simulation results for higher numbers of users. Figs. 4.23 to 4.28 show the BER for ten to thirty users, in steps of five. As with the previous results, these figures show that as the number of users increase, all the codes suffer loss in performance. More importantly however is the BER for N = 63, which can be seen to degrade at an alarming rate, such that for 30 users, its performance has basically flattened out to a BER of about 0.5. The BER for N = 255 can also be seen to follow a similar trend. In addition, a close look at the figures indicates that BER for N = 1023 is following the same behaviour. Therefore we can expect that with further increase in number of users, the BER for N = 255 and N = 1023 will develop error floors, and ultimately system saturation, of the kind that we now see for N = 63.

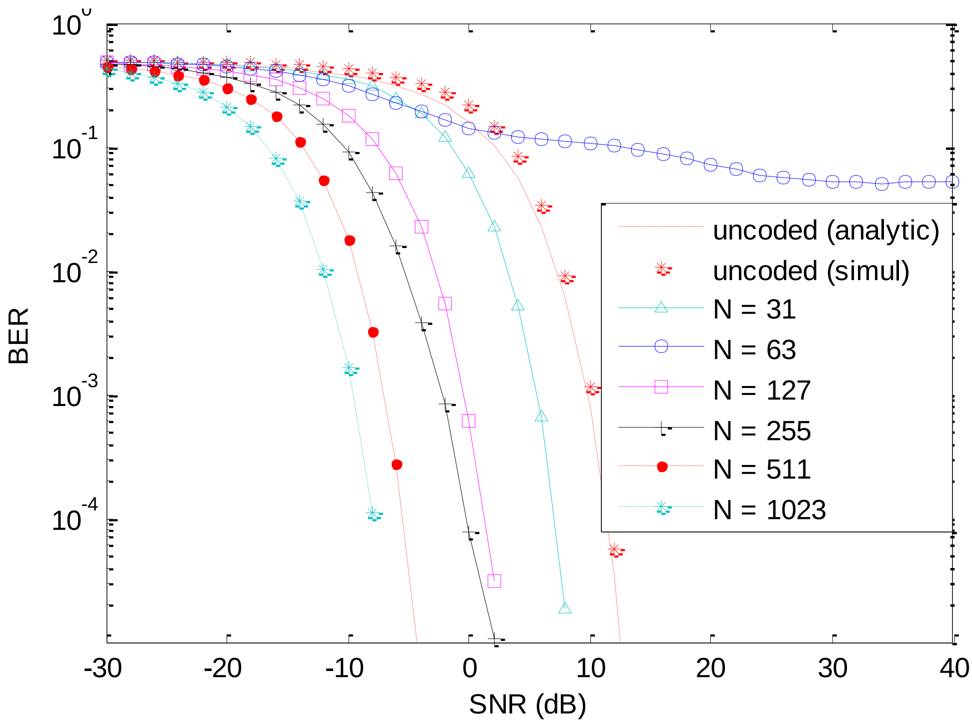

Fig. 4.23. Bit-error rate for 10 users

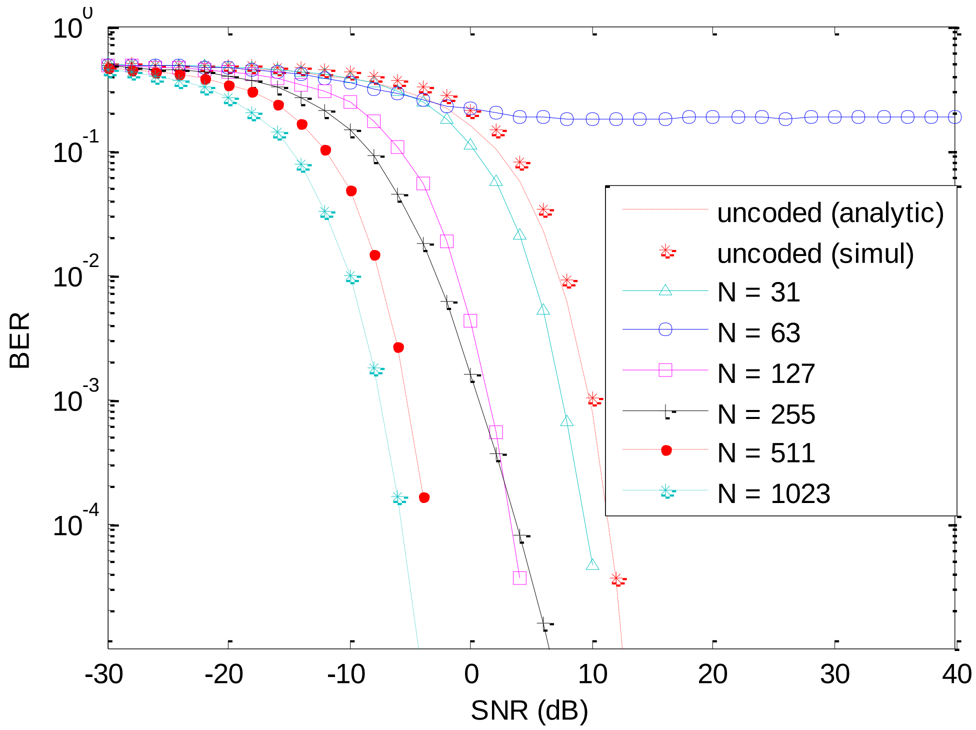

Fig. 4.24. Bit-error rate for 15 users

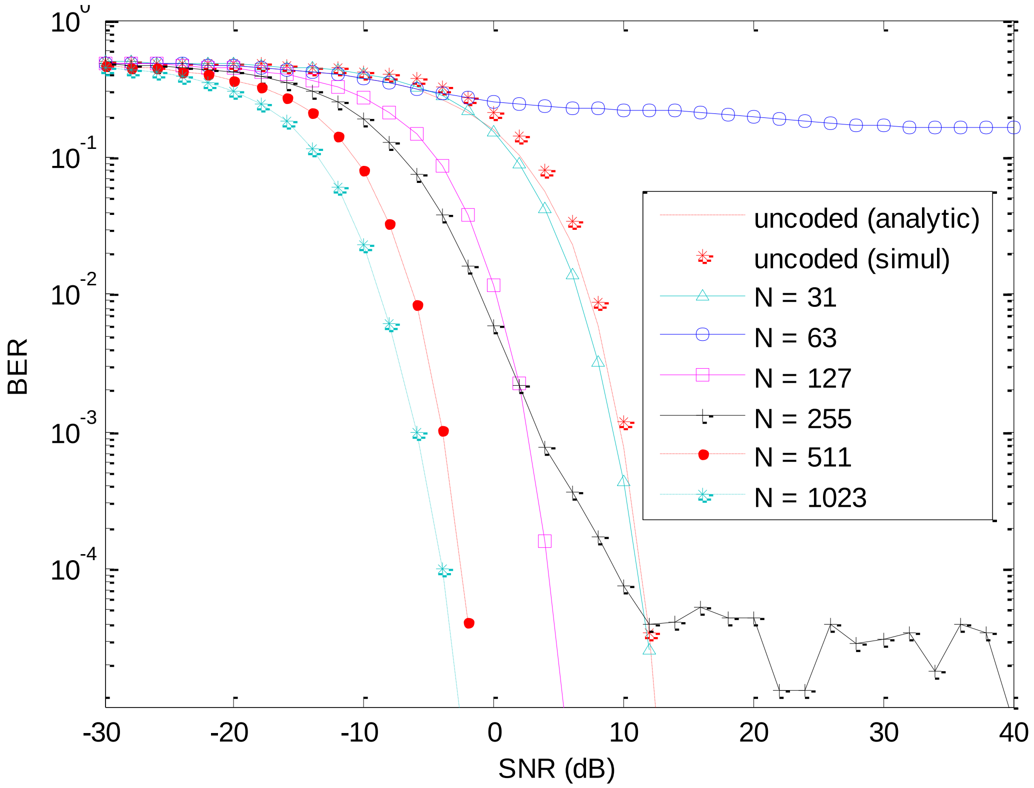

Fig. 4.25. Bit-error rate for 20 users

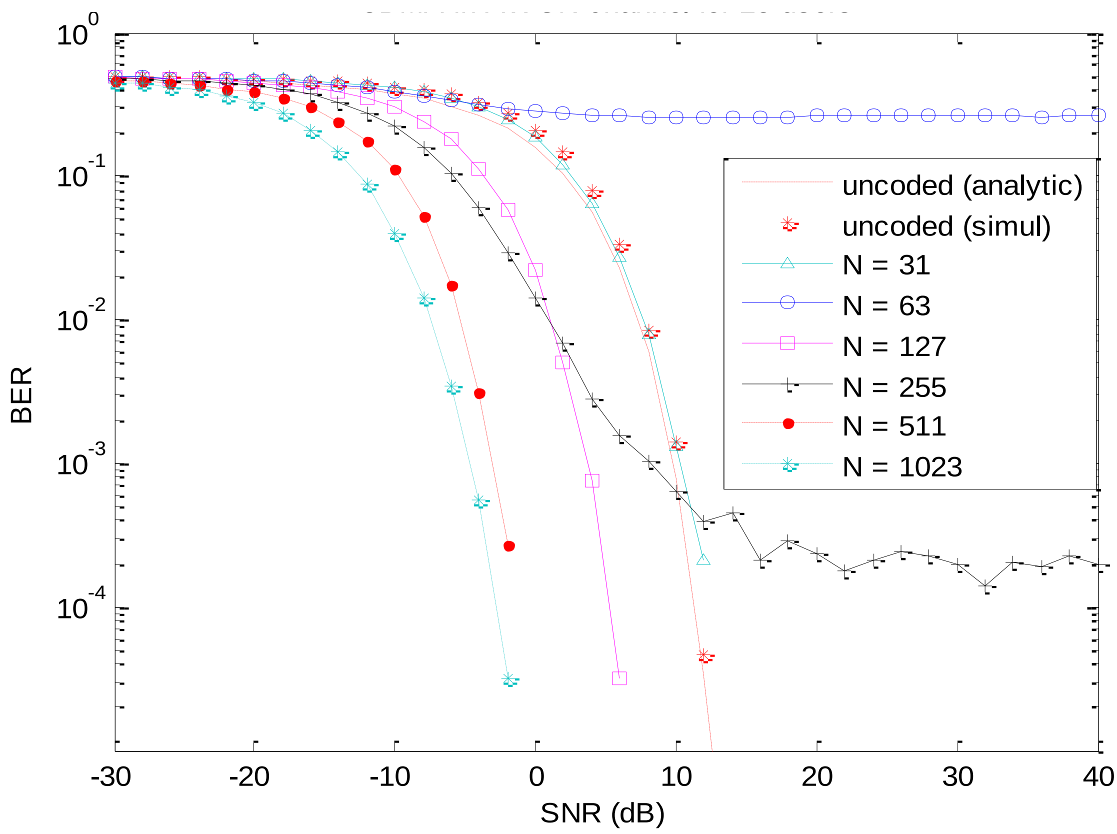

Fig. 4.26. Bit-error rate for 25 users

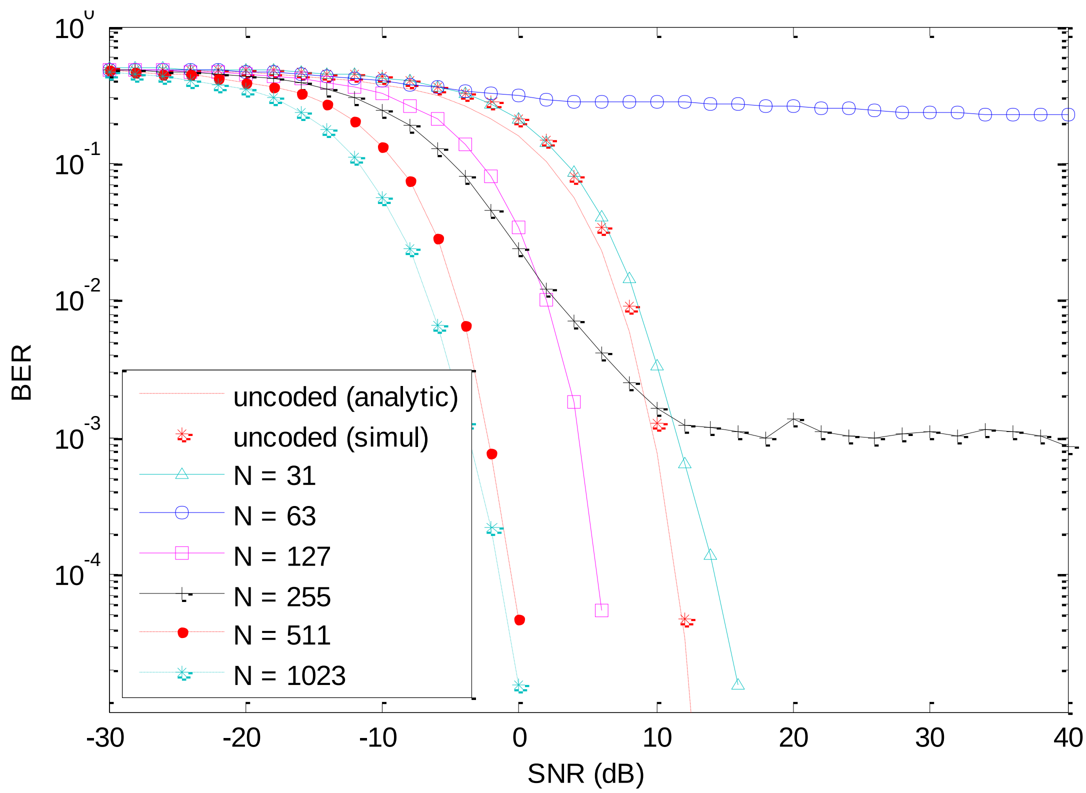

Fig. 4.27. Bit-error rate for 30 users

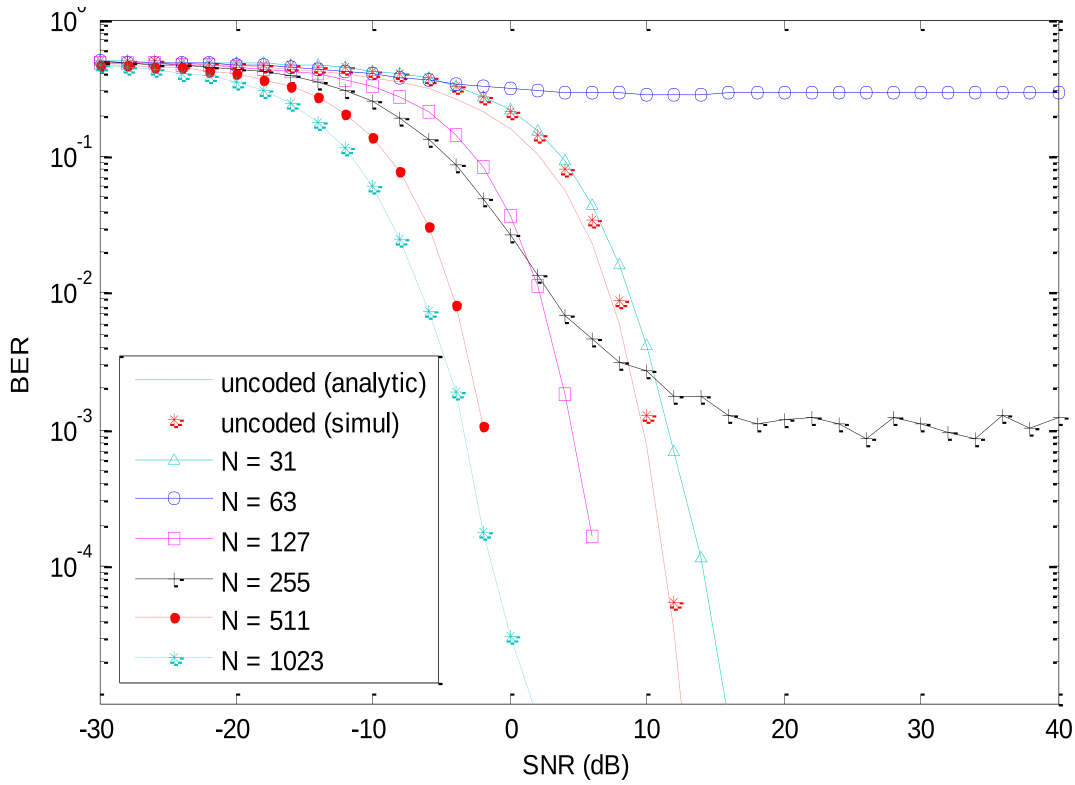

Fig. 4.28 Bit-error rate for 31 users.

4.4.4 Deductions

The simulation results that have just been presented confirm that, generally, the system BER becomes worse when the number of simultaneous users increases, which is expected. However, the sharp difference in the rate of degradation for different code lengths demands some consideration. Being from the same family, all the codes would normally be expected to exhibit similar behaviour. In contrast, the simulation results showed that this is not the case. An attempt is hereby made as follows to explain this situation.

Compared to other code lengths, the simulation results show that the BER for $N = 63$ degrade more rapidly when the number of users increases. This resulted in early emergence of an error floor for the code length, ultimately resulting in premature system saturation. The results also give good indication that $N = 255$ and $N = 1023$ have similar behaviour. Now, these three sets of codes are even-degree codes (n even). This implies that this behaviour is peculiar to even-degree Gold codes.

In contrast to the above, the simulation results show that BER for N = 31, 127 and 511 exhibited relatively marginal degradation in performance when the system was loaded. The codes suffered less dB-loss, and maintained their steep, high-SNR slopes regardless of elevated number of users. Now, these set of codes are odd-degree codes (n odd), meaning that the positive characteristics are peculiar to odd-degree Gold codes. Hence, we conclude that in a multi-user environment, odd-degree Gold codes have better BER performance than even-degree Gold codes. An implication of this is that the odd-degree Gold codes have better cross-correlation properties than their even-degree counterparts.

There is a further observation on the present discourse. Ordinarily for a given family of spreading codes, a longer code is expected to give better performance than a shorter code. In contrast, the simulation results show that when the number of users is four or more, 63-chip Gold codes give progressively worse performance than 31-chip Gold codes. The same pattern is noticeable among the remaining even- and odd-degree codes. Thus we conclude that a longer code will not necessarily give a better performance.

4.5 Loading characteristics of even-degree Gold codes

The on-going examination of the performance of the Gold codes was further investigated by considering the loading characteristics of a complete set of codes for each degree or code length. The code set for each degree was subjected to loading, from light to heavy loading. The outcome of the investigation is presented as follows, starting with even-degree codes, for n = 6, 8 and 10, corresponding to code length N = 63, 255 and 1023 respectively.

4.5.1 Performance of degree-6 Gold codes

Fig. 4.29 shows the simulation results for degree-6 Gold codes. This figure shows that as the number of users increases, the system BER becomes worse. Furthermore, when full-load is approached, the rate of the performance degradation becomes rapid, resulting in emergence of an error floor. This behaviour is expected, in connection with increase in multiple-access interference (MAI) when the number of users increases. As at 10 users (about one-sixth full-load), the performance can be seen to flatten out to a BER of about 10^{-1}.

4.5.2 Performance of degree-8 Gold codes

We shall now consider simulation results for degree-8 Gold codes, which corresponds to $N = 255$. Fig. 4.30 shows the results. As with the previous figure, this figure shows that BER becomes worse when the number of users increases, ultimately resulting in emergence of an error floor. However, comparing Fig. 4.29 with Fig. 4.30 shows that the 255-chip code is able to support more users. This is in agreement with fundamental theory, the 255-chip code being a longer code. Whereas only 10 users cause the BER of a 63-chip code to flatten out to a BER of 10^{-1}, it takes about 100 users (two-fifth full-load) to make the performance a 255-chip code to degrade to the same BER.

4.5.3 Performance of degree-10 Gold codes

We shall now consider simulation results for degree-10 Gold codes, which corresponds to $N = 1023$. Fig. 4.31 shows the results for the codes. A look at this figure shows a behaviour similar to that observed in the other even-degree codes that have just been considered. There is degradation in BER, resulting in emergence of an error floor when number of users is elevated. For the 1023-chip codes however, the results show that it takes about 500 users (about half full-load) for the BER to degrade to about 10^{-1}.

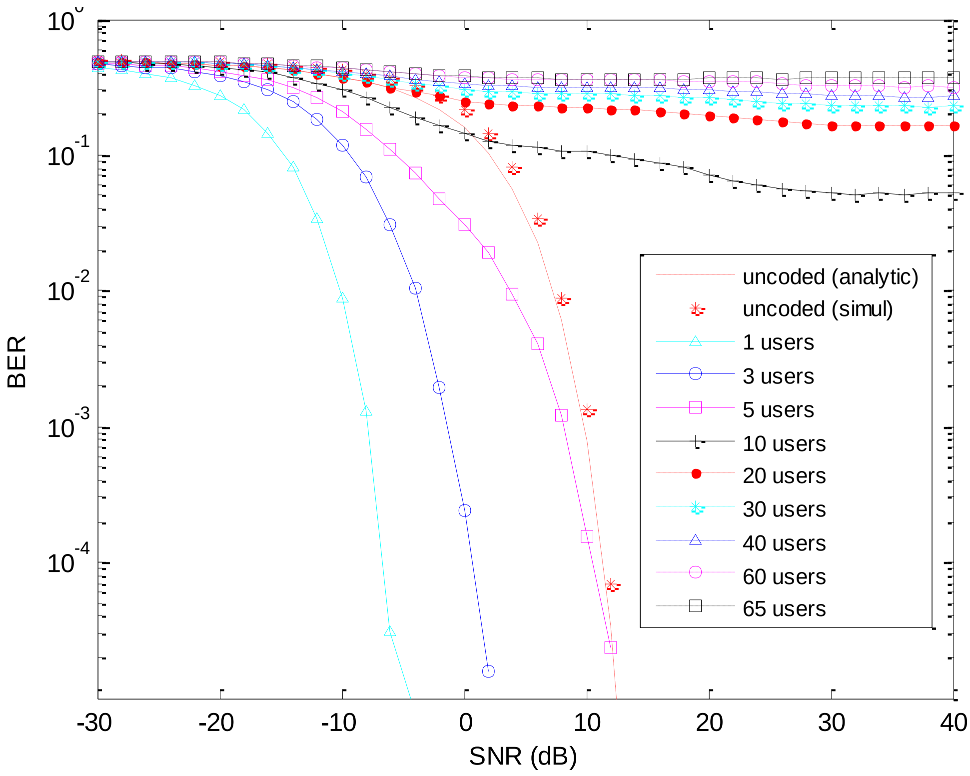

Fig. 4.29. Performance of degree-6 Gold codes

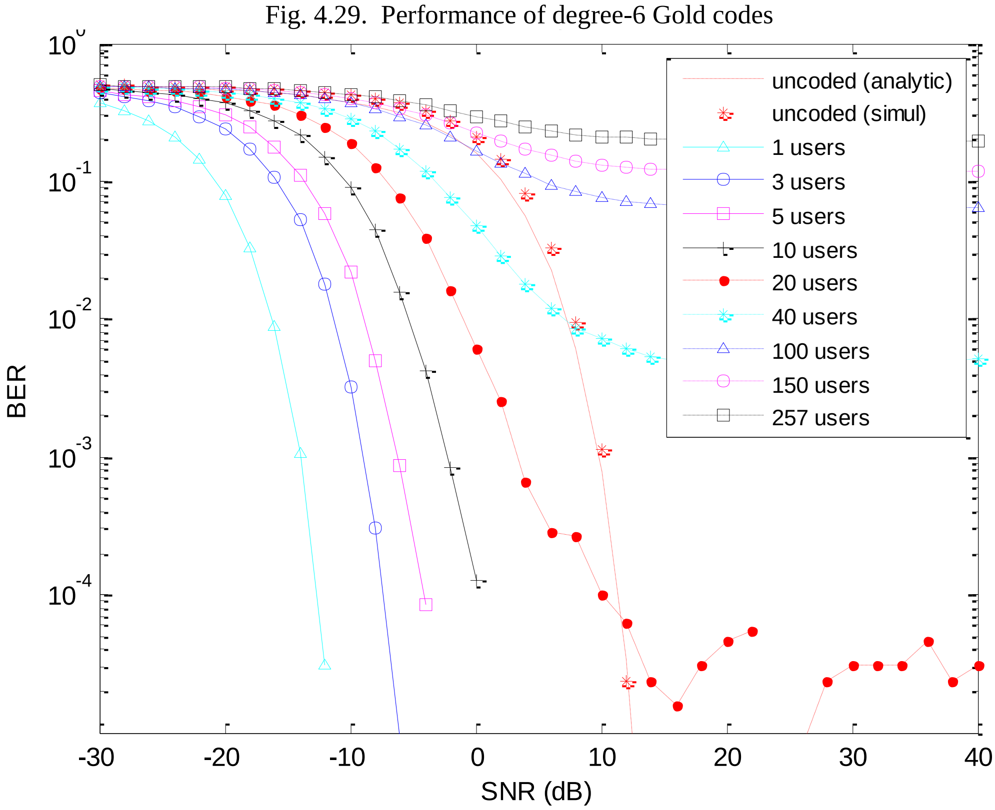

Fig. 4.30 Performance of degree-8 Gold codes

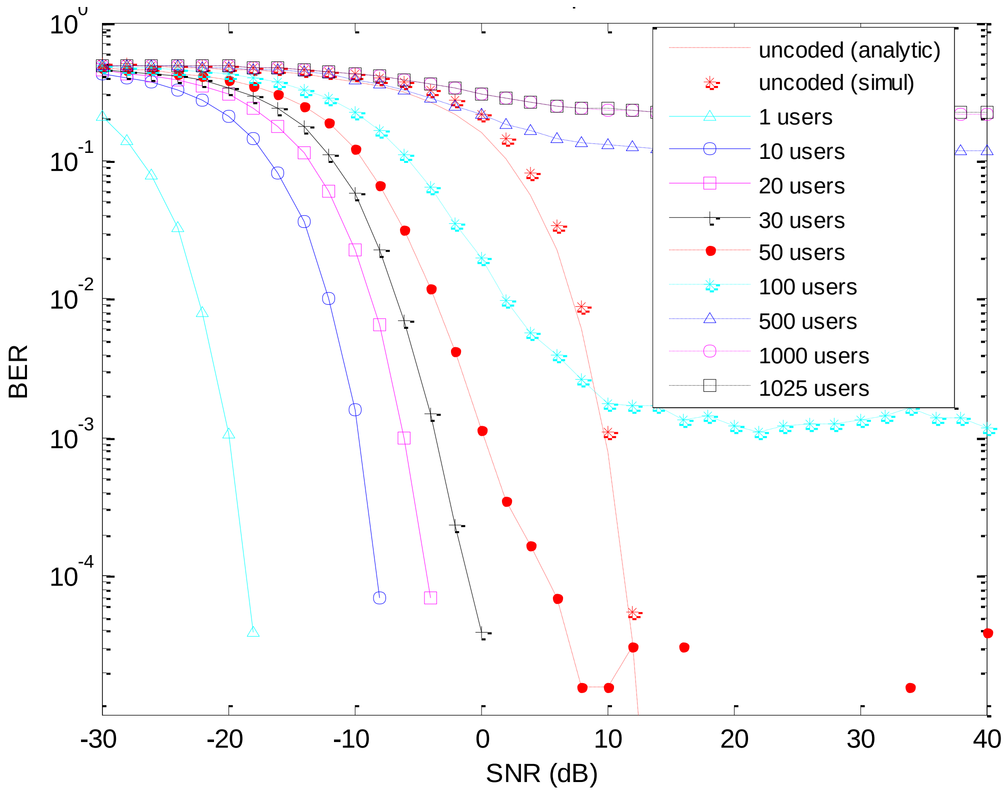

Fig. 4.31 Performance of degree-10 Gold codes

4.6 Loading characteristics of odd-degree Gold codes

Having examined loading performance of even-degree codes, we shall now consider simulation results for odd-degree Gold codes, for $n = 5$, 7 and 9, corresponding to code length $N = 31$, 127 and 511 respectively.

4.6.1 Performance of degree-5 Gold codes

Here we consider simulation results for degree-5 Gold codes, Fig. 4.32. A look at this figure shows that the performance of this code set is strikingly different from the ones that have just been considered. The differences are enumerated as follows:

i. Performance degradation is not rapid but gradual for this current set of codes.
ii. When the system is heavily loaded, the codes maintain their high-SNR steep slope.
iii. There is no serious system saturation when the system is heavily loaded, even up to full system load.
iv. For this code set, the BER performance curves exhibit no error floor.

v. When fully loaded, the code performance is still as good as that of an uncoded, single-user system.

The performance of this set of codes is surprisingly better than expected. We shall now consider simulation results for other sets of odd-degree codes.

4.6.2 Performance of degree-7 and degree-9 Gold codes

Fig. 4.33 shows simulation results for degree-7 Gold codes. By comparing this figure with the previous one, it is obvious that the two set of codes have similar performance characteristics, enumerated in the previous subsection. The same behaviour can be seen in Fig. 4.34 for degree-9 Gold codes. These indicate that the desirable behaviour is peculiar to the odd-degree Gold codes.

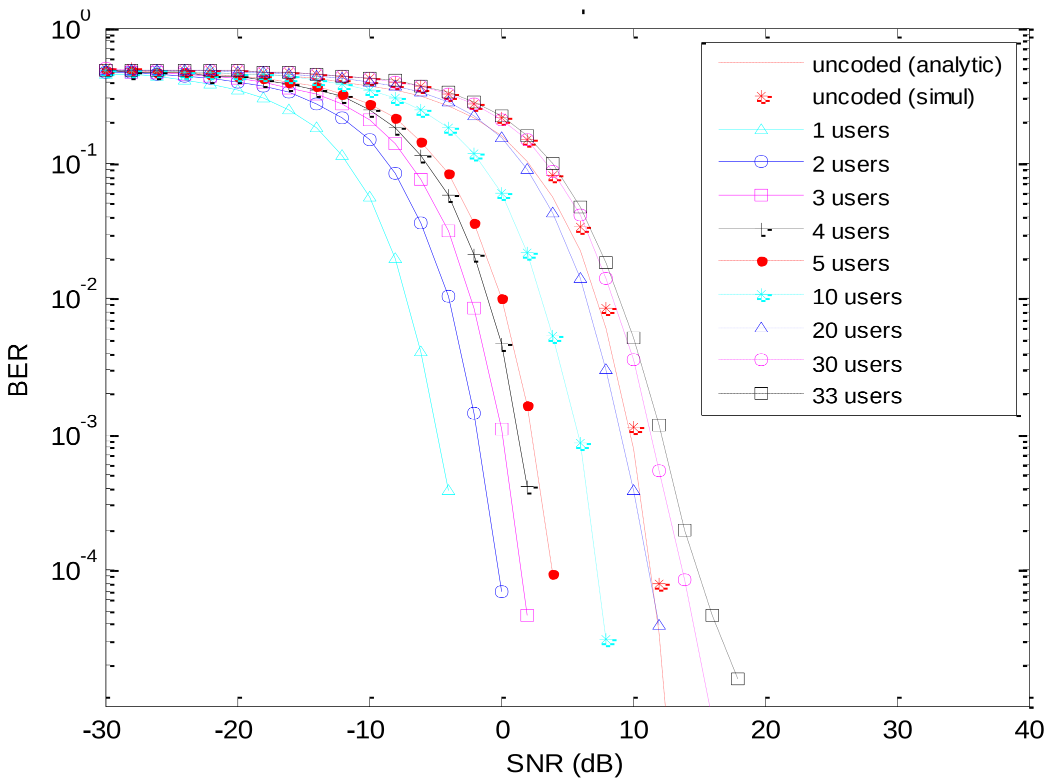

Fig. 4.32 Performance of degree-5 Gold codes

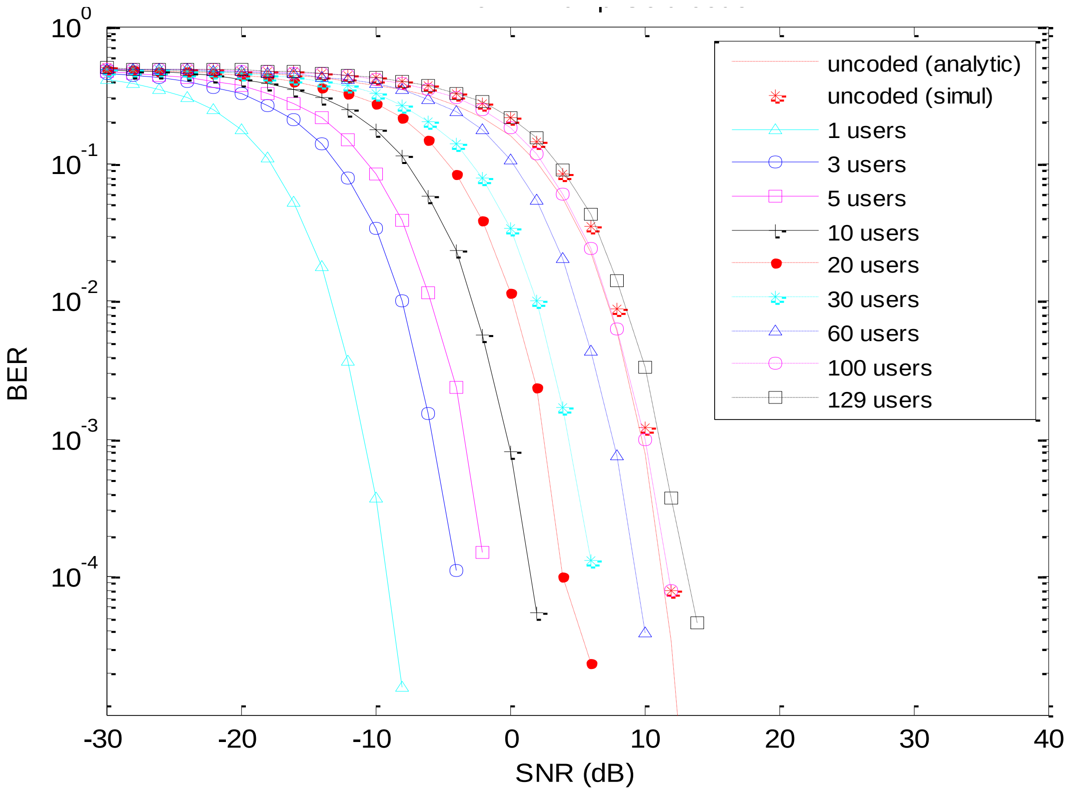

Fig. 4.33 Performance of degree-7 Gold codes

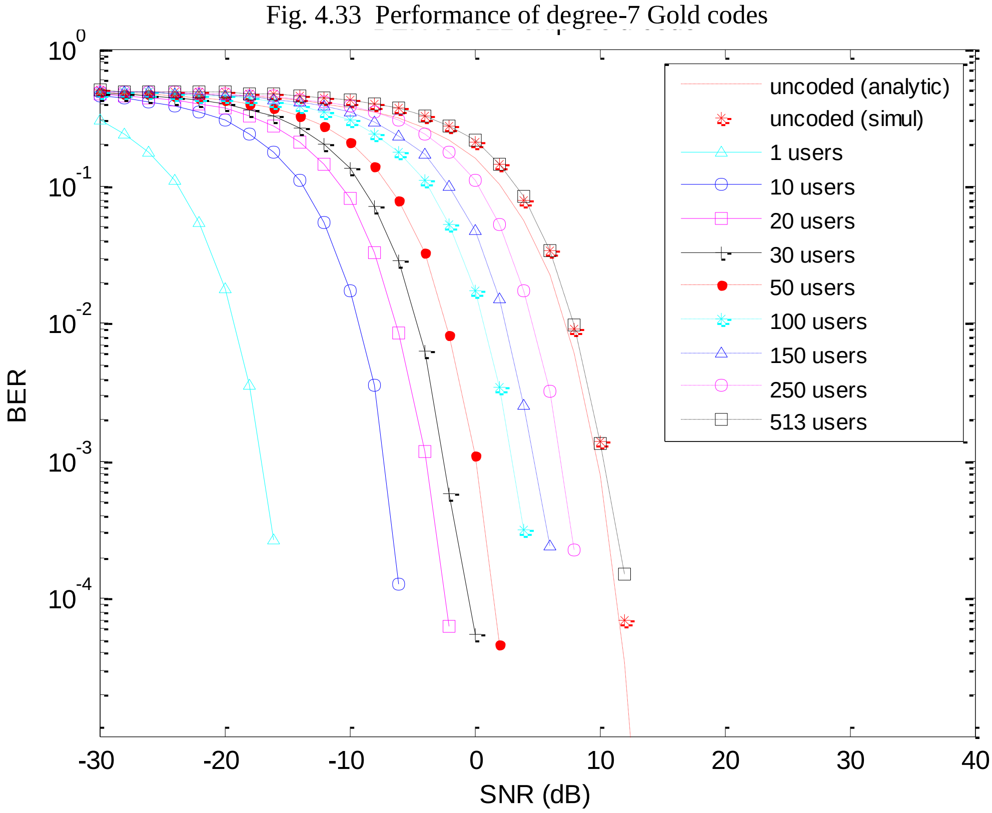

Fig. 4.34 Performance of degree-9 Gold codes

4.7 Chapter summary

This chapter investigated the performance of even- and odd-degree Gold codes in a multi-user direct-sequence spread-spectrum system. The investigation entailed software simulations for different sets of codes, ranging from 31-chip to 2047-chip Gold codes, from light to heavy system loading, involving up to about a thousand simultaneous users. Results of the investigation showed that odd-degree Gold codes have better multiple-access performance than their even-degree counterparts. Whereas the latter exhibited error floor and system saturation when the system was loaded, no such performance degradation was noticeable in the former. The results suggest that odd-degree Gold codes are better suited for multiple-access applications than their even-degree counterparts.

Chapter 5

Performance of a multicarrier CDMA system

5.0 Introduction

The previous chapter entails the performance of Gold codes using a direct sequence CDMA system. The current chapter extends the treatment by introducing multi-carrier transmission, to give a multicarrier CDMA system.

The significance of wireless communication in today's technology cannot be over-emphasised. It is one of the fastest-growing segments of modern technology. However, many challenges remain in the design of wireless systems. One of this is performance degradation due to channel fading. Diversity is known to be one of the best techniques for mitigating the effects of fading, and is the main idea behind performance advantage provided by a multicarrier CDMA system, which happens to be a focus of this chapter. This chapter models the performance of a DS-CDMA system and a multicarrier CDMA system in Rayleigh fading channels.

The rest of this chapter is organised as follows. Basic concepts on channel fading are presented in Section 5.1, followed by fading models in Section 5.2. Section 5.3 and 5.4 give an overview of diversity techniques and multicarrier CDMA respectively. Section 5.5 presents simulation results on the system performance in a Rayleigh fading channel. This chapter concludes with a summary in Section 5.6.

5.1 Channel fading

In wireless communications, **fading** [146-148] refers to variation or loss in received signal strength resulting from reflection or obstructions of the transmitted signal. Fading may vary with time, geographical position or radio frequency. It may either be due to multi-path propagation or shadowing from obstacles affecting the wave propagation. Multi-path propagation originates from the presence of reflectors in the environment, creating multiple signal paths. As a result, the receiver sees the superposition of multiple copies of the transmitted signal coming from different paths. Each signal copy experience differences in attenuation, phase shift and path delay while travelling from source to receiver. This can cause interference, which is either constructive or destructive, amplifying or attenuating the signal power seen at the receiver. Strong destructive interference is often referred to as a **deep fade** and may result in temporary failure of communication due to a severe drop in signal strength.

Depending on the rate of change of received signal strength, fading can either be *slow-fading* or *fast-fading*, and is measured relative to channel coherence time. Coherence time is a measure of the minimum time required for the magnitude change of the channel to become uncorrelated from its previous value. **Slow-fading** arises when the coherence time of the channel is large relative to the delay constraint of the channel. It describes a situation where the channel impulse response varies at a rate much slower that the rate of change of the transmitted signal. In this case, the time duration of a transmitted symbol T_s is small compared with the channel coherent time T_c. Such a channel can be assumed to be time-invariant over a number of symbol intervals. Slow fading can be caused by events such as shadowing, where a large obstruction such as a hill or large building obscures the main signal path between the transmitter and the receiver. **Fast-fading** occurs when the coherence time of the channel is small relative to the time duration of transmitted symbol. In this regime, the amplitude and phase change imposed by the channel varies considerably over the period of use.

In a fast-fading channel, the transmitter may take advantage of the variations in the channel conditions using time diversity to help increase robustness of the communication to a temporary deep fade. In a slow-fading channel, it is not possible to use time diversity because the transmitter sees only a single realization of the channel within its delay constraint. A deep fade therefore lasts the entire duration of transmission and cannot be mitigated using coding.

The coherence time of the channel is related to a quantity known as the **Doppler spread,** which results from Doppler shift. Doppler spread refers to the difference in Doppler shifts between different signal components. In general, coherence time T_c is inversely related to Doppler spread D_s, typically expressed as $T_c \approx 1/D_s$.

In terms of range of frequencies involved, fading can also be described as being *frequency non-selective* or *frequency-selective*. In **frequency non-selective** fading, otherwise known as **flat-fading**, the coherence bandwidth of the channel is larger than the signal bandwidth. Therefore, all frequency components of the signal will experience the same magnitude of fading. In **frequency-selective fading**, the coherence bandwidth of the channel is smaller than the bandwidth of the signal. Different frequency components of the signal therefore experience different degrees of fading. The coherence bandwidth measures the bandwidth over which two frequencies of a signal are likely to experience comparable or correlated amplitude fading.

5.2 Fading models

The wireless channel is a multipath channel. The channel impulse response *h(t)* can be represented by

$$h_k(t) = \sum_{l=1}^{L} \beta_{kl} e^{j\gamma_{kl}} \delta(t - \tau_{kl}) \quad , \tag{5.1}$$

where l is path index, L is number of paths, β_l is path amplitude, τ_l is propagation delay and γ_l, the phase shift. Interference among the multipath components results in fading. Amplitude fading in a multipath environment follows different distributions depending on the presence or absence of a dominating strong component, among other factors. In the absence of a strong dominating component, the amplitude has a Rayleigh distribution (and hence Rayleigh fading) with a probability density function (pdf) given by [2, 4, 5, 79]:

$$P(r) = \frac{r}{\sigma^2} \exp\left(-\frac{r^2}{2\sigma^2}\right), \qquad r \geq 0, \tag{5.2}$$

where σ is the Rayleigh parameter. The mean and the variance of the distribution are $\sqrt{\pi/2}\sigma$ and $(2-\frac{\pi}{2})\sigma^2$ respectively. If, in addition to low-level scattered paths, there is a strong dominating path (e.g. a line-of-sight path), the amplitude follows Rician distribution, whose pdf is given by [2, 4, 5, 79]:

$$P(r) = \frac{r}{\sigma^2} \exp\left(\frac{-r^2 + v^2}{2\sigma^2} \right) I_o \left(\frac{rv}{\sigma^2} \right), \quad r \geq 0, \tag{5.3}$$

where I_o is zeroth-order modified Bessel function of the first kind, v is the magnitude of the dominant component, and σ^2 is proportional to the power of the scatter Rayleigh components. The *Rician parameter* $K = \frac{v^2}{2\sigma^2}$, represents the ratio of the power associated with the dominant component and the scattered path components in the multipath channel [2, 4, 5, 79]. For a non-fading channel, the channel has an infinite bandwidth and the channel impulse response is equal to a delta-dirac function, i.e. $h(t) = \delta(t)$.

5.3 Diversity Techniques

Diversity can be achieved in time, frequency, or space [147, 148]. **Time diversity** is achieved when different time slots are used to transmit identical message with the time separation between different transmissions to ensure independent fade. This provides replicas of the transmitted signal across time by a combination of channel coding and time interleaving. In time diversity, the receiver suffers from time delay before receiving the entire transmitted signal for onward processing. This time delay results in bandwidth inefficiency.

Spatial diversity is implemented by using multiple antennas separated enough to ensure that individual signals are uncorrelated. Spatial diversity may be *receive or transmit diversity*. In receive diversity, multiple antennas are employed at the receive side, while in transmit diversity, multiple antennas are deployed at the transmit side. Two other forms of *spatial diversity* are *polarization diversity* and *angular diversity*. Angular diversity uses directional antennas to achieve diversity, and it involves different versions of the sent signals being collected from different angular directions. Polarization diversity method uses vertically and horizontally polarized signals to achieve diversity. Polarization diversity does not require separate location of the antenna but its diversity is limited to two.

In **frequency diversity,** different carrier frequencies are used to transmit identical messages. To ensure independent fades across different replica of the transmitted signal, the carrier frequencies must be separated by more than the coherence bandwidth of the channel.

5.4 Multicarrier CDMA

In a frequency-selective channel, since different frequency components of the signal are affected independently, it is highly unlikely that all parts of the signal will be simultaneously affected by a deep fade. A multicarrier (MC) CDMA systems take advantage of this fact to employ frequency diversity to provide robustness to fading, and is one of the basis why multicarrier modulation provides performance improvement to the wireless communication system. Orthogonal frequency-division multiplexing (OFDM), as found in the MC-CDMA, simply converts a frequency-selective channel into a parallel collection of flat-fading channels. The sub-carriers (sub-channels) have the minimum frequency separation required to make their time domain waveforms orthogonal while the signal frequency spectrum corresponding to the different subcarriers overlap. As a result, the available bandwidth is utilized more efficiently. In general, OFDM technique for wireless communication systems has a high spectral efficiency compared with frequency division multiplexing (FDM) scheme. In addition, it is very robust to selective fading and has a low computational complexity due to the type of computational method with which it is implemented.

Orthogonal frequency division multiplexing (OFDM) is a class of multicarrier modulation in which information is carried over many lower rate subcarriers. Modern version of OFDM involves the use of fast Fourier transform, which helps in reducing implementation complexity of the multi-carrier system. Considering that the complex symbols to be transmitted in a P-subcarrier OFDM system with a pass bandwidth B are denoted by $\left(X_{-P/2}, \ldots, X_{-1}, X_1 X_2, \ldots, X_P\right)$, one P-subcarrier OFDM symbol can be represented mathematically by [149]

$$s(t) = \begin{cases} \sum_{p=P/2, k\neq 0}^{P/2} X_n e^{j2\pi f_k t}, & for\; pT - T_w - T_g \leq t \leq kT + T_{FFT} + T_w \\ 0 & otherwise \end{cases} \quad (5.4)$$

where f_p is the frequency of the pth subcarrier, $T_{FFT} = PT_s$ is the duration of the total number of FFT-points, T_s is the sampling rates, T_g is the duration of the cyclic prefix, and T_w is the duration of the windowing. The transmitted OFDM signal can be demodulated by applying inverse operations to (1.14) as

$$x_p = \frac{1}{T_{FFT}} \int_{t=0}^{T_{FFT}} s(t) e^{-2\pi f_p t} dt. \quad (5.5)$$

FFT operation ensures that the generated subcarriers are orthogonal because each bin of an IFFT corresponds to the amplitude and phase of a set of orthogonal sinusoid.

Although there are different variants of the multicarrier CDMA system [4-7, 9, 10, 74, 75, 109-124], all are based on the same principle, which is the breaking of the wideband signal bandwidth into a set of parallel orthogonal frequency sub-channels.

5.5 Simulations results and discussion

Software simulations were carried out to investigate the performance of a DS-CDMA system in a flat-fading Rayleigh channel as well as a MC-CDMA system in a frequency-selective channel. Random QPSK symbols generated and transmitted through the channel using different sets of Gold codes as spreading sequences. The influence of code length on the system performance was investigated for a given number of tones and data rate. At the receiving end, recovered data were compared to the original transmitted data for the determination of bit-error-rate (BER). Parametric BER graphs were generated for the evaluation of the system performance. Results of the simulations will now be presented as follows.

5.5.1 Performance in a flat-fading channel

Here we shall be presenting the performance of a direct-sequence CDMA system in a flat-fading channel. Multicarrier transmission is not used here for the simple reason that there is no advantage in using multiple carriers in a flat-fading channel. (The essence of using multicarrier transmission is to convert a frequency-selective channel to flat-fading channels. Since the channel currently under consideration is flat-fading, the use of multi-carrier transmission is not necessary.)

We shall now examine the performance of the DS-CDMA system in a Rayleigh flat-fading channel for a sample frequency of 10 kHz and a maximum Doppler shift of 83.3 Hz. Fig. 5.1 shows the results for uncoded and coded data transmission for a single user. This figure clearly shows the effects of channel fading on the system performance. It is obvious that the system has worse BER in the flat-fading channel than in a Gaussian channel. Higher SNR (or power) is required to obtain any given BER in the fading channel than in a Gaussain channel. As with a Gaussian channel however, it can be seen that the use of Gold codes provides better BER, if compared to uncoded data transmission. The codes provide constant coding gain between adjacent code lengths. At a BER of 10^{-4}, the Gold codes provide coding gain of about 11.0, 17.4 and 22.5 dB for N = 31, 127 and 511 respectively. This is equivalent to a constant coding gain of about 5.75 dB between adjacent code lengths, which is just a little less than that of a Gaussian channel. The results also show that a longer code gives better error rate performance, though at the expense of increased transmission bandwidth.

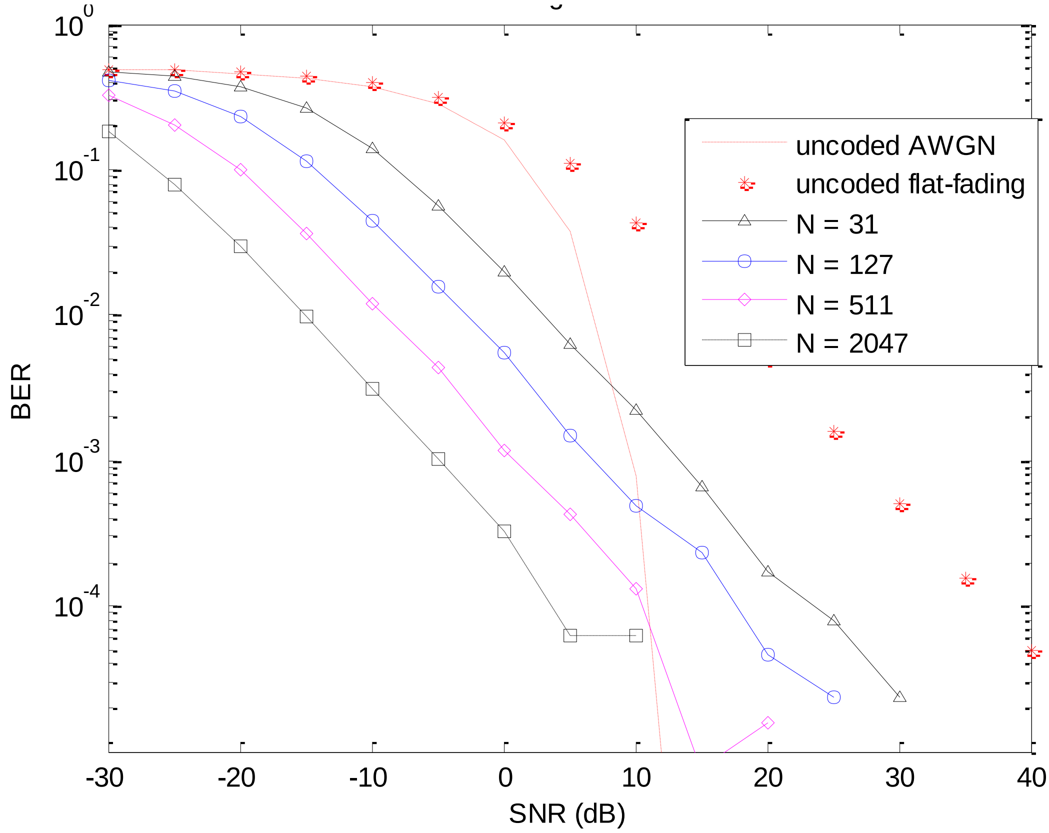

Fig. 5.1 Performance for a single user in a flat-fading channel

Next, we shall examine results for multiple users in the flat-fading channel. Fig. 5.2 shows BER for a particular user in the presence of another interfering user. It is easy to see the degrading effects of fading on the system performance. Of particular interest is the emergence of an error floor, a feature that is absent in a Gaussian channel. While it is true that the presence of an interfering user and hence multiple-access interference (MAI) is a factor in the emergence of the error floor, the results show that channel fading is more responsible for it than does code properties. This is buttressed by the fact that in a Gaussian channel, there was no error floor, even when the system was fully loaded (Chapter 4). This can be compared to the present situation in which error floor appears even for only two users.

Hence, with a mitigation of the fading effect of the channel, it should be possible to get the codes to perform significantly well as in a Gaussian channel.

It is noteworthy that the emergence of the irreducible error floor is delayed for longer codes. Also the error floor is significantly less for longer codes. This is due to the fact that longer codes have higher capacity for accommodating more users.

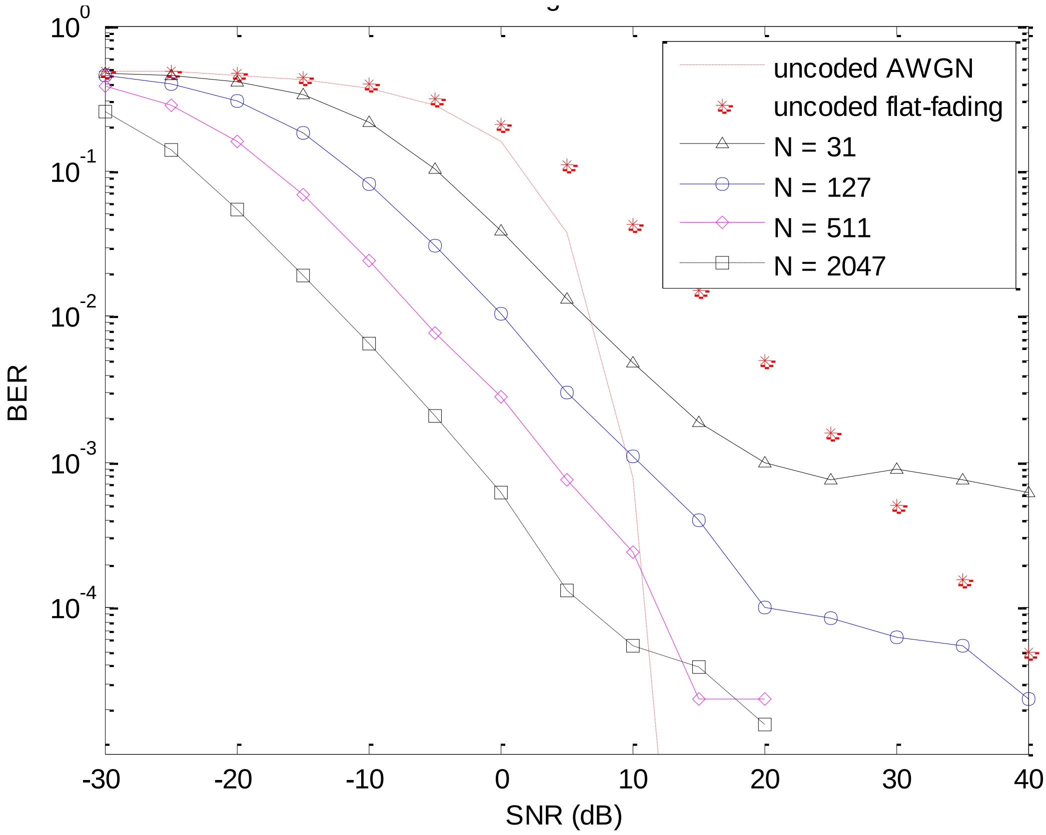

Fig. 5.2. Performance for two users in a flat-fading channel

We shall now examine results for higher number of users in the flat-fading channel. Fig. 5.3 and 5.4 show BER for three to six multiple users. Here again, effects of channel fading on the system performance can be seen. Ignoring the error floor region, it can be seen that coding gain between adjacent code lengths remains constant when the number of users is elevated, which is similar to the behaviour observed for the codes in a Gaussian channel.

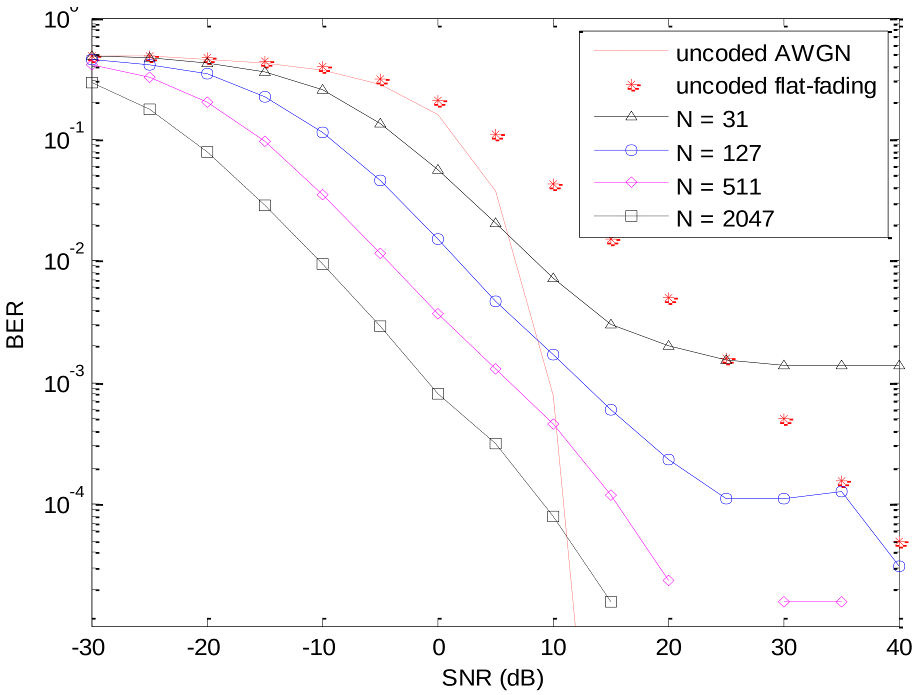

(a)

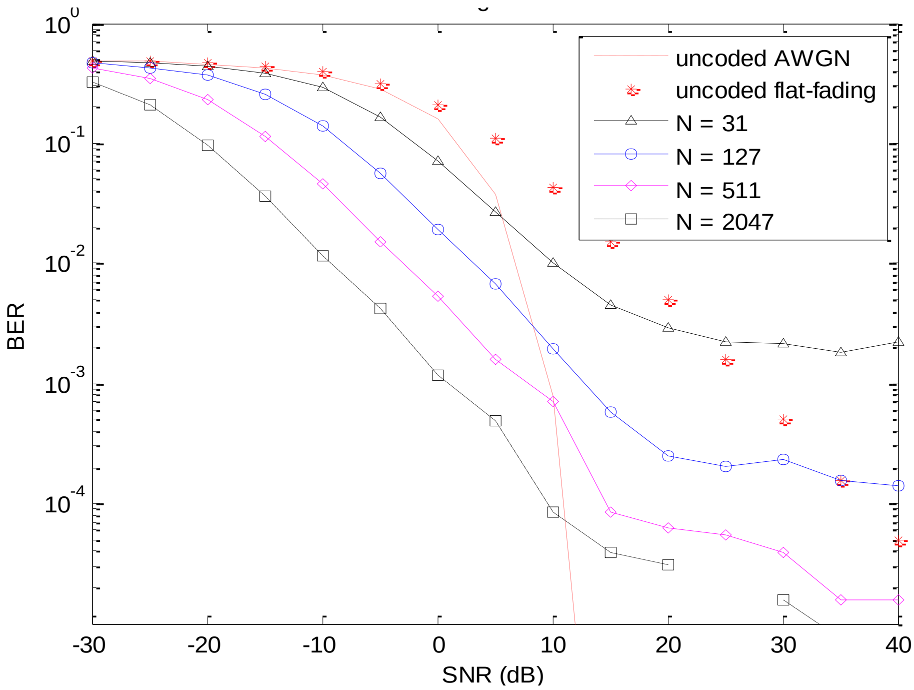

(b)

Fig. 5.3 . Performance in a flat-fading channel for (a) three and (b) four users

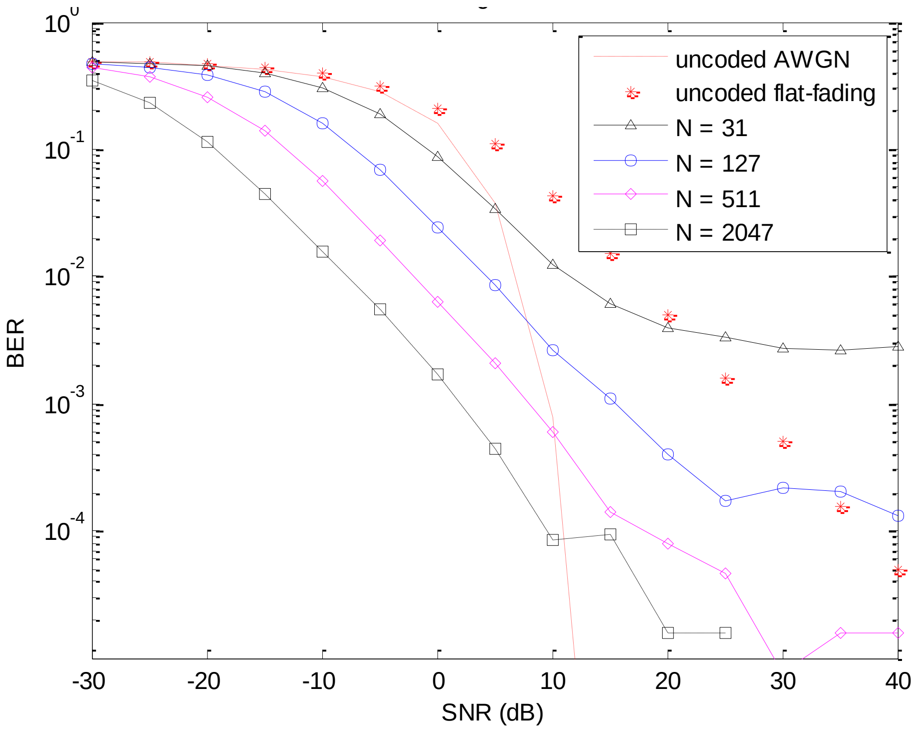

(a)

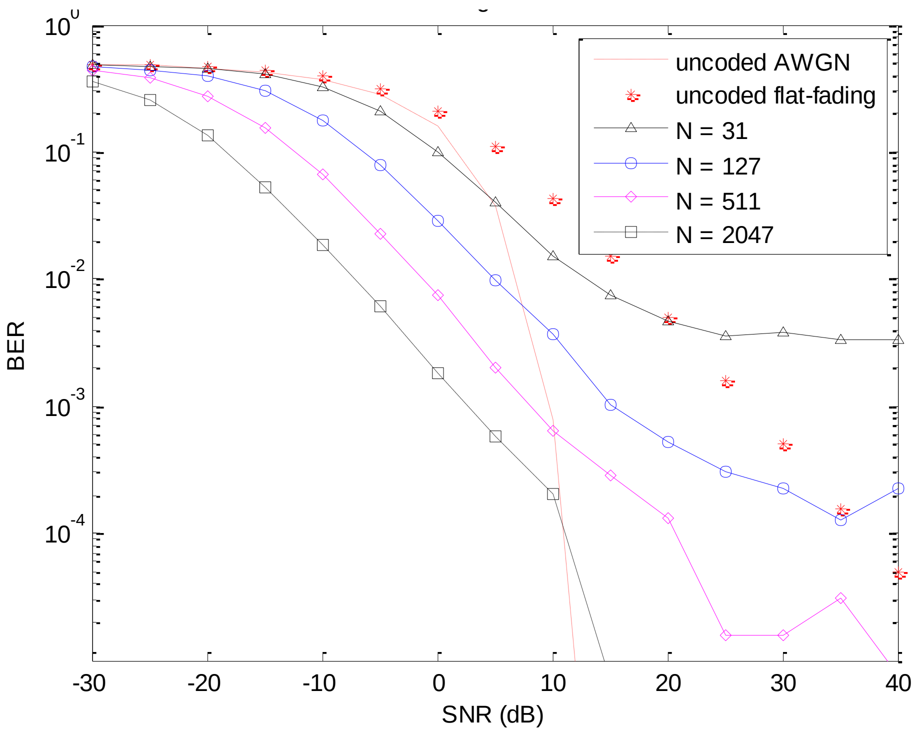

(b)

Fig. 5.4. Performance in a flat-fading channel for (a) five and (b) six users.

5.5.2 Performance in a frequency-selective channel

The system performance in a frequency-selective, Rayleigh channel was also modelled for a MC-CDMA system. A four-path channel with constant path delays was assumed. Number of subcarriers was kept fixed at 64. Table 5.1 shows the simulation parameters. Simulation results for the MC-CDMA system will now be presented.

Table 5.1 Simulation parameters for the MC-CDMA system

Modulation type	QPSK
Frame size	64 QPSK symbols
No. of subcarriers	64
Cyclic extension (25%)	16 symbols
Carrier frequency	900 MHz
Max Doppler shift	83.33 Hz
Sample Frequency	10 kHz
Number of paths	4
Path gains(dB)	0 -20 -30 -40
Path delays (μs)	0 1 5 10

Fig. 5.5 shows BER versus signal-to-noise ratio for a single user. There is no interfering user. This curve clearly shows that in terms of BER, the system performance is better for longer codes, which is expected. In the performance curves, the appearance of irreducible error floor can be seen. This error floor cannot be attributed to MAI, as there is no interfering user here. Rather, the error floor can be attributed to destructive interference originating from multi-paths. This observation is important because it indicates that primarily, irreducible error floor is not due to multiple-access performance of the codes, but channel fading. This situation can be compared to that of a flat-fading (single-path) channel where there is no error floor for a single user.

Another look at these results shows that for N = 31 and 127, the BER performance is worse in a frequency-selective channel than in a flat-fading channel. The opposite is the case for N = 511 and 2047. Among other things, the results show that for N = 31 and 127, error floor emerges earlier in a frequency-selective channel than in a flat-fading channel. In addition, the level of error floor is higher in the frequency-selective channel than in a flat-fading channel.

Now turning to N = 511 and 2047, no error floor is visible up to the BER regions that was considered by this work. While it is desirable to see the system performance in lower BER regions, investigating this would require generating results for lower BER regions, but the time required to run simulations for this makes it impracticable. For example, obtaining results for a BER of 10^{-7} may require running the simulations continuously for about 700 days[1], which is not feasible.

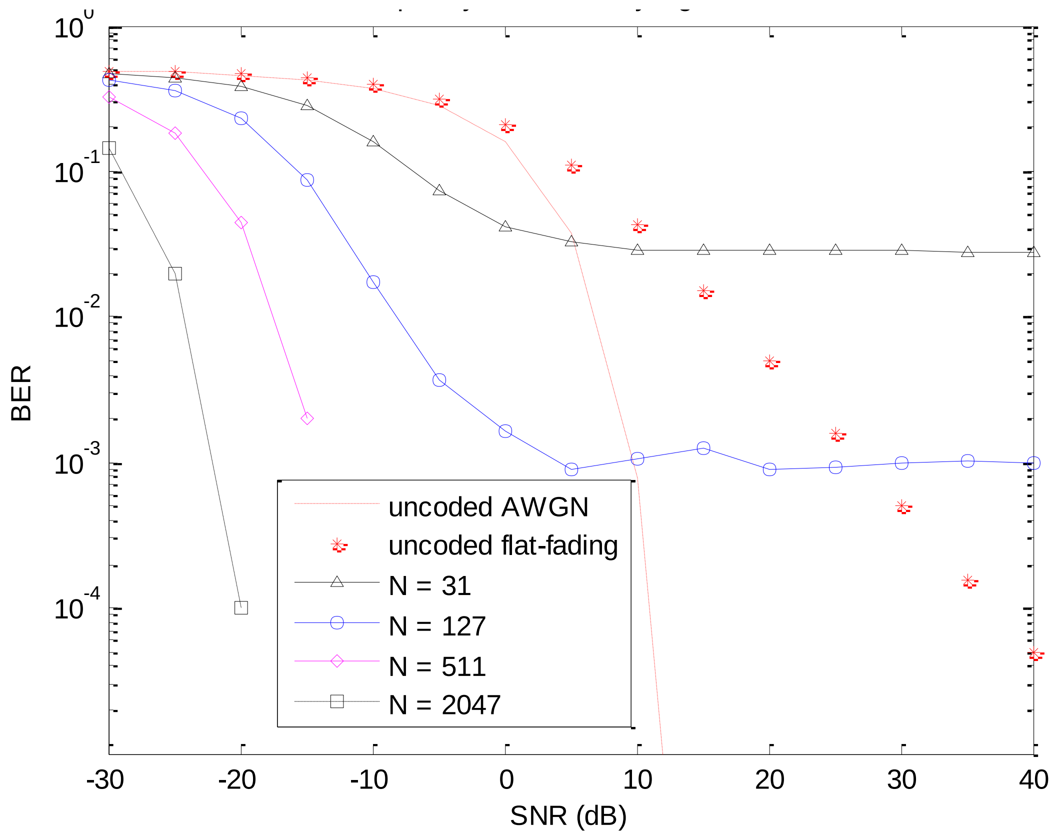

Fig. 5.5 Performance of a multicarrier CDMA system in a frequency-selective channel for a single user

It is useful to note that in Fig. 5.5, the error floor is notably reduced for longer codes. In fact, for the BER range under consideration, the error floor cannot be seen for 511 and 2047 code lengths. Another point of interest is the presence of diversity gain on the performance curves. It can be seen that longer codes provides higher diversity gain. The origin of these desirable features can be explained as follows. As we increase code length for a fixed data rate, chip duration decreases. This increases transmission bandwidth, such that the signal is spread over wider bandwidth. Since different frequency components of the signal are affected independently, it is very unlikely that every part of the signal will be affected at the same time by a deep fade. This frequency diversity makes longer codes more resilient to fading

[1] The simulation results reported here involves a minimum BER of about 10^{-5}, and the simulation took about a week (7 days) to run. Going down to a BER of 10^{-7} requires processing hundred-fold the number of data samples for the BER of 10^{-5}. This would therefore require the simulation running continuously for about 700 days, which is not practicable.

effects, thereby making the longer codes to give better BER, at the expense of wider transmission bandwidth.

We shall now examine the performance of the multicarrier system for multiple users. Fig. 5.6 shows the BER for a particular user in the presence of an interfering user. It can be seen that the system BER is slightly worse than when there was no interfering user, which obviously is due to MAI. As expected, the results confirm again that longer Gold codes give better error rate performance.

Fig. 5.7 (a) and (b) shows performance curves for four and five users. This also shows that the MAI effect of interfering users is marginal. Furthermore, the results show that for multiple users (five users in this case), the multicarrier CDMA in the frequency-selective channel outperforms the DS-CDMA in a flat-fading channel.

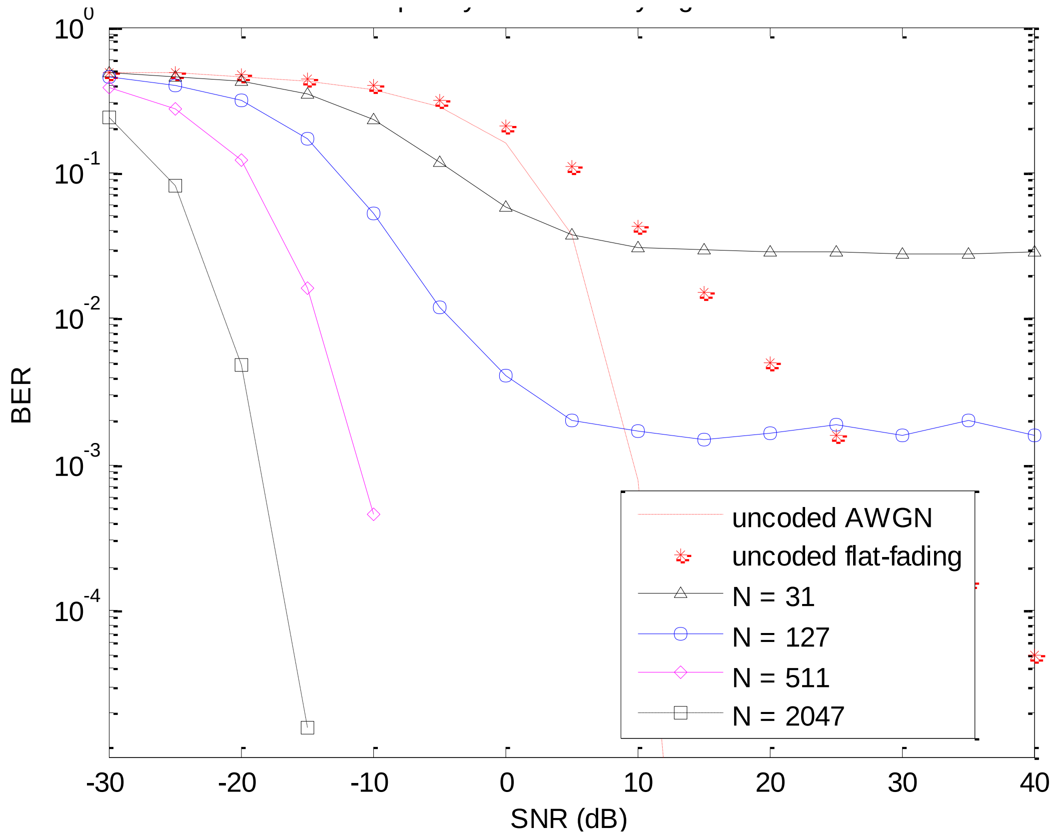

Fig. 5.6 Performance of a multicarrier CDMA system in a frequency-selective channel in the presence of an interfering user

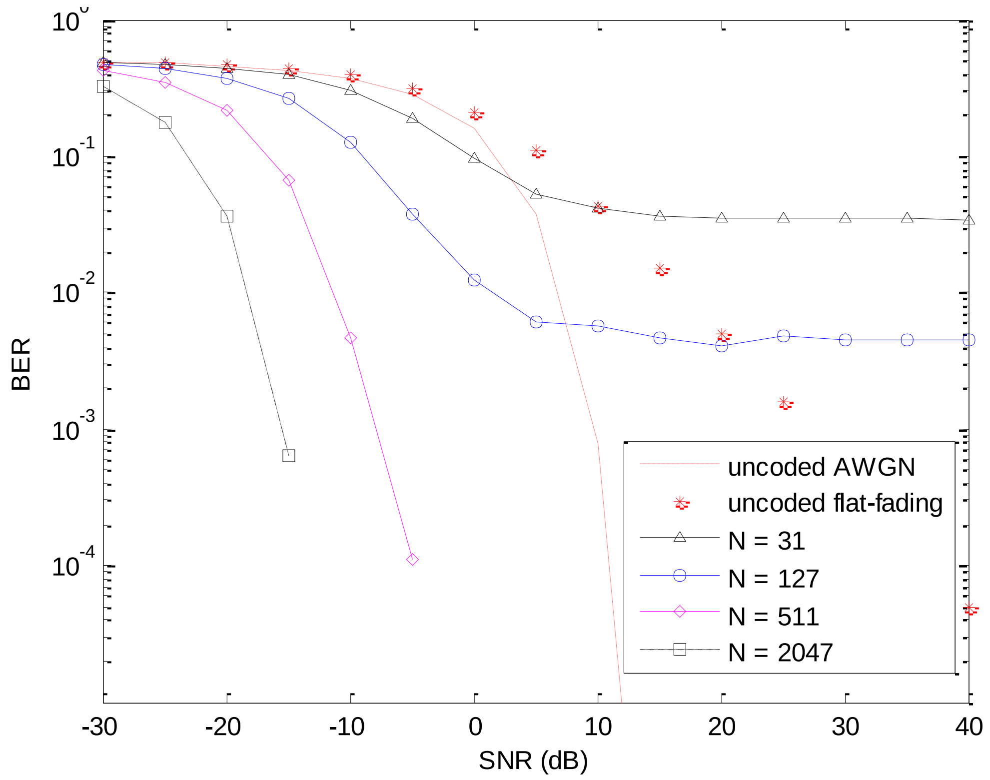

(a)

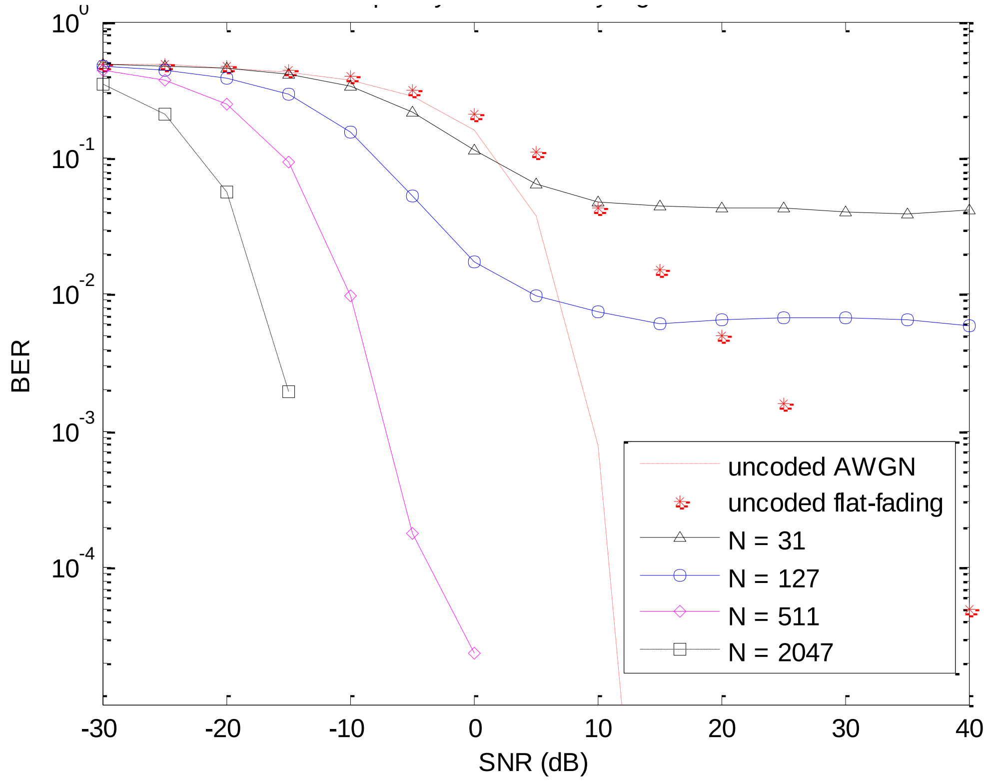

(b)

Fig. 5.7 Performance in a frequency-selective channel for (a) four and (b) five users.

It might have been observed that results presented here for the fading channels are limited to a few users. Reason for this is explained as follows. The simulation model for the system in a fading channel is computationally intensive and takes long time to run. Sometimes, the simulation has to run continuously for days before giving an output. The higher the number of users, the longer the time required. Hence to minimise the time penalty, it was necessary to limit the number of users to just a few.

5.6 Chapter Summary

This chapter presented results of simulations for the performance of the communication system in a Rayleigh fading channel. The results show that in a flat-fading channel, the codes provide a constant coding gain close to that obtainable in a Gaussian channel. The impact of longer spreading codes is more pronounced for the MC-CDMA system in a frequency-selective channel as indicated by significant lowering of error floors. Also, frequency diversity associated with the use of longer codes coupled with multi-carrier modulation makes the MC-CDMA system resilient to multi-path effects. In the next chapter, simulation results on a space-time coded MC-CDMA system shall be presented.

Chapter 6

Space-time Coded Multi-carrier CDMA System

6.0 Introduction

Space-time coding (STC) is known to be an effective diversity technique for combating channel fading without bandwidth penalty. STC combines transmit diversity with coding scheme. This chapter models the performance of a multiple-antenna space-time coded multi-carrier (MC) code-division multiple-access (CDMA) system.

Although significant amount of work has been done on space-time-coded MC-CDMA systems, available literature shows that existing works have been largely limited to the use of Walsh-Hadamard codes as spreading sequences, as confirmed by the following references [11-62]. To the best of our knowledge, cases involving the use of Gold codes as spreading sequences in space-time coded MC-CDMA systems are not common in literature. In this chapter, we investigate the performance of Gold codes in a space-time block-coded CDMA system.

Space-time coding is designed primarily for flat-fading channels. However, many wideband wireless channels are frequency-selective in nature. Consequently, STC schemes cannot be applied as-is to wideband systems. However, the combination of multi-carrier modulation with CDMA removes this barrier. Multicarrier modulation, as found in orthogonal frequency-division multiplexing (OFDM) converts a wideband frequency-selective channel to a set of narrow-band, flat-fading channels, thereby giving the opportunity to use STC schemes in broadband frequency-selective channels. In a MC-CDMA system, multiple-access is achieved by having different users transmit on the same set of sub-carriers but with different spreading sequences.

STC systems are multi-antenna systems. Therefore, Sections 6.1 to 6.3 gives basics of multi-antenna systems. This is followed by fundamental theory on STC in Section 6.4 and 6.5. Section 6.6 gives system description of a space-time coded MC-CDMA system. Section 6.7 develops a mathematical model of the communication system. Section 6.8 presents results and discussion of software simulations that were carried out on the system performance. This chapter concludes with a summary in Section 6.9.

6.1 MIMO systems

In. Multiple-input multiple-output (MIMO), which involves the use of multiple antennas at both transmitter and receiver ends of wireless communication systems, has received attention both from industries as well as from academic communities. On the other hand, OFDM technique has emerged as a popular multi-carrier modulation technique to combat some problems associated with physical properties of wireless channels such as multipath fading and inter-symbol interference. The combination of MIMO technology with OFDM technique, along with CDMA is a promising solution for future broadband wireless communication systems. Amalgamation of these techniques is a potential means of increasing the throughput and quality of service of future wireless communication.

In general, a MIMO system comprises n_T transmit antennas and n_R receive antennas. Consequently, the system has a channel matrix H having n_T x n_R dimensions. Fig. 6.1 shows a schematic diagram of a MIMO system.

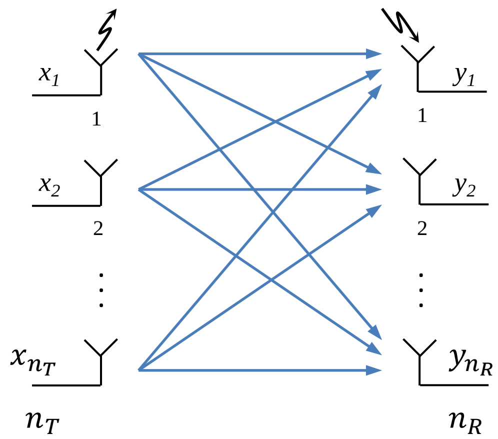

Fig. 6.1. A MIMO system

Because of the advantages associated with the use of multiple antennas at both the transmitter and the receive end of a communication system, MIMO systems have been an important subject of modern research. Prominent among the advantages are *diversity gain* and *multiplexing gain* [147, 148].

Diversity gain can be achieved with the aid of STC techniques. The deployment of STC enables the transmission of the same data symbol from multiple transmit antennas. The received data symbols, at each of the receive antennas, are superposition of all the transmitted data symbols. As such, the receiver will detect the same transmitted data symbol several times and at different antenna positions in space. As long as the fading for each transmission link between a pair of transmit and receive antennas in the MIMO system can be assumed to be independent of each other, the transmitted data symbols can be detected with higher accuracy at the receiver of the MIMO system. In this way, the bit–error-rate (BER) performance of the system can be significantly enhanced. The performance improvement is referred to as diversity gain.

Multiplexing gain is achieved with the aid of spatial multiplexing techniques. The technique involves simultaneous transmission of multiple streams of data symbols independently on different transmit antennas, and received via different receive antennas. This increases the data rate since instead of sending symbols via the same antenna serially, consecutive symbols equal to the number of transmit antennas can be sent in parallel. Multiplexing gain refers to this increase in data rate, and is obtained at no additional bandwidth expenditure. Whereas achieving diversity gain only requires multiple antennas at either end of the communication system, achieving multiplexing gain requires multiple antennas at both ends of the link.

6.2 MIMO channel model

Consider a MIMO communication system [147, 148] having n_T transmit and n_R receive antennas as shown by Fig. 6.2. At time *t*, the signals $x_{t,i}, i = 1, \dots, n_T$ are simultaneously transmitted from n_T transmit antennas. Each transmitted signal is affected by channel fading, and received at each of n_R receive antennas. If we consider a flat-fading channel with the channel gain $h_{i,j}$ between receive antenna j and transmit antenna i, then the received signal at received antenna j at time t is given by

$$r_t^j = \sum_{i=1}^{n_T} h_{i,j} x_{t,i} + \eta_{t,j} \ , \tag{6.1}$$

where $\eta_{t,j}$ is the additive Gaussian noise at the receiving antenna j at time t. Consider that the channel is quasi-stationary, that is, the fading coefficients (or path gains) $h_{i,j}$ are constant over a certain time period T', and from period to period they are varied independently. The rate of fading is determined by the value of T'. If the data block is transferred during the time $T < T'$, the fading is said to be slow. In this case the coefficients $h_{i,j}$ are constant during the entire transmission period. The signals transmitted during the time period T from n_T transmitting antennas can be represented using a $(T \times n_T)$ matrix $\mathbf{X}$ given by

$$\mathbf{X} = \begin{bmatrix} x_{1,1} & \cdots & x_{1,n_T} \\ \vdots & \ddots & \vdots \\ x_{T,1} & \cdots & x_{T,n_T} \end{bmatrix}. \tag{6.2}$$

Similarly, the received signal can be represented in the form of $(T \times n_R) -$ matrix $\mathbf{R}$ given by

$$\mathbf{R} = \begin{bmatrix} r_{1,1} & \cdots & r_{1,n_R} \\ \vdots & \ddots & \vdots \\ r_{T,1} & \cdots & r_{T,n_R} \end{bmatrix} . \tag{6.3}$$

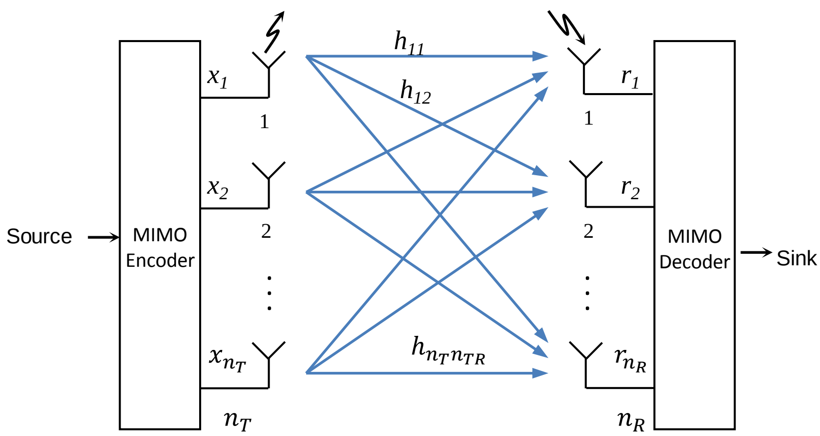

Fig. 6.2. MIMO system with n_T transmit and n_R receive antennas

Assuming $T < T'$, such that the channel fading coefficient are constant during the transmission period, the fading channel coefficients may also be written in the form of $(n_T \times n_R) -$ matrix $\mathbf{H}$ given by

$$\mathbf{H} = \begin{bmatrix} h_{1,1} & \cdots & h_{1,n_R} \\ \vdots & \ddots & \vdots \\ h_{n_T,1} & \cdots & h_{n_T,n_R} \end{bmatrix}. \tag{6.4}$$

.

Then, we can write (6.1) in matrix form as

$$\boldsymbol{R} = \boldsymbol{H}.\boldsymbol{X} + \boldsymbol{\mathcal{N}}. \tag{6.5}$$

where $\boldsymbol{\mathcal{N}}$ is noise matrix given by

$$\boldsymbol{\mathcal{N}} = \begin{bmatrix} \eta_{1,1} & \cdots & \eta_{1,n_R} \\ \vdots & \ddots & \vdots \\ \eta_{T,1} & \cdots & \eta_{T,n_R} \end{bmatrix}. \tag{6.6}$$

6.3 MIMO channel capacity

It has been shown in information-theoretical studies of wireless channels that MIMO channel capacity is increased significantly compared to the capacity of single-input/single-output (SISO) systems. Recently, researchers have actively engaged in an effort to exploit this new potential of MIMO channel capacity.

Channel capacity can be defined as the maximum error-free data rate that a channel can support. Claude Shannon in [146] derived the capacity of an AWGN channel as

$$C = B\log_2(1 + \gamma), \tag{6.7}$$

where B is channel bandwidth, and γ is the average received signal–to-noise-ratio (SNR). The capacity of a deterministic SISO channel is given by [14]

$$C = \log_2(1 + \rho|H|^2), \tag{6.8}$$

where $|H|^2$ is the normalized channel power transfer characteristic and ρ is the average SNR at each receiver.

For a deterministic MIMO channel, the channel capacity is given by [147, 148]

$$C = \log_2\left[\det\left(\mathbf{I}_{\mathrm{n_R}} + \frac{\rho}{n_T}\mathbf{H}\mathbf{H}^{\boldsymbol{H}}\right)\right], \tag{6.9}$$

while for an ergodic MIMO channel, the capacity is given by [146]

$$C = E_{\mathrm{H}}\left\{B \log_2 \left[\det\left(\mathbf{I}_{\mathrm{n_R}} + \frac{\rho}{n_T}\mathbf{H}\mathbf{H}^{\boldsymbol{H}}\right)\right]\right\}, \tag{6.10}$$

where $E_{\mathbf{H}}$ denotes expectation with respect to **H**, $\mathbf{I}_{\mathrm{n_R}}$ is $n_T \times n_R$ identity matrix and det[**A**] is the determinant of matrix **A**.

6.4 Spatial diversity

Fading can cause the effective SNR at the receiver of a communication system to drop drastically thereby making reliable recovery of the transmitted signal impossible. The inability of a communication system to recover the transmitted signal at the receiver, results in loss of communication (outage) which is undesirable in any communication system. Diversity is a technique used in MIMO systems to combat channel impairments by providing replicas of the transmitted signal to the receiver, which fades independently. If the multiple transmitted signals undergo independent fading, the probability that the entire transmitted signal will undergo simultaneous deep fade is minimized. As a result, the probability of outage is reduced in system employing spatial diversity. The diversity gain G_d is given as [147, 148]

$$G_d = \lim_{\gamma\to\infty} \frac{log(P_e)}{log(\gamma)} , \tag{6.11}$$

where P_e is the error probability of the received signal and γ is the received SNR.

6.5 Space-time coding

A key feature of MIMO systems is the ability to turn multi-path propagation, traditionally a pitfall in wireless transmission into a benefit for the user. MIMO effectively takes advantage of random channel fading. The prospect of many orders of magnitude improvement in wireless communication performance at no extra cost of the spectrum is largely responsible for the interest in MIMO systems.

Space-time coding schemes combine the channel code design and the use of multiple transmit and receive antennas. The encoded data is split into N streams that are simultaneously transmitted using n_T transmit antennas. The received signal is a linear superposition of these simultaneously transmitted symbols corrupted by noise and fading. Space-time decoding algorithms as well as channel estimation techniques are incorporated at the receiver in order to achieve diversity advantage and coding gain.

Different types of space-time codes have been proposed in literature. These include space-time block codes (STBC), orthogonal space-time block codes (OSTBC), space-time trellis codes (STTC) and super-orthogonal space-time trellis codes (SOSTTC) [129, 147, 148]. STTC provides both diversity and coding gain, but its complexity of decoding increases exponentially with diversity level and transmission rate. In contrast, STBC [130-132] as an alternative provides diversity but no coding gain. However, the attractiveness in STBC includes its ability to achieve maximum possible diversity advantage, coupled with the simplicity of its implementation and decoding algorithm [12].

Consider a space-time block code transmit diversity scheme involving two transmit antennas. Its generator matrix *G* for orthogonal design is given by [130, 131]:

$$\boldsymbol{G_2} = \begin{pmatrix} x_1 & x_2 \\ -x_2^* & x_1^* \end{pmatrix} \tag{6.12}$$

where columns signifies transmit antennas and the rows signifies time instances. Thus, at time t = 1, x_1 and x_2 will be transmitted from antenna 1 and 2 respectively, while at time t = 2, $-x_2^*$ and x_1^* will be transmitted from antenna 1 and 2 respectively. Assuming a single receive antenna and fading coefficient to be constant over two consecutive time slots, the received signal is given as

$$r_1 = h_1 x_1 + h_2 x_2 + \eta_1, \tag{6.13}$$

$$r_2 = -h_1 x_2^* + h_2 x_1^* + \eta_2, \tag{6.14}$$

where h_1 and h_2 signifies the coefficients of the channel and $\eta_1$and η_2 the channel noise.

For a space-time block code scheme involving four transmit antennas, transmission matrix *G* for real orthogonal design is given by [131, 147, 148]

$$\boldsymbol{G_4} = \begin{pmatrix} x_1 & x_2 & x_3 & x_4 \\ -x_2 & x_1 & -x_4 & x_3 \\ -x_3 & x_4 & x_1 & -x_2 \\ -x_4 & -x_3 & x_2 & x_1 \end{pmatrix} \tag{6.15}$$

6.6 *Space-time coded MC-CDMA system*

A space-time coded MC-CDMA system combines the positive advantages of STC, multicarrier (OFDM) modulation with that of a CDMA system. Fig. 6.3 shows system block of a space-time coded MC-CDMA system for a single user. Here, the user source signal, represented by the vector ***X***, is first space-time coded by the STC encoder into parallel sub-streams x_i, where i = 1, 2, 3,…, n_T, where n_T is the number of transmit antennas. The CDMA encoder then encodes each sub-stream using the user's unique code. Following this, each of the encoded sub-streams is placed on a subcarrier for onward transmission via the multiple transmit antennas through the wireless channel. The transmitted sub-streams convolves with the channel, and are then picked up by the receive antennas. At any time instant, the signal detected by each receive antenna is a summation of all the signals coming from the n_T transmit antennas. To recover the original signal, the receiver carries out the reverse process on the detected signal.

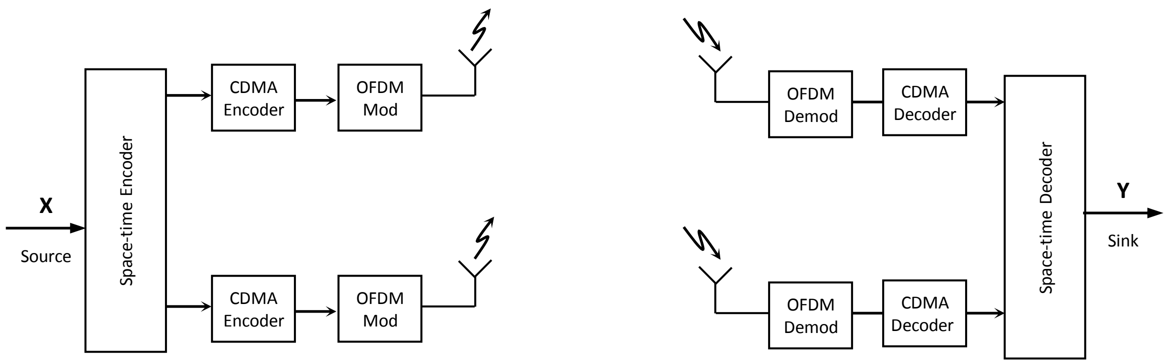

Fig. 6.3 Space-time coded MC-CDMA system.

Fig. 6.4 is another block diagram of the STC MC-CDMA system showing details of signal transformation through the communication system. This is described as follows. In the transmitter, the source signal is first space-time coded by the STC encoder into sub-streams. Each sub-stream is converted from serial to, say, N_p parallel symbol streams, having a symbol duration T_s. Each symbol stream is multiplied by the user code $c(t)$, after which the resulting signal for the pth symbol stream modulates a subcarrier f_p. The subcarriers are orthogonal on the symbol duration and are given by $f_p = f_o+p/T_s$, where f_o is RF frequency. The multicarrier signal $s(t)$ is obtained from addition of the different subcarrier signals. The resulting OFDM symbols are transmitted simultaneously from the individual transmit antennas. The received signal $r(t)$ is a convolution of $s(t)$ and the channel impulse response, corrupted by noise. To recover the original data, the receiver carries out the reverse of what the transmitter does. In actual implementation , inverse fast Fourier transform (IFFT) and fast Fourier transform (FFT) are normally employed by the OFDM modulator at the transmit and the receive end respectively for improved system efficiency. For details, the reader may refer to Chapter 2 of this thesis.

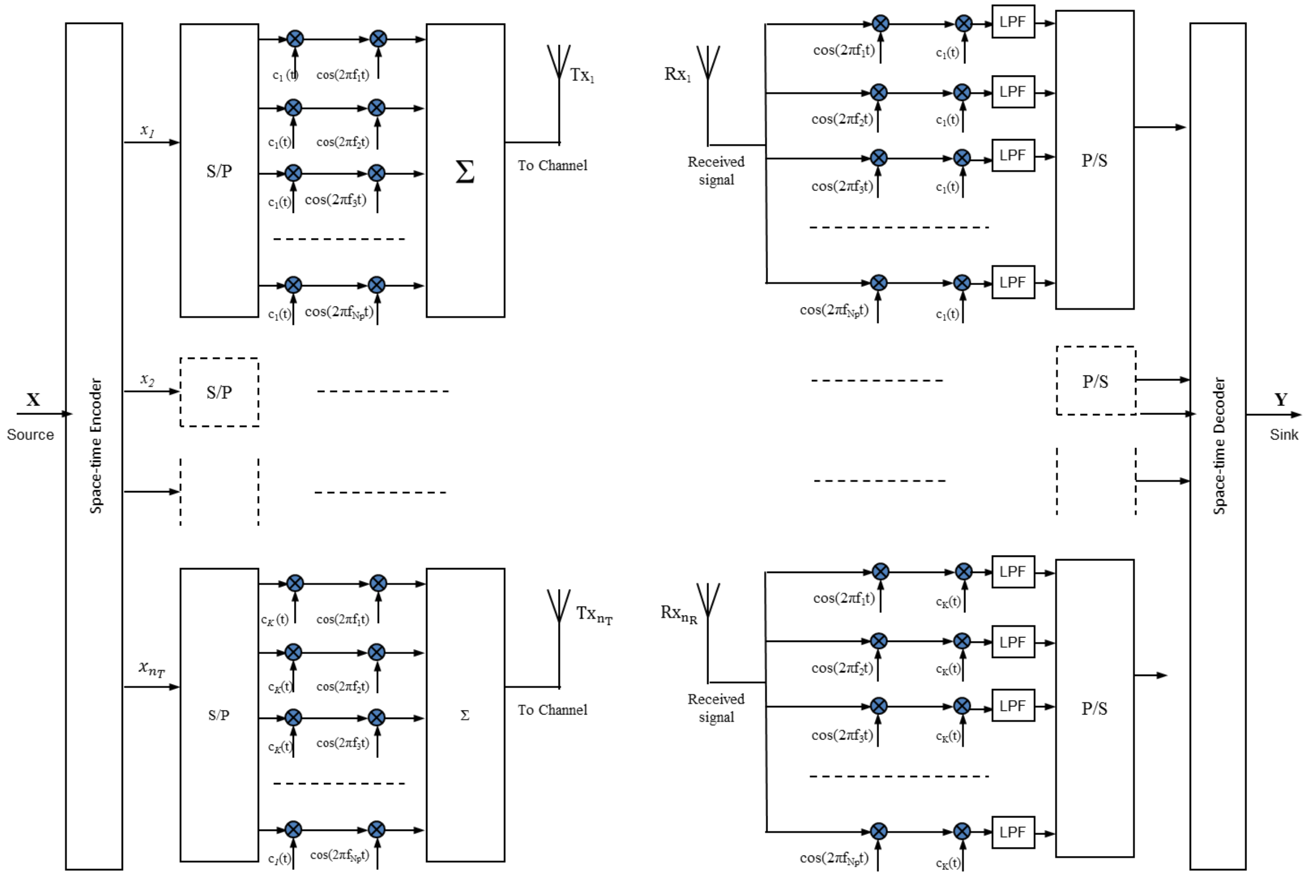

Fig. 6.4 A space-time coded MC-CDMA system

Fig. 6.4 represents an MC-CDMA system for a *single* user. A multi-user system has as many of these structures as the number of users running in parallel.

6.7 System model

Starting from basic principles, we shall now be developing a mathematical description of the communication system.

6.7.1 CDMA without transmit diversity

Let us first describe a CDMA system without transmit diversity nor multicarrier modulation. The transmitted signal $s_{k,t}$ for user k at time t can be expressed as

$$s_{k,t} = c_k(t)b_{k,t}cos(\omega_c t - \theta_k)$$

where c_k(t) is a code sequence for the user, b_k is the user binary data, ω_c is carrier frequency, and θ_k is phase angle. The code sequence c_k(t) can be expressed as

$$c_k(t) = \sum_{i=1}^{N} c_k^i P_c(t - iT_c), \qquad c_k^i \in \{-1,1\}, \tag{6.16}$$

where P_c is a pulse having a chip duration T_c. Let $h_k(t)$ represent channel impulse response for the user, where

$$h_k(t) = \sum_{l=1}^{L} \beta_{kl} e^{j\gamma_{kl}} \delta(t - \tau_{kl}). \tag{6.17}$$

where $\beta_{kl,}$ is path gain for user k and path l, τ_{kl} is propagation delay, γ_{kl} *is* phase shift, l is path index and L is number of paths. Received signal $r_{k,t}$ for the user at time t is given by

$$r_{k,t} = \int_{-\infty}^{\infty} s_{k,t}(\tau) h_k(t - \tau) d\tau \ + \ n_{k,t} \tag{6.18}$$

where $n_{k,t}$ represents channel noise. By substituting the expressions for $s_{k,t}$ and $h_k(t)$ into this integral, we can show that:

$$r_{k,t} = \sum_{l=1}^{L} \beta_{kl} e^{j\gamma_{kl}} \ c_k(t - \tau_{kl}) \ b_k(t - \tau_{kl}) \ cos(\omega_c(t - \tau_{kl}) - \theta_{kl}) + \ n_{k,t} \tag{6.19}$$

For a multi-user system comprising K users, the received signal $r(t)$ is a linear superposition of the signals for all users, and is given by

$$r(t) = \sum_{k=1}^{K} \sum_{l=1}^{L} A\beta_{kl} e^{j\gamma_{kl}} \ c_k(t - \tau_{kl}) \ b_k(t - \tau_{kl}) \ cos(\omega_c(t - \tau_{kl}) - \theta_{kl}) + \ n_{k,t} \tag{6.20}$$

Let user-1 be the reference user. Assuming coherent demodulation, the receiver output $z(m)$ for m^{th} bit during the bit duration T_b of the user is given by

$$z_1(m) = \int_{mT_b}^{(m+1)T_b} r(t)c_1(\mathrm{t}) \cos \omega_c t \, dt$$

$$= \int_{mT_b}^{(m+1)T_b} \left\{ \sum_{k=1}^{K} \sum_{l=1}^{L} A\beta_{kl} e^{j\gamma_{kl}} \; c_k(t - \tau_{kl}) \, b_k(t - \tau_{kl}) \, cos(\omega_c(t - \tau_{kl}) - \theta_{kl}) + \; n_{k,t} \right\} c_1(\mathrm{t})\mathrm{cos}\omega_c t \, dt \quad (6.21)$$

6.7.2 Space-time coded CDMA system

Now consider a CDMA transmit diversity scheme having n_T transmit antennas. Let $\boldsymbol{b_{k,t}}$ be the user data, space-time coded onto the n_T transmit antennas. The user data can be represented by a vector as

$$\boldsymbol{b_{k,t}} = \{b_{k,t}^i\}, \qquad i = 1,2, \ldots, n_T$$

$$= \{b_{k,t}^1, b_{k,t}^2, \ldots, b_{k,t}^{n_T}\}, \quad (6.22)$$

where $b_{k,t}^i$ is the user data for antenna *i* at time *t*. Transmitted signal $s_{k,t}^i$ for the user at antenna *i* and time *t* can be expressed as

$$s_{k,t}^i = \frac{1}{\sqrt{n_T}} c_{k,t} b_{k,t}^i cos(\omega_c t - \theta_k) \quad (6.23)$$

Channel impulse response $h_k^i(t)$ for the i^{th} transmit antenna is given by

$$h_k^i(t) = \sum_{l=1}^{L} \beta_{kl}^i e^{j\gamma_{kl}^i} \delta\left(t - \tau_{kl}^i\right). \quad (6.24)$$

Received signal $r_{k,t}$ for the user at time *t* is a superposition of the signals coming from all the transmit antennas, and is given by

$$r_{k,t} = \frac{1}{\sqrt{n_T}} \sum_{i=1}^{n_T} \int_{-\infty}^{\infty} s_{k,t}^i(\tau) h_k^i(t - \tau) d\tau \; + \; n_{k,t}. \quad (6.25)$$

By following an argument similar to that of the previous section, we can show that:

$$r_{k,t} = \frac{1}{\sqrt{n_T}} \sum_{i=1}^{n_T} \sum_{l=1}^{L_i} \beta_{kl}^i{}_{kl} e^{j\gamma_{kl}^i} \; c_k\left(t - \tau_{kl}^i\right) b_k\left(t - \tau_{kl}^i\right) cos\left(\omega_c\left(t - \tau_{kl}^i\right) - \theta_{kl}^i\right) + \; n_{k,t}$$

$$(6.26)$$

where L_i is number of paths for the signal transmitted from antenna *i*. For a multi-user system comprising *K* users, the received signal *r(t)* is a linear superposition of the signals for the users, and is given by

$$r(t) = \frac{1}{\sqrt{n_T}} \sum_{k=1}^{K} \sum_{i=1}^{n_T} \sum_{l=1}^{L_i} \beta_{kl}^{i} e^{j\gamma_{kl}^{i}} \; c_k\left(t - \tau_{kl}^{i}\right) b_k\left(t - \tau_{kl}^{i}\right) cos\left(\omega_c\left(t - \tau_{kl}^{i}\right) - \theta_{kl}^{i}\right) + \; n_{k,t} \tag{6.27}$$

6.7.3 Space-time coded CDMA system with transmit and receive diversity

The space-time coded CDMA system of the previous section involves multiple transmit but single receive antenna. The treatment is now extended to a case involving multiple antennas at both ends. Consider a CDMA system having multiple n_T transmit and n_R receive antennas. The space-time coded user data $\boldsymbol{b_{k,t}}$ is given by Equation 6.22 stated earlier. Received signal $r_{k,t}^{j}$ at j^{th} receive antenna and time *t* is a superposition of the signals coming from all the transmit antennas. Received signals for the all the receive antennas can be represented by:

$$\begin{aligned} \boldsymbol{r_{k,t}} &= \; \{r_{k,t}^{j}\}, \qquad\qquad j = 1,2, \ldots \; n_R \\ &= \{r_{k,t}^{1}, \; r_{k,t}^{2}, \ldots, r_{k,t}^{n_R}\} \end{aligned} \tag{6.28}$$

Channel impulse response $h_k^{i,j}$ for the i^{th} transmit antenna and j^{th} receive antenna is given by

$$h_k^{i,j}(t) = \sum_{l=1}^{L_{i,j}} \beta_{kl}^{i,j} e^{j\gamma_{kl}^{i,j}} \delta\left(t - \tau_{kl}^{i,j}\right). \tag{6.29}$$

Following a similar argument to that of the previous section, it can be shown that the signal received at the j^{th} receive antenna at time *t* for a multi-user system comprising *K* users is given by

$$r^{j}(t) = \frac{1}{\sqrt{n_T}} \sum_{k=1}^{K} \sum_{i=1}^{n_T} \sum_{l=1}^{L_{i,j}} \beta_{kl}^{i,j} e^{j\gamma_{kl}^{i,j}} \; c_k\left(t - \tau_{kl}^{i,j}\right) b_k\left(t - \tau_{kl}^{i,j}\right) cos\left(\omega_c\left(t - \tau_{kl}^{i,j}\right) - \theta_{kl}^{i,j}\right) + \; n_{k,t}^{j} \tag{6.30}$$

The array of signals $\{r_{k,t}^{1}, \; r_{k,t}^{2}, \ldots, r_{k,t}^{n_R}\}$ from the n_T transmit antennas can be combined using a receive diversity technique such as maximal ratio combining, equal gain combining and selection combining.

6.7.4 Space-time coded multi-carrier CDMA system

Theoretical treatment so far involves single carrier transmission. We shall now be developing theory for a multicarrier CDMA system. In doing this, we shall approach the problem by considering OFDM modulation.

Assume that each serial data symbol sub-stream, after space-time coding is converted to, say, N_p parallel symbols, having a symbol duration T_s. Each OFDM frame consists of N_p coded symbols, which modulate N_p subcarrier frequencies f_0, f_1, f_2,…, f_{Np-1}, where the subcarrier frequency $f_p = f_o+p/(N_pT_s)$, where f_o is RF frequency, and p = 1,2,3, …, N_p-1. Considering that the complex symbols to be transmitted in a N_P-subcarrier OFDM system to be represented by $\left(X_{-N_p/2},\ldots,X_{-1},X_1,X_2,\ldots,X_{N_p/2}\right)$, one OFDM symbol can be represented mathematically by [149]

$$s(t)=\begin{cases}\displaystyle\sum_{p=-Np/2,p\neq 0}^{Np/2} X_n e^{j2\pi f_p t}, & for\ pT-T_w-T_g\leq t\leq pT+T_{FFT}+T_w \\ 0 & otherwise\end{cases} \quad (6.31)$$

where f_p is the frequency of the pth subcarrier, $T_{FFT}=N_pT_s$ is the duration of the total number of FFT-points, T_s is the sampling rates, T_g is the duration of the cyclic prefix, and T_w is the duration of the windowing. The transmitted OFDM signal can be demodulated by applying inverse operations to (6.31) as

$$x_p=\frac{1}{T_{FFT}}\int_{t=0}^{T_{FFT}} s(t)e^{-j2\pi f_p t}dt. \quad (6.32)$$

The multicarrier signal *s(t)* is obtained from addition of the different subcarrier signals. The resulting OFDM symbols are transmitted simultaneously from the individual transmit antennas. The received signal *r(t)* is a convolution of these and the channel impulse response corrupted by noise. To recover the original data, fast Fourier transform (FFT) is used at the receiver to reverse the effect of OFDM. In actual implementation in OFDM systems, to avoid inter-symbol-interference (ISI), cyclic prefix is appended to each OFDM frame. The cyclic prefix is a copy of the last L_p samples of the OFDM frame, so that the overall OFDM frame length is N_p + L_p. The cyclic prefix is added after IFFT at the transmitter, and removed at the receiver before FFT.

6.8 Simulation results and discussion

Software simulations were carried out to investigate the performance of an OFDM-modulated as well as a space-time block-coded (STBC) MC-CDMA system in a Rayleigh frequency-selective fading channel. The channel is modelled as being quasi-static, meaning that the fading process remains constant during transmission of each data frame. We shall begin by looking at results for transmit and receive space diversity, followed by the performance of a CDMA system in flat-fading channel.

6.8.1 Transmit versus receive diversity

This section compares simulation results for transmit and receive diversity for transmission over a Rayleigh flat-fading channel. The transmit diversity (2 x 1) corresponds to the so-called Alamouti scheme. For comparison, the results for a no-diversity link (single transmit-receive antenna) is also shown (Fig. 6.5).

The results (Fig. 6.5) show that using two transmit antennas and one receive antenna (2x1) provides the same diversity order as the maximal-ratio combined (MRC) system of one transmit antenna and two receive (1x2) antennas. Also the receive diversity has a 3 dB advantage when compared to the transmit diversity.

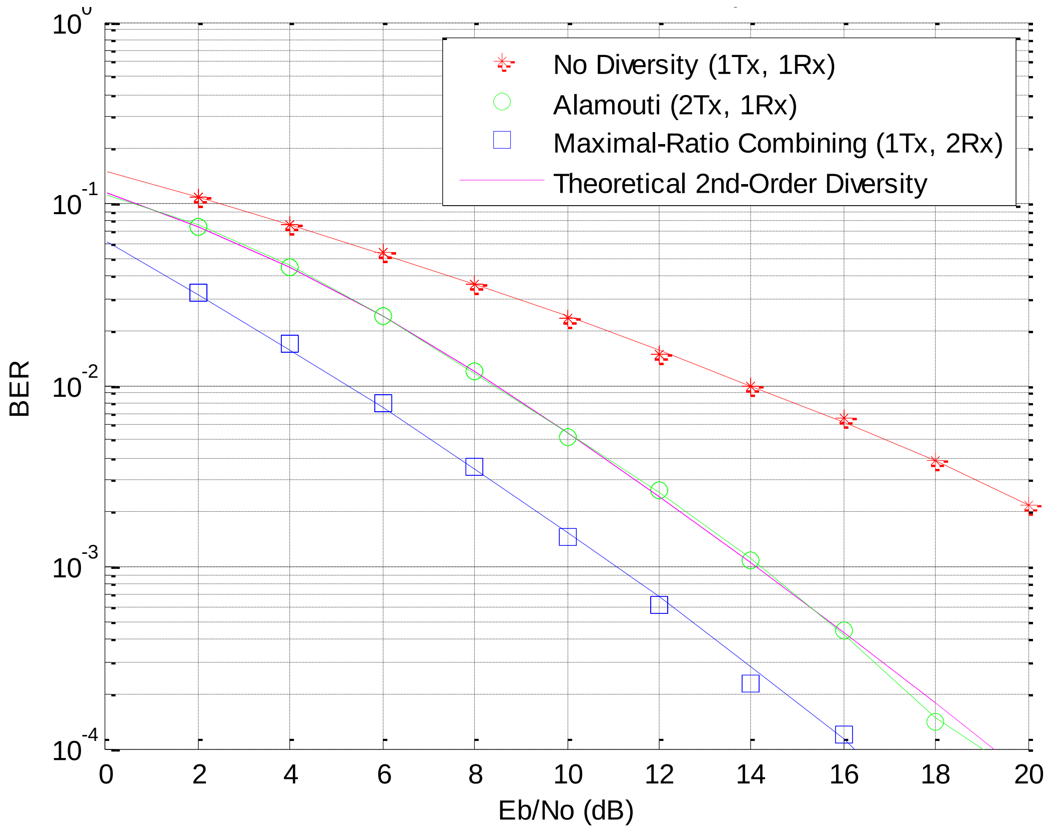

Fig. 6.5 Transmit versus receive diversity for BPSK modulation

The previous result involves binary phase shift keying (BPSK) symbols. The next figure shows similar results for transmission of quadrature phase shift keying (QPSK) modulation. It can be seen that the change of modulation order does not affect the system diversity. It can be observed that the 2x1 transmit antenna still provides the same diversity gain as the 1x2 receive diversity, and that the latter has a 3dB advantage over the former. However, the results show that the analytic 2nd order curve now coincides with the 1x2 system, and not the 2x1 system.

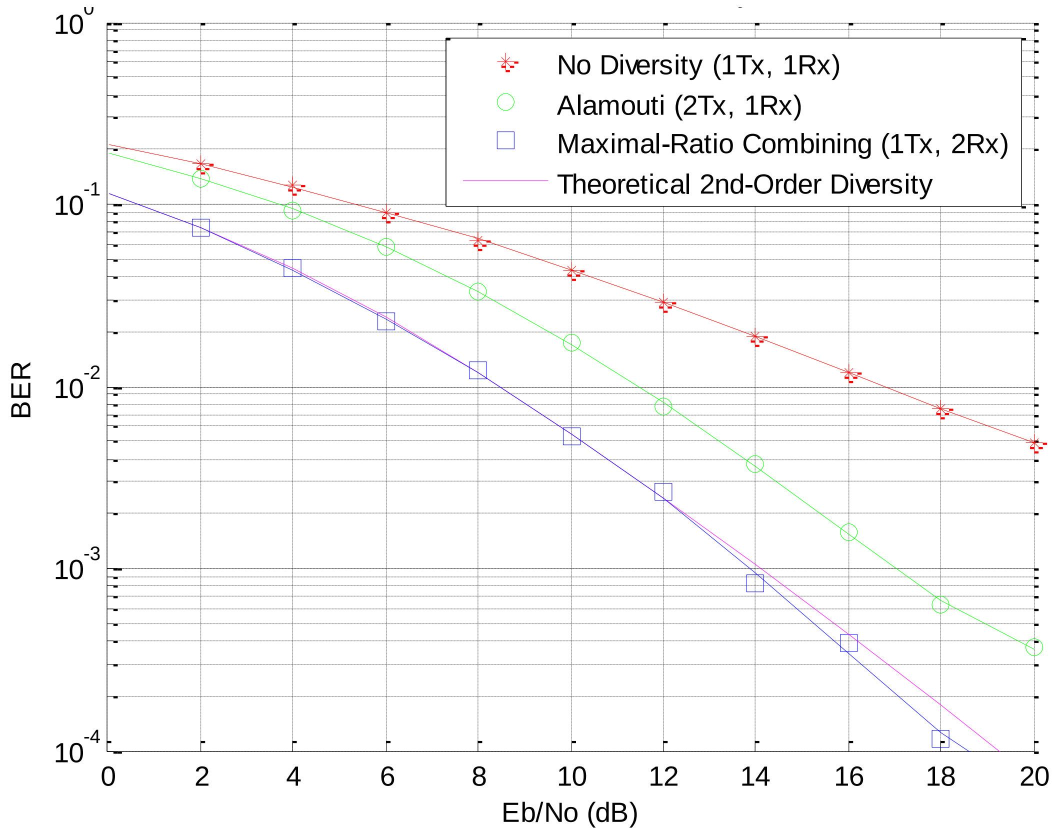

Fig. 6.6 Transmit versus receive diversity for QPSK modulation

6.8.2 Space-time block-coded versus CDMA system

This section compares the performance of a Gold-coded CDMA system with that of transmit 2x1 and receive 1x2 diversity system for a single user in a flat-fading Rayleigh channel. For the CDMA, 31-chip Gold code was used as spreading sequence for BPSK symbols. The next figure shows the results. For comparison, uncoded data transmission for a no-diversity, transmit and receive diversity are included. Looking at this figure, it can be seen that the use of Gold code provides coding gain of about 16 dB, compared to the uncoded, no-diversity case. However, the Gold code provides no diversity gain. This is expected, particularly in a flat-fading channel. Another look at this results show that in terms of BER, at low SNR (or Eb/No) the coding gain provided by the Gold code surpasses the diversity advantage provided by the use of the multiple antenna.

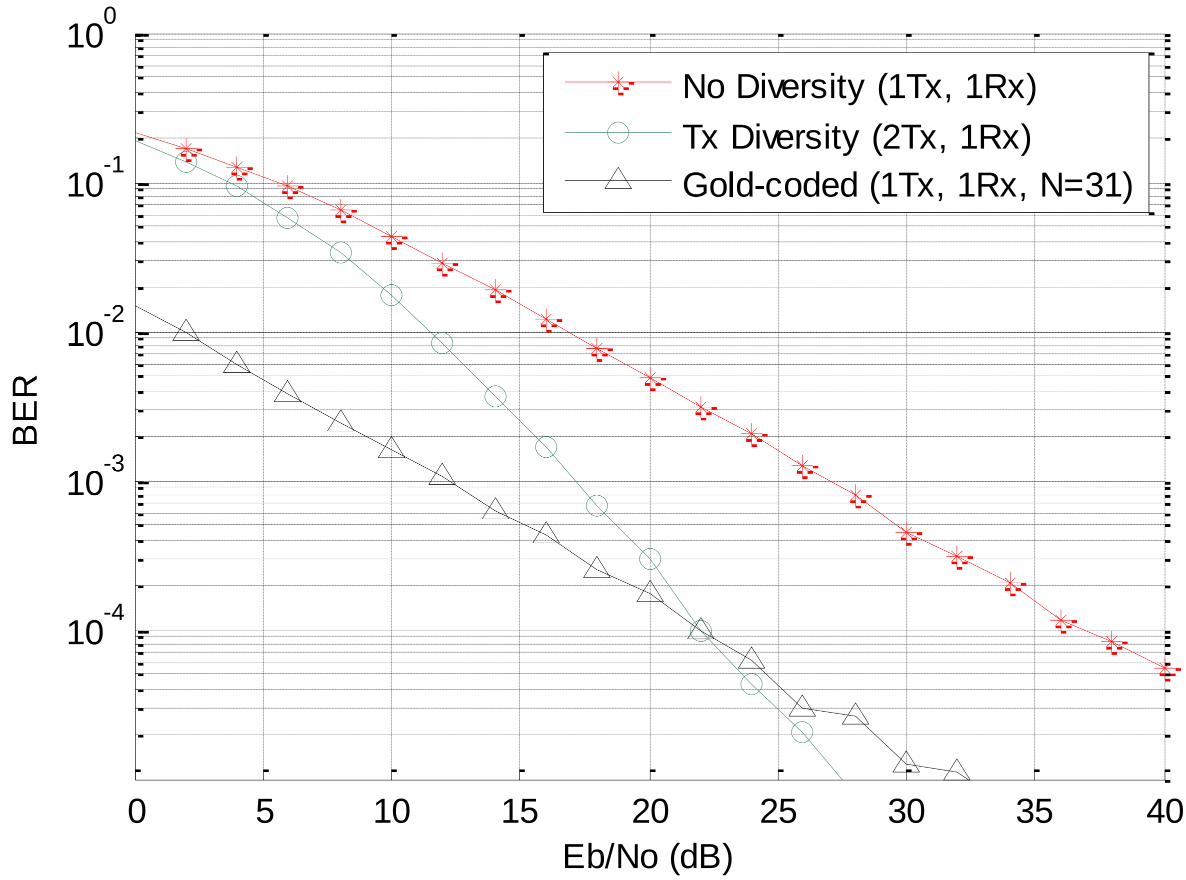

Fig. 6.7 Performance of a Gold coded CDMA system versus STBC

6.8.3 Space-time block-coded CDMA system

This section presents the performance of a space-time block-coded (STBC) CDMA system. Fig. 6.8 shows the results for a 31-chip Gold code. Looking at this figure, it can be seen that the STBC-CDMA system provides both diversity and coding gain. The curve for the plain 2x1 system is seen to be parallel to that of the STBC-CDMA system, which clearly shows that the space-time coding is solely responsible for the diversity gain, while Gold code encoding is responsible for the coding gain. In the composite STBC-CDMA system, the diversity advantage of the STBC is complemented by the coding gain of the CDMA, giving better system performance. Diversity decreases the asymptotic error rate as a function of signal-to-noise ratio (SNR), while coding gain provides vertical shift of the error performance curve. At a BER of 10^{-3}, there exists about 12 dB difference between the coding gain of a CDMA-only system and its space-time-coded counterpart. This difference in coding gain grows with decent in BER. Apart from these, the figure also shows that the coding gain between the no-diversity link and its Gold-coded counterpart is the same as that between the transmit-diversity link and its Gold–coded counterpart.

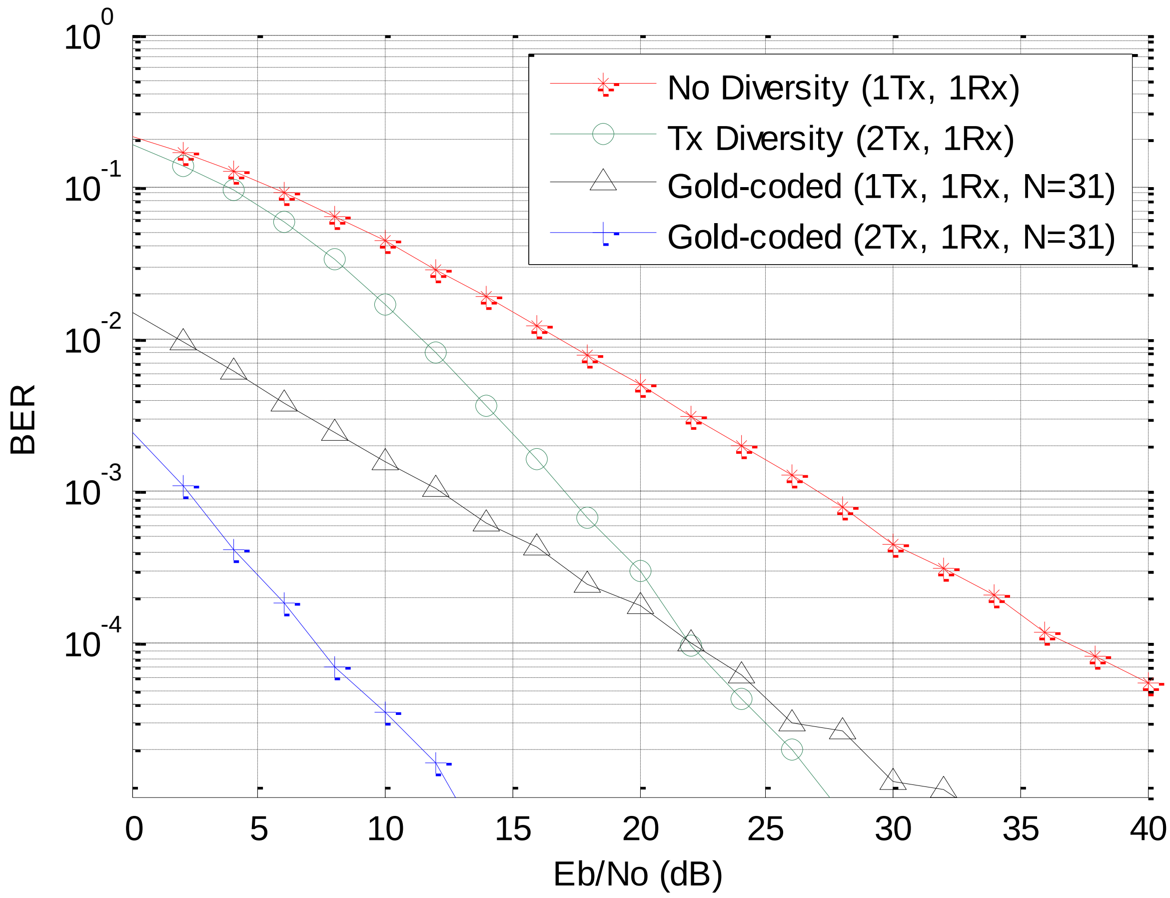

Fig. 6.8 Performance of a STBC-CDMA system using a 31-chip Gold code as spreading sequence.

Fig. 6.9 shows simulation results for a 127-chip Gold code. It can be seen that this figure has similar features with the results for 31-chip Gold code. However, the 127-chip provides greater coding gain than the 31-chip Gold code. This is expected, consequent to difference in process gains of the codes. Fig. 6.10 and 6.11 shows results for a 511-chip and 2047-chip Gold codes respectively. These figures agree with the observations stated earlier. As expected, it is clear that a longer code give better error-rate performance, but at the expense of greater transmission bandwidth as a penalty.

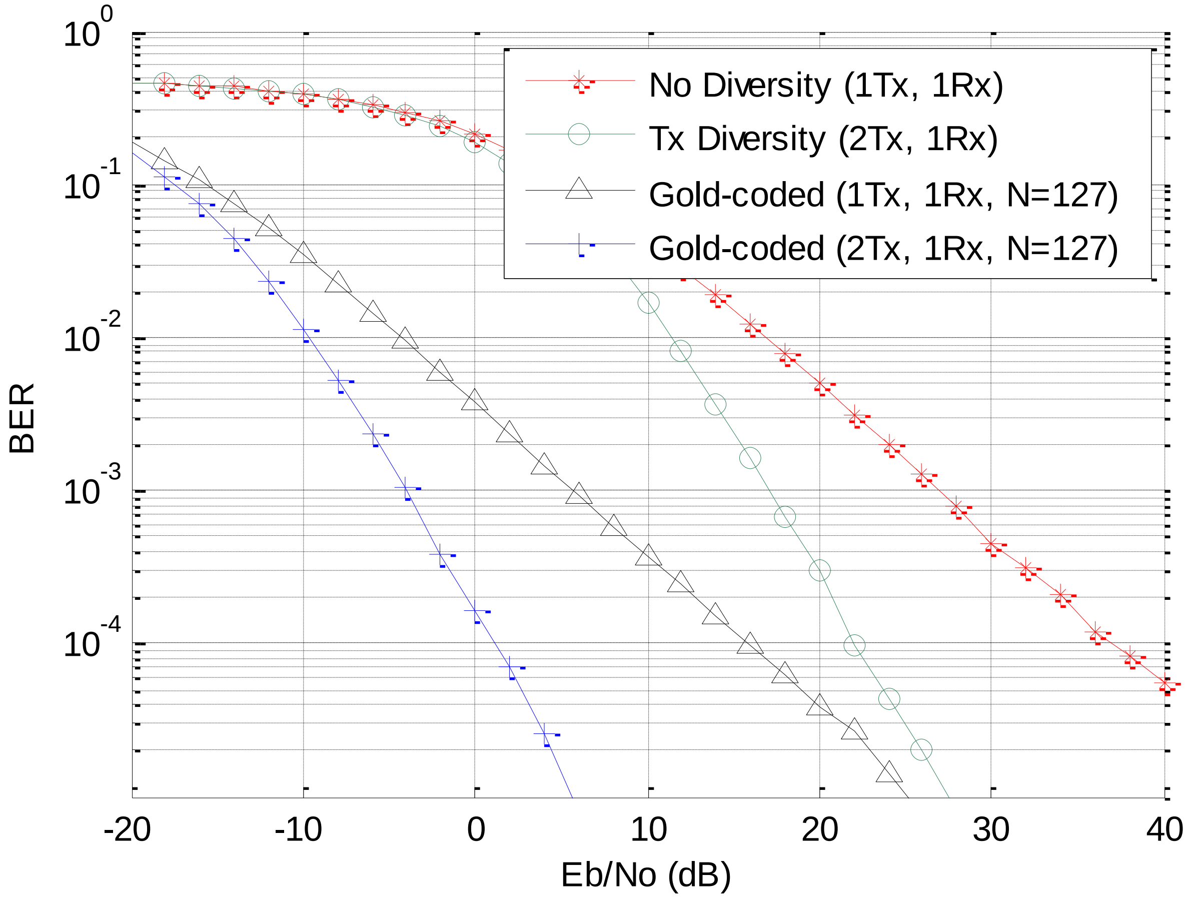

Fig. 6.9 Performance of a STBC-CDMA system for a 127-chip Gold code

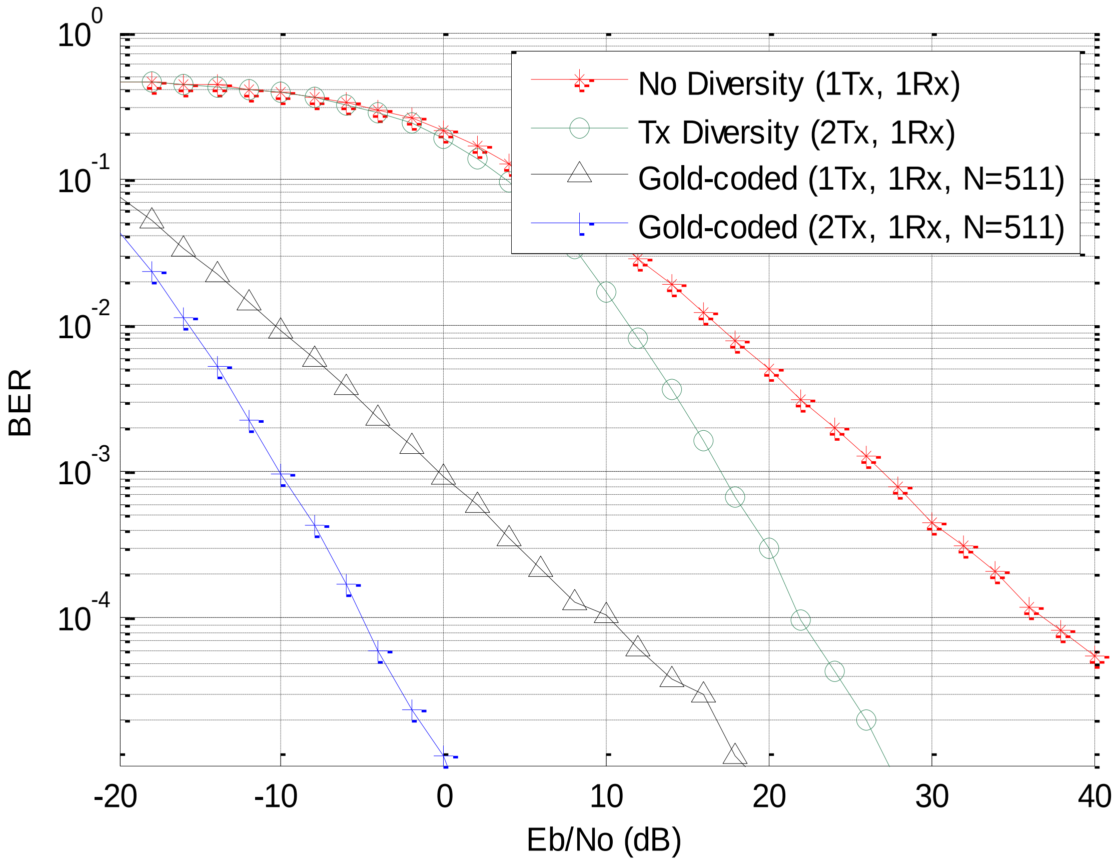

Fig. 6.10 Performance of a STBC-CDMA system for a 511-chip Gold code

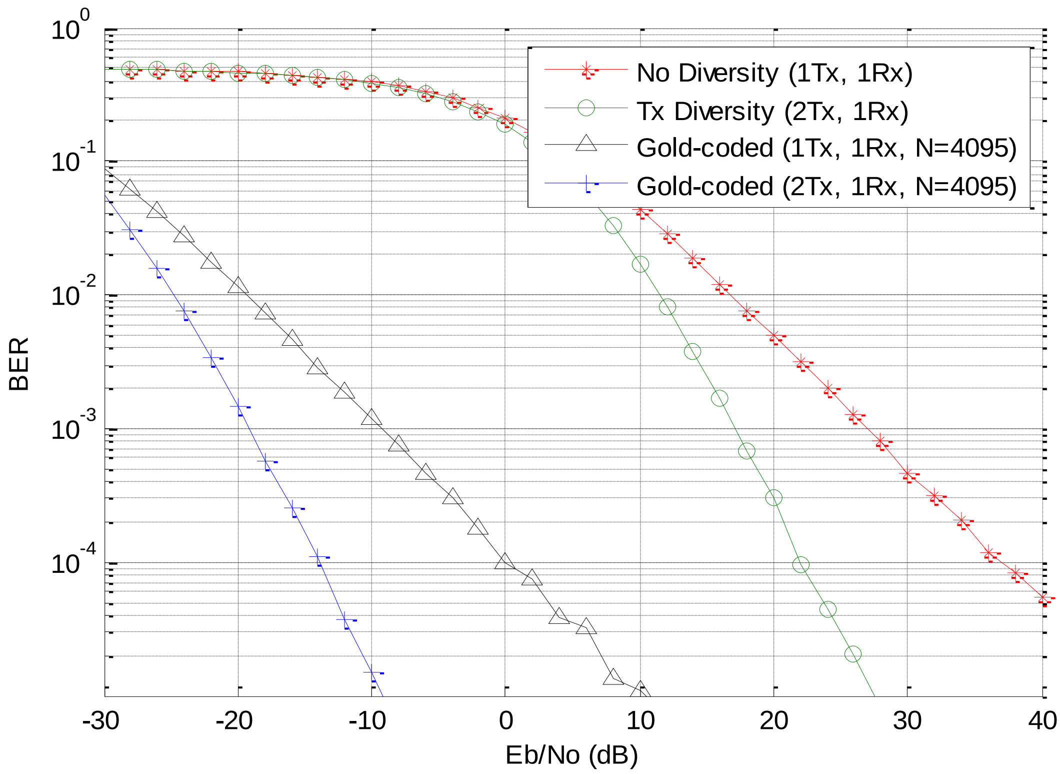

Fig. 6.11 Performance of a STBC-CDMA system for a 2047-chip Gold code

6.8.4 Performance in a frequency-selective channel

In addition to performance in a flat-fading channel, the system performance in a frequency-selective Rayleigh channel was also investigated for coded as well as uncoded data transmission. A four-path channel with fixed path delays and path gains were considered for a sample frequency of 10 kH. Table 6.1 shows the simulation parameters. The performance of a space-time coded OFDM system as well as a MC-CDMA system were investigated for a single user. The number of subcarriers was kept fixed at 64. The channel was modelled as being quasi-static, meaning that the fading process remains constant during transmission of each OFDM frame. Cyclic prefix was added after IFFT at the transmitter, and removed at the receiver before FFT. The simulation results shall now be presented as follows.

Table 6.1. Simulation parameters for the STBC MC-CDMA system

Modulation type	QPSK
Frame size	64 QPSK symbols
No. of subcarriers	64
Cyclic extension (25%)	16 symbols
Carrier frequency	900 MHz
Max Doppler shift	83.33 Hz
Sample Frequency	10 kHz
Number of paths	4
Path gains(dB)	0 -20 -30 -40
Path delays (μs)	0 1 5 10

6.8.5 Space-time coded OFDM system

Here, the performance of a space-time coded OFDM system in the frequency-selective channel is considered. For comparison, the results, Fig. 6.12, show the performance for a single-antenna, no-diversity (1x1) case, for transmit diversity and MRC receive diversity. The water-fall region of this figure shows that the transmit and the receive diversity schemes provide the same diversity gain. This agrees with expectation, both being second-order diversity schemes. However, the figure shows that the receive diversity has a 3-dB advantage over the transmit diversity. This is because total transmitted power is modelled to be the same in both cases, such that the power transmitted from each transmit antenna of the latter is half that of the former. If the transmitted power is made to be the same in both cases, then the performance would be identical. It is noteworthy that these features are similar to those observed for a flat-fading channel.

Another important feature of Fig. 6.12 is the appearance of error floor. This error floor cannot be attributed to multi-user interference, as there is no interferer here. Rather, it originates from multi-paths characteristic of a frequency-selective channel. The figure shows that the receive diversity's 3-dB advantage is lost in the error floor region, such that both thetransmit and the receive diversity schemes exhibit the same level of error floor.

Compared to no-diversity scheme, the benefit of using multiple-antenna is obvious, as revealed by the lowering of error floor by the latter. A close look at the performance curves (see data tips, Fig. 6.13) shows that whereas error floor for no-diversity is about 0.1475, it is about 0.0738 for transmit diversity (see data tips). Dividing the former by the latter gives 2.001, which indicates that the diversity scheme reduced the error floor by a factor of two.

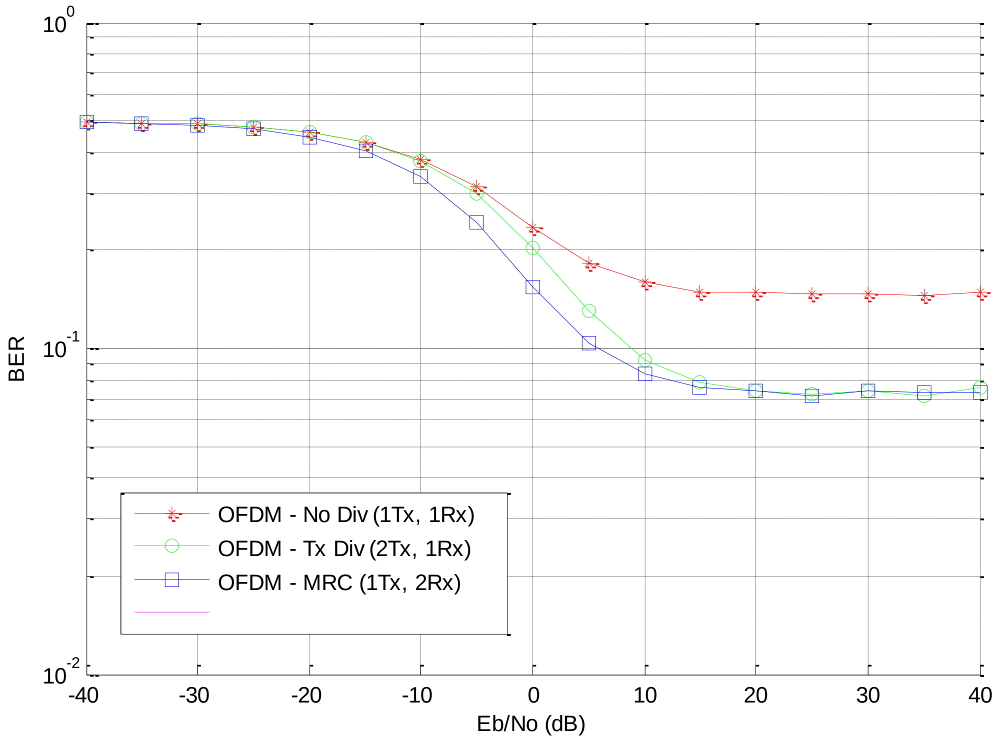

Fig. 6.12 Performance of a space-time coded OFDM system in a four-path frequency selective Rayleigh channel.

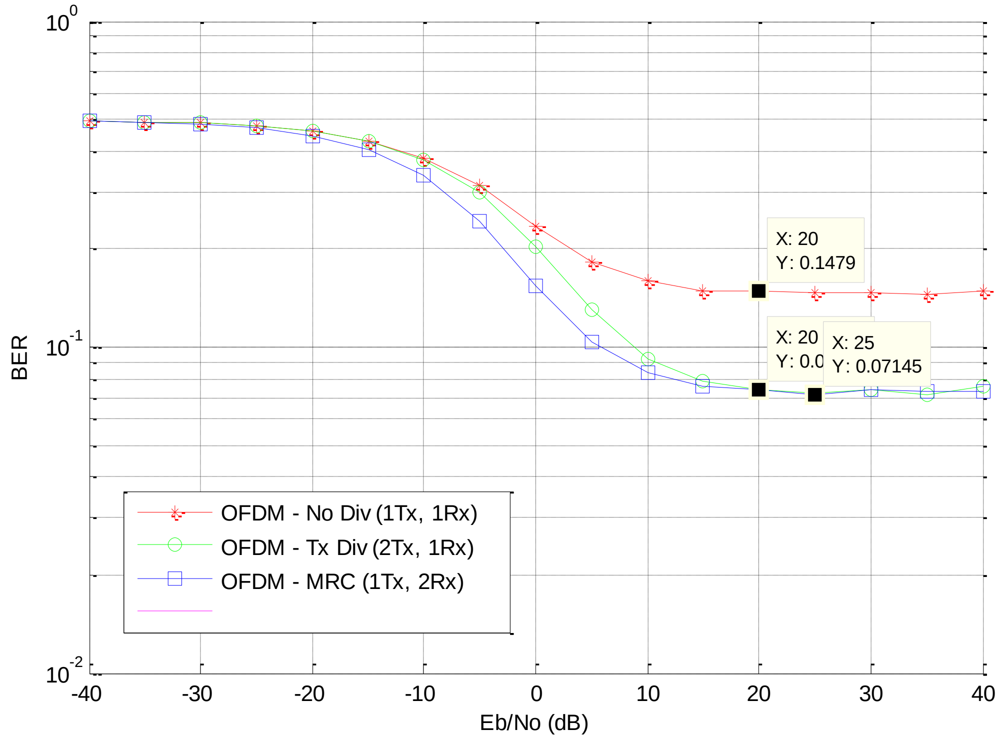

Fig. 6.13 Data tips showing the level of error floor for no-diversity and transmit-diversity transmission for the OFDM system.

6.8.6 Space-time coded MC-CDMA system

This section presents simulation results on the performance of a space-time coded multi-carrier CDMA system in the frequency-selective channel. Results for STC-OFDM are also included for the purpose of comparison. Simulations were carried out to investigate the system performance for Gold codes of different code lengths. Fig. 6.14 shows the results for a 31-chip Gold code. It is obvious from this figure that a STC MC-CDMA system has better performance than its STC-OFDM counterpart. Comparing no-diversity transmission shows that at a BER of 10^{-1}, the use of the 31-chip Gold codes in the MC-CDMA system provides a coding gain of about 16.272 dB relative to the OFDM system. For the transmit diversity scheme, the STC MC-CDMA provides a coding gain of about 15.516, relative to the OFDM system. Another look at the figure shows that the performance curves of STC MC-CDMA and the STC OFDM has similar slopes in the waterfall region. This indicates that the MC-CDMA provides no additional diversity gain to the STC MC-CDMA system. That is, for the 31-chip Gold-coded STC MC-CDMA system, diversity gain originates solely from the use of the multiple antennas, while coding gain comes from the Gold codes.

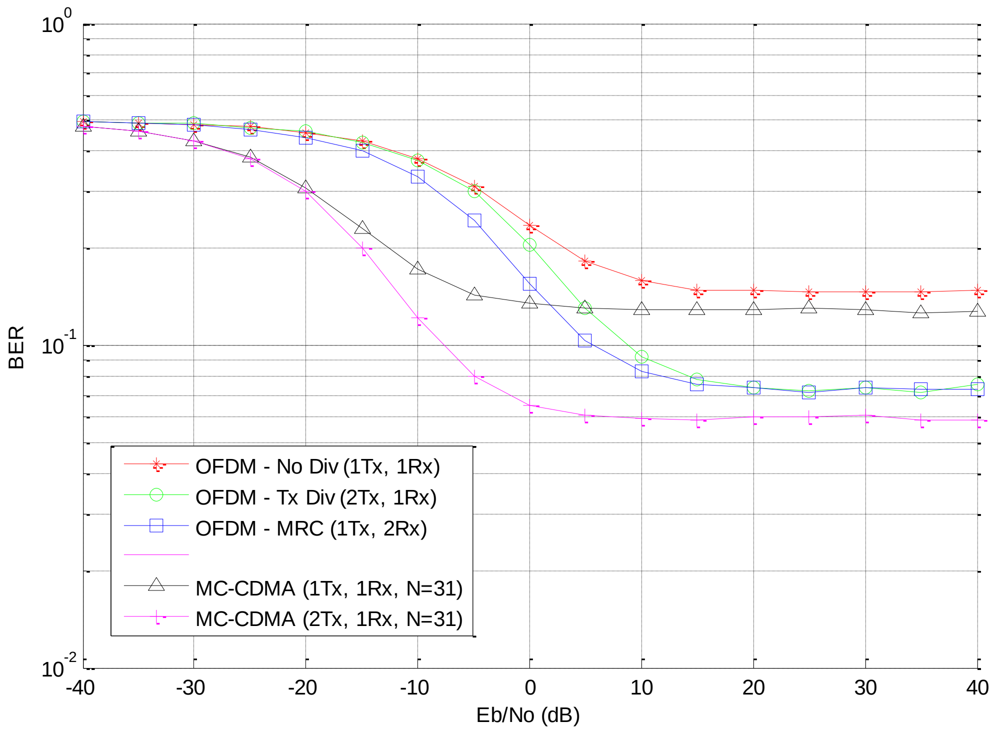

Fig. 6.14 Performance of a space-time coded MC-CDMA system for a 31-chip Gold code

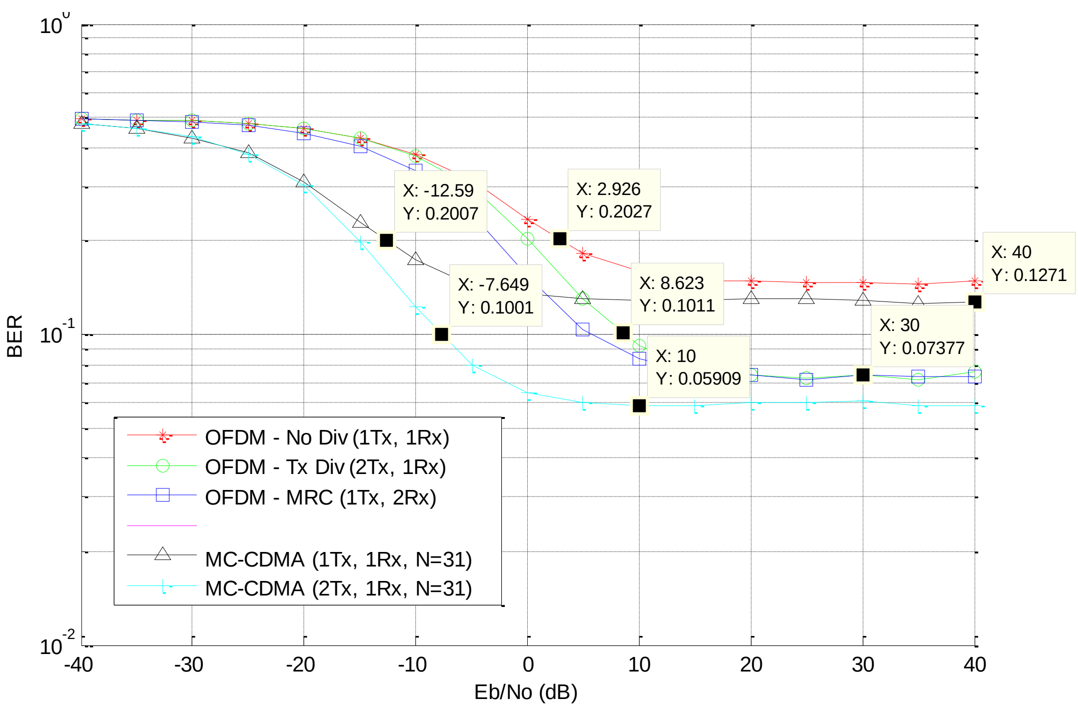

Fig. 6.15 Data tips showing data points for evaluating the performance of the MC-CDMA system for a 31-chip Gold code

Another important feature in this figure is the level of error floor. It is obvious from Fig. 6.15 that the STC MC-CDMA system has lower error floor than the STC-OFDM system. For the no-diversity scheme, error floor is about 0.1479 (Fig. 6.13) for OFDM transmission, and 0.1271 for MC-CDMA. For transmit-diversity scheme, error floor is about 0.0738 for OFDM transmission, and 0.0591 for MC-CDMA. For the MC-CDMA system, the results show that the use of transmit diversity provides about 2.164 reduction in error floor.

We shall now consider simulation results for a 127-chip Gold code, as shown by Fig. 6.16. Looking at this figure, it is obvious that this longer code gives a better performance than its 31-chip counterpart in terms of BER, coding gain, diversity gain and level of error floor. For the no-diversity transmission at a BER of 0.2, the 127-chip Gold codes provides a coding gain of about 24.944 dB relative to the OFDM system. Looking at the results for the transmit diversity scheme shows that for the 127-chip code, the performance curve for the STC MC-CDMA has steeper slope in the waterfall region than its STC-OFDM counterpart. This implies that the former has a higher diversity gain than the latter. This can be compared to the results for 31-chip Gold code, for which the two systems have similar slopes in the waterfall region. The extra diversity gain observable in the 127-chip system could only be attributed as coming from MC-CDMA counterpart. The use of a 127-chip code, the MC-CDMA provides not only coding gain, but also diversity gain.

Now turning to the level of error floor, the results show that for the no-diversity case, error floor is about 0.04214 for 127-chip MC-CDMA system. With reference to the OFDM system, this is equivalent to a factor of about 3.51 reduction in error floor. For transmit-diversity scheme, error floor is about for 0.0088 for the 127-chip MC-CDMA, which is equivalent to a factor of about 8.4164 reduction in error floor with reference to the OFDM case.

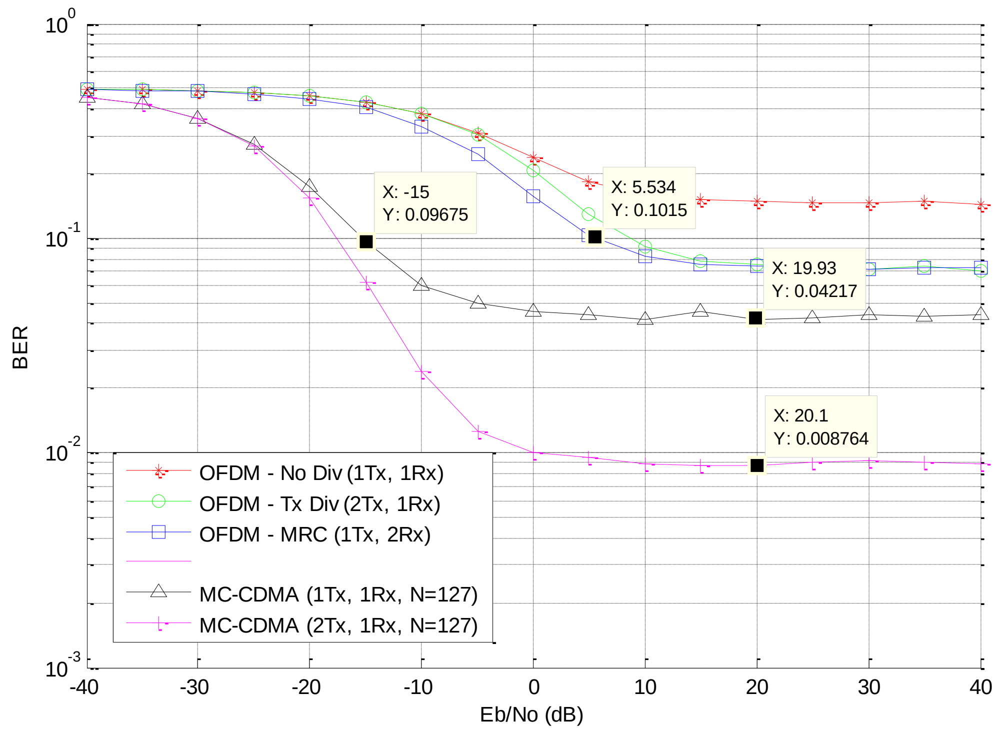

Fig. 6.16 Performance of a space-time coded MC-CDMA system for a 127-chip Gold code

The system performance was also investigated for longer codes. Fig. 6.17 shows the results for a 511-chip Gold code. Obviously from this figure, this longer code gives better performance, as indicated by the dramatic increase in diversity gain, and significant drop in the level of error floor. It is obvious that the slope of the STC MC-CDMA system is significantly steeper, indicating higher diversity gain. The increase in diversity gain for the longer 511-chip could only be attributed as coming from the MC-CDMA

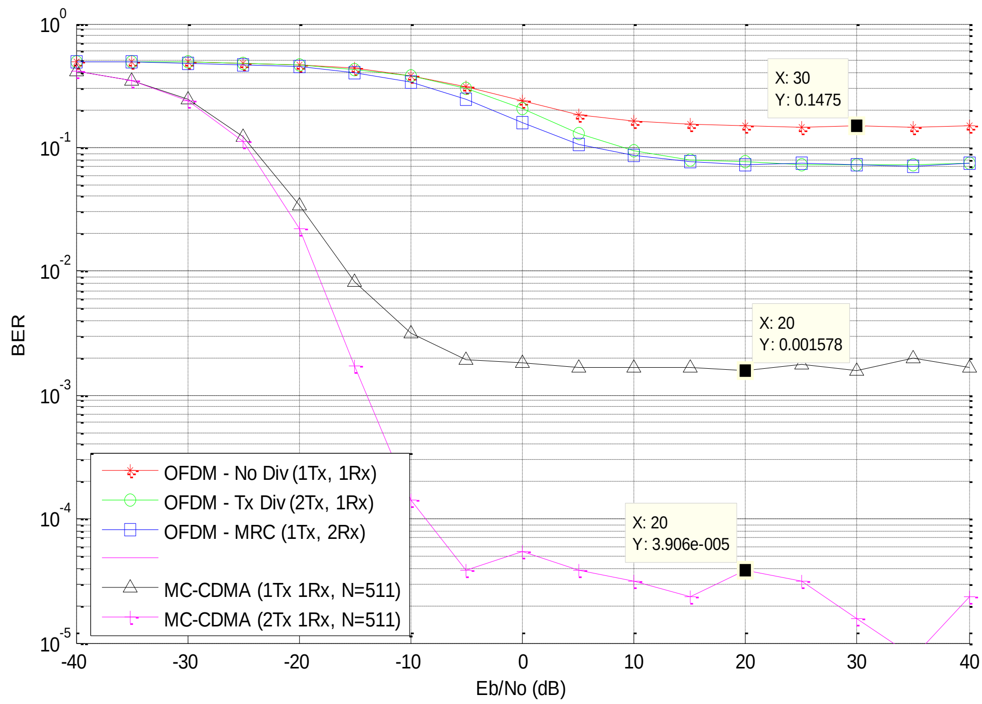

Fig. 6.17 Performance of a space-time coded MC-CDMA system for a 511-chip Gold code

Considering level of error floor, the results show that for the no-diversity case, error floor is about 0.0016 for 511-chip MC-CDMA system. With reference to the OFDM system, this is equivalent to a factor of about 93.726 reduction in error floor. For transmit-diversity scheme, error floor is about for 3.906×10^{-5} for the 511-chip MC-CDMA, which is equivalent to a factor of about 3,786 reduction in error floor with reference to the OFDM case.

We shall now consider simulation results for the performance of a 2047-chip code, as shown by Fig. 6.18. This figure shows dramatic increase in the system performance. The slope of the performance curves for the 2047-chip code is incomparably steep. The graph also shows sharp drop in error floor such that the error floor is not even visible within the limit of lowest BER shown by the figure. Intuition suggests making an attempt to find out the error floor for the code. However, this would require generating results for lower BER, but the time penalty required for doing this does not make it feasible. (Results shown here took about two days of continuous running of simulations. Hence going down in BER by, say, two orders of magnitude to give a BER of 10^{-7} would entail processing 100-fold the data samples, and that will require about 200 days of continuous simulation, which is not practicable.)

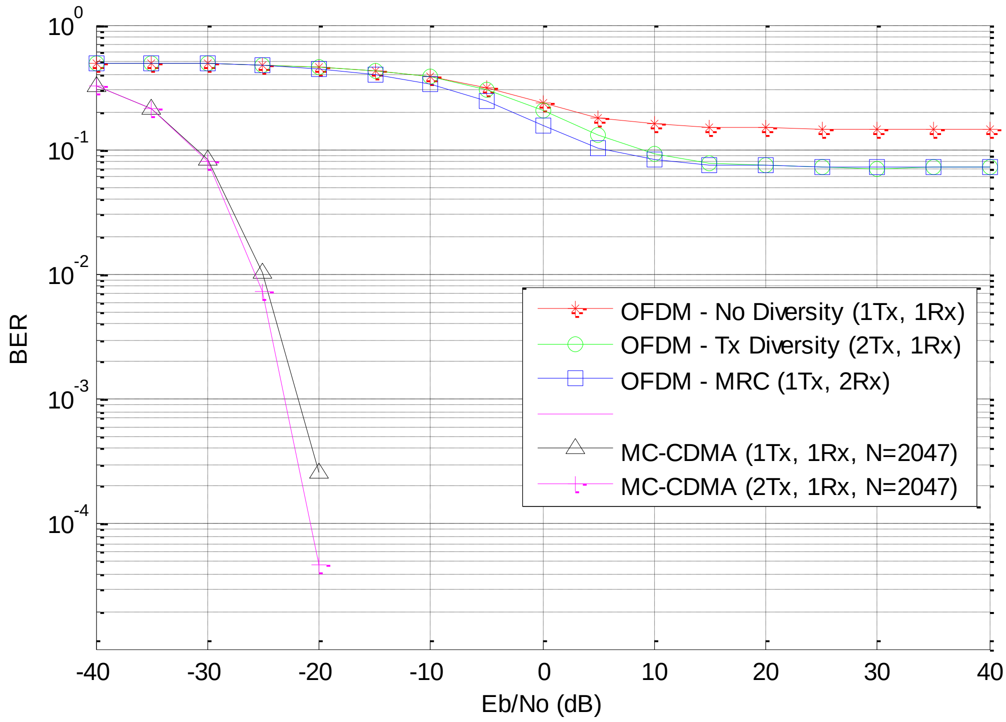

Fig. 6.18 Performance of a space-time coded MC-CDMA system for a 2047-chip Gold code

6.9 Chapter summary

Among other things, this chapter presents results for the performance of a space-time block-coded multi-carrier CDMA system. The treatment began by examining results for 2x1-transmit and 1x2-receive diversity schemes, both of which gave similar diversity gain, both being second-order diversity schemes. This chapter then investigated the performance of a STBC CDMA system for different chip lengths. Results showed that at low signal-to-noise ratio, the coding gain provided by the codes surpasses the diversity advantage provided by the use of the multiple antennas. The results also showed that in a flat-fading channel, coding gain between no-diversity link and its Gold-coded counterpart is the same as that between the transmit-diversity link and its Gold–coded counterpart. The independence of the diversity advantage provided by multiple transmit antennas and the coding gain obtainable from the use of the spreading sequences enables the prediction of the performance of composite space-time block-coded CDMA systems.

This chapter also investigated the performance of a space-time coded OFDM system in a frequency-selective channel. Results showed that the receive diversity's 3-dB advantage over its transmit diversity counterpart was lost in the error floor region, such that both the transmit and the receive diversity schemes exhibited the same level of error floor. The results also showed that with reference to no-diversity transmission, the diversity schemes reduced the system error floor by a factor of two.

Results of investigation on the performance of a STC MC-CDMA system was also presented, and the outcome of which showed that the combination of diversity gain in the use of multiple antennas, coupled with coding gain provided by the Gold codes of the CDMA system, plus the diversity gain resulting from frequency diversity of multi-carrier transmission and the spectrum-spreading by the CDMA makes the composite system resilient to fading. This fact is particularly the case for long codes.

Chapter 7

Conclusion and Future Work

7.0 Introduction

This concluding chapter gives a brief summary of the main contributions and findings of this thesis. Suggestions on likely extension of the work are also itemized in this chapter.

The significance of wireless communication in the present information age cannot be over-emphasized. From the early days of mobile communication, code-division multiple-access (CDMA) has been one of the primary multiple-access techniques in mobile technology. The technique, whose evolution dates back to the 1940s, was primarily for military applications in its early days, due to its jam-resistant and signal-hiding capability. Over the years however, CDMA has become an important access technique not only in mobile technology, but also in satellite communication. This thesis is a contribution to the development of CDMA technology. A summary of the outcome of the work reported in this thesis is hereby given as follows.

7.1 Thesis summary

CDMA relies on coding to achieve its multiple-access property. It assigns each user a unique code, which is used to encode the user signal at the transmitter end. The receiver, knowing the code sequence of the user, decodes the received signal after reception to recover the original signal. CDMA codes, called spread-spectrum codes, pseudo-noise (PN) codes or pseudo-random noise (PRN) codes play a critical role in the performance of CDMA systems. A CDMA system can do no better than the properties of its codes allow. Poor codes yield poor system performance. In line with this, initial aspect of this PhD work was directed at learning about CDMA codes. Different types of codes were considered, out of which Gold codes were selected.

Following the code selection process, different sets of Gold codes were generated, after which software simulations were carried out on their correlation properties. This was necessary to confirm that the codes possess expected properties. After experimenting with the correlation properties of the codes, a CDMA baseband model was simulated for signal transmission through a noiseless, non-fading channel. Basically, this involved PN-encoding-decoding, and it helps to further validate the Gold codes. This signal transmission was carried out for different data sizes, ranging from a few data bits (e.g. 4 bits) up to a million random bits. Since the transmission was through a noiseless channel, it is expected that every transmitted signal should be received without any errors. Simulation results agreed with this. Furthermore, the codes were tested for signal transmission through a noisy channel. In this case, it was expected that as signal-to-noise ratio (SNR) goes down, errors should creep into the recovered bit streams. Simulation results confirmed this to be the case: as SNR decreased, bit-error-rate (BER) worsened. The results were also tested with the aid of scatter plots.

Following the code testing process, multiple-access performance of even- and odd-degree Gold codes in a multi-user system was investigated. The investigation entailed software simulations for different sets of Gold codes, ranging from 31-chip to 4095-chip Gold codes, from light to heavy system loading, involving up to about a thousand simultaneous users. Results of the investigation showed that odd-degree Gold codes have better multiple-access performance than their even-degree counterparts. Whereas the latter exhibited error floor and system saturation when the system was loaded, no such performance degradation was noticeable in the former. The results suggest that the odd-degree Gold codes are better suited for multiple-access applications than their even-degree counterparts.

Any particular code is normally expected to have a maximum number of users that would be tolerated, a number that is believed to be well below full load. In contrast, simulation results presented in this thesis showed that with good choice of codes, the number of available codes can go up to full-load. This is another important contribution of this thesis.

Furthermore in this thesis, software simulations were carried to investigate the performance of a direct-sequence (DS) CDMA system in a flat-fading Rayleigh channel, and a multi-carrier (MC) CDMA system in a frequency-selective channel. Random QPSK symbols were generated and transmitted through the channel using different sets of Gold codes as spreading sequences. The influence of code length on the system performance was investigated for a given number of tones and data rate for coded as well as uncoded data transmission. The results showed that a longer code gives better error rate performance, though at the expense of increased transmission bandwidth. In addition, the results indicated that primarily, irreducible error floor is not due to multiple-access performance of the codes, but channel fading. The results also showed that in a flat-fading channel, the Gold codes provide a constant coding gain close to that obtainable in a Gaussian channel. Apart from this, this thesis showed that the impact of longer spreading codes was more pronounced for the MC-CDMA system in a frequency-selective channel as indicated by significant lowering of error floors. Also, frequency diversity associated with the use of longer codes coupled with multi-carrier modulation makes the MC-CDMA system resilient to multi-path effects.

Further still, this thesis presented simulation results on the performance of a space-time block-coded (STBC) MC-CDMA system. The treatment began by examining the performance of simple transmit and receive diversity schemes, followed by the performance of a STBC CDMA system. Results showed that at low signal-to-noise ratio, the coding gain provided by the codes surpasses the diversity advantage provided by the use of the multiple antennas. The results also showed that in a flat-fading channel, coding gain between no-diversity link and its Gold-coded counterpart is the same as that between the transmit-diversity link and its Gold–coded counterpart.

The work on transmit-receive diversity was followed by an investigation of the performance of a STBC OFDM system in a frequency-selective channel, after which the performance of the same was compared with that of a STBC MC-CDMA system. Results showed that the combination of diversity gain from the use of multiple antennas, coupled with coding gain provided by the Gold codes of the CDMA system, plus the diversity gain resulting from frequency diversity of multi-carrier transmission and the spectrum-spreading by the CDMA makes the composite STBC MC-CDMA system resilient to channel fading. This fact is particularly the case for long codes. For example, with reference to the OFDM transmission, the results showed that a 511-chip Gold-coded STC MC-CDMA system provided a factor of about 3,786 reduction in error floor.

7.2 Future work

Some recommendations on possible future work shall now be highlighted as follows.

Throughout this thesis, perfect synchronization was assumed, which generally does not apply in practice, particularly in the uplink. Investigating effects of lack of synchronization might be a worthwhile future work.

In this thesis, knowledge of channel impulse response (CIR) at the receiver was assumed. As an extension of this work, effect of imperfect knowledge of CIR may be considered.

For the multi-carrier transmission, this thesis assumed fixed number of sub-carriers. A consideration of the effect of number of sub-carriers on the system performance might be a useful future work.

This work involved variable transmission bandwidth, consequent to the variable code lengths. Future work may consider effects of having fixed transmission bandwidth.

This work assumed constant path gains and constant path delays. Future considerations may extend this work to the case of variable path gains and path delays.

For the frequency-selective channel, *four* multi-paths were assumed. As an extension, the simulation may be repeated for some other number of paths.

The investigation on multiple-access performance of Gold codes was carried out for some representative sets of codes. Thus in the future, the simulation can be carried out on more code samples. Furthermore, the possibility of developing an analytic solution for the problem may be explored.

In the simulations for space-time coded systems, single user rather than multiple users was assumed. Thus, this work can be extended to the case of multiple users.

For space-time coding, considerations was limited to two antennas. Hence, this work can be extended to that involving higher number of antennas. Apart from this, this work only considered space-time block codes. As a future extension, other types of space-time codes can be considered.

In this work, effect of interleaver was not considered. As a future extension, effect of interleaver on the system performance may be investigated.

References

[1] O. O. Oyerinde, "Channel Estimation for SISO and MIMO OFDM Communication Systems," PhD, School of Electrical, Electronic and Computer Engineering, University of KwaZulu-Natal, Durban, 2010.

[2] R. Prasad, *CDMA for Wireless Personal Communications* Artech House, 1996.

[3] Z. Wei, X.-G. Xia, and K. Ben Letaief, "Space-Time/Frequency Coding for MIMO-OFDM in Next Generation Broadband Wireless Systems," *Wireless Communications, IEEE*, vol. 14, pp. 32-43, 2007.

[4] Q. M. Rahman and A. B. Sesay, "Non-coherent MT-CDMA system with diversity combining," in *Electrical and Computer Engineering, 2001. Canadian Conference on*, 2001, pp. 1351-1356 vol.2.

[5] Q. M. Rahman and A. B. Sesay, "MT-CDMA system with two stage maximum likelihood symbol estimation," in *56th Vehicular Technology Conference, September 24, 2002 - September 28, 2002*, Vancouver, BC, Canada, 2002, pp. 539-543.

[6] Q. M. Rahman and A. B. Sesay, "Performance analysis of MT-CDMA system with diversity combining," in *Military Communications Conference, 2001. MILCOM 2001. Communications for Network-Centric Operations: Creating the Information Force. IEEE*, 2001, pp. 1360-1364 vol.2.

[7] Q. M. Rahman and A. B. Sesay, "Two-stage maximum likelihood estimation (TSMLE) for MT-CDMA signals," in *Canadian Conference on Electrical and Computer Engineering, May 13, 2001 - May 16, 2001*, Toronto, Ont., Canada, 2001, pp. 111-116.

[8] K. Pietikäinen. (11 Nov). *Orthogonal Frequency Division Multiplexing*. Available: http://www.comlab.hut.fi/opetus/333/2004_2005_slides/ofdm_text.pdf

[9] R. Prasad and S. Hara, "An overview of multi-carrier CDMA," in *Spread Spectrum Techniques and Applications Proceedings, 1996., IEEE 4th International Symposium on*, 1996, pp. 107-114 vol.1.

[10] S. Hara and R. Prasad, "Overview of multicarrier CDMA," *Communications Magazine, IEEE*, vol. 35, pp. 126-133, 1997.

[11] B. Golkar and F. Danilo-Lemoine, "Bit error rate analysis of multiuser and space-time coded MC-CDMA systems," in *Military Communications Conference, MILCOM 2007, October 29, 2007 - October 31, 2007*, Orlando, FL, United states, 2007.

[12] L. K. Bansal and A. Trivedi, "Comparative Study of Different Space-Time Coding Schemes for MC-CDMA Systems," *International Journal of Communications, Networks and System Sciences*, vol. 3, pp. 418-24, 2010.

[13] Z. Yanxing, Y. Qinye, Z. Yivven, D. Ke, L. Ming, and R. Aifeng, "Direct decoding of uplink space-time block coded multicarrier code division multiple access systems," in *Communications, 2004 IEEE International Conference*, 2004, pp. 2372-2376 Vol.4.

[14] K. Deng, Q. Yin, H. Zhang, and A. Ren, "Direct multiuser symbol detector for space-time block coded MC-CDMA systen with uniform linear array," in *2004 IEEE 59th*

Vehicular Technology Conference, VTC2004-Spring: Towards a Global Wireless World, May 17, 2004 - May 19, 2004, Milan, Italy, 2004, pp. 1456-1460.

[15] A. Ling and L. Milstein, "The effects of spatial diversity and imperfect channel estimation on wideband MC-DS-CDMA and MC-CDMA," *Communications, IEEE Transactions*, vol. 57, pp. 2988-3000, 2009.

[16] M. Mehrkam and A. Z. Asli, "EM-based Multi-User Detection for STBC-MC-CDMA communication systems," in *Signal Processing and Communication Systems, 2009. ICSPCS 2009. 3rd International Conference on*, 2009, pp. 1-6.

[17] D. Falconer, S. L. Ariyavisitakul, A. Benyamin-Seeyar, and B. Eidson, "Frequency domain equalization for single-carrier broadband wireless systems," *Communications Magazine, IEEE*, vol. 40, pp. 58-66, 2002.

[18] P. L. Kafle, A. B. Sesay, and J. McRory, "An iterative MMSE-decision feedback multiuser detector for space-time coded multicarrier CDMA system," in *Canadian Conference on Electrical and Computer Engineering; Technology Driving Innovation, 2004, May 2, 2004 - May 5, 2004*, Niagara Falls, Canada, 2004, pp. 2281-2286.

[19] P. L. Kafle and A. B. Sesay, "Iterative semiblind multiuser receivers for a space-time block-coded MC-CDMA uplink system," *IEEE Transactions on Vehicular Technology*, vol. 53, pp. 601-610, 2004.

[20] M. El-Hajjar, O. Alamri, R. G. Maunder, and L. Hanzo, "Layered Steered Space–Time-Spreading-Aided Generalized MC DS-CDMA," *Vehicular Technology, IEEE Transactions*, vol. 59, pp. 999-1005, 2010.

[21] S. Bangwon and A. Jae Young, "LMS adaptive receiver for uplink space-time coded MC-CDMA systems," in *Advanced Communication Technology (ICACT), 2010 The 12th International Conference on*, 2010, pp. 839-843.

[22] J.-L. Yu, C.-H. Wu, and M.-F. Lee, "MC-CDMA MIMO systems with quasi-orthogonal space-time block codes: Channel estimation and multiuser detection," *International Journal of Communication Systems*, vol. 25, pp. 294-313, 2012.

[23] J.-L. Yu, C.-C. Lin, and M.-F. Lee, "MC-CDMA multiple-input multiple-output systems with space-time block codes," in *MAPE2005: IEEE 2005 International Symposium on Microwave, Antenna, Propagation and EMC Technologies for Wireless Communications, August 8, 2005 - August 12, 2005*, Beijing, China, 2005, pp. 1492-1495.

[24] M. Juntti, M. Vehkapera, J. Leinonen, V. Zexian, D. Tujkovic, S. Tsumura, *et al.*, "MIMO MC-CDMA communications for future cellular systems," *Communications Magazine, IEEE*, vol. 43, pp. 118-124, 2005.

[25] P. Nagaradjane, S. N. Chandrasekaran, K. S. Vishvaksenan, and M. Ramakrishnan, "MIMO multi carrier interleave division multiple access system with multiuser detection," in *Wireless Communication and Sensor Computing, 2010. ICWCSC 2010. International Conference on*, 2010, pp. 1-4.

[26] P. Nagaradjane, S. N. Chandrasekaran, and K. S. Vishvaksenan, "MIMO Multi Carrier Interleave Division Multiple Access System with Multiuser Detection: Performance Results," in *Int'l J. of Communications, Network and System Sciences*, 2010, pp. 413-417.

[27] S. Wei and M. G. Amin, "Minimum variance receiver for multicarrier CDMA systems with space-time coding," in *Conference Record of the 37th Asilomar Conference on Signals, Systems and Computers, 9-12 Nov. 2003*, Piscataway, NJ, USA, 2003, pp. 1152-5.

[28] W. Sun, H. Li, and M. Amin, "MMSE detection for space-time coded MC-CDMA," in *2003 International Conference on Communications (ICC 2003), May 11, 2003 - May 15, 2003*, Anchorage, AK, United states, 2003, pp. 3452-3456.

[29] Y. Jung-Lang and W. Chun-Hsien, "Multiuser detection for QO-STBC MC-CDMA MIMO systems," in *Communications and Networking in China, 2009. ChinaCOM 2009. Fourth International Conference on*, 2009, pp. 1-5.

[30] Y. Jung-Lang, W. Chun-Hsien, and L. Ming-Feng, "Multiuser receiver design for MC-CDMA systems with quasi-orthogonal STBCs," in *Signal Processing, 2008. ICSP 2008. 9th International Conference*, 2008, pp. 1731-1734.

[31] J.-L. Yu, M.-F. Lee, and C.-C. Lin, "Multiuser receivers for MC-CDMA MIMO systems with space-time block codes," *Signal Processing,* vol. 89, pp. 99-110, 2009.

[32] V. T. Vakili and M. T. Mohebbi, "A new scheme for signal reception in MC-CDMA systems with space-time block coding," in *Wireless and Optical Communications Networks, 2005. WOCN 2005. Second IFIP International Conference on*, 2005, pp. 463-467.

[33] Z. Li and M. Latva-aho, "Nonblind and semiblind space-time-frequency multiuser detection for space-time block-coded MC-CDMA," *IEEE Transactions on Wireless Communications,* vol. 4, pp. 1311-1318, 2005.

[34] A. Gusmao, R. Dinis, and N. Esteves, "On frequency-domain equalization and diversity combining for broadband wireless communications," *Communications, IEEE Transactions,* vol. 51, pp. 1029-1033, 2003.

[35] H. Zhihua and V. K. Dubey, "Performance analysis for downlink MC-CDMA systems with space-time block codes in frequency-selective Rayleigh fading channels," in *ICICS-PCM 2003. Proceedings of the 2003 Joint Conference of the Fourth International Conference on Information, Communications and Signal Processing and Fourth Pacific-Rim Conference on Multimedia, 15-18 Dec. 2003*, Piscataway, NJ, USA, 2003, pp. 658-62.

[36] C. Kotchasarn, "Performance analysis of uplink MIMO MC-CDMA systems with V-BLAST over frequency selective Rayleigh fading channel," in *Industrial Electronics & Applications, 2009. ISIEA 2009. IEEE Symposium on*, 2009, pp. 733-736.

[37] P. Xiaoming, L. Zhongding, and F. P. S. Chin, "Performance comparison of different MIMO configurations for downlink MC-CDMA systems," in *Communications Systems, 2004. ICCS 2004. The Ninth International Conference on*, 2004, pp. 281-285.

[38] H. M. Elkamchouchi and A. M. Medra, "Performance comparison of MIMO space-time block coded MC-CDMA systems in Nakagami-m fading channel," in *Radio Science Conference, 2009. NRSC 2009. National*, 2009, pp. 1-7.

[39] A. Lodhi, F. Said, M. Dohler, and A. H. Aghvami, "Performance comparison of space-time block coded and cyclic delay diversity MC-CDMA systems," *Wireless Communications, IEEE,* vol. 12, pp. 38-45, 2005.

[40] M. Valipour and H. Shafiee, "Performance comparison of space-time coded MC-CDMA systems," in *2005 International Conference on Wireless and Optical Communications Networks, 6-8 March 2005*, Piscataway, NJ, USA, 2005, pp. 458-62.

[41] N. Kumaratharan, E. E. Arnold, J. Venkatesan, and P. Dananjayan, "Performance Improvement of ICE for Orthogonal STBC MC-CDMA Systems over MIMO Channels," in *Industrial and Information Systems, 2008. ICIIS 2008. IEEE Region 10 and the Third international Conference on*, 2008, pp. 1-5.

[42] A. Narzullaev, K. Ryu, and Y. Park, "Performance investigation of space-time block coded multicarrier DS-CDMA in time-varying channels," *ETRI Journal*, vol. 28, pp. 684-687, 2006.

[43] J. Bastos and A. Gameiro, "Performance of extended space-time coding techniques for MIMO MC-CDMA systems," in *European Conference on Antennas and Propagation: EuCAP 2006, November 6, 2006 - November 10, 2006*, Nice, France, 2006.

[44] M. Valipour and H. Shafiee, "Performance of MC-CDMA systems with space-time block codes in frequency selective fading channels," in *Communications Systems, 2004. ICCS 2004. The Ninth International Conference on*, 2004, pp. 645-649.

[45] J. M. Auffray and J. F. Helard, "Performance of multicarrier CDMA technique combined with space-time block coding over Rayleigh channel," in *IEEE ISSTA 2002 - IEEE International Symposium on Spread Spectrum Techniques and Applications, 2-5 Sept. 2002*, Piscataway, NJ, USA, 2002, pp. 348-52.

[46] Z. Li and M. Latva-aho, "Performance of space-time block coded MC-CDMA in Nakagami fading channels," *Electronics Letters*, vol. 39, pp. 222-224, 2003.

[47] L. Hang, Y. Wei, T. Zhenhui, and C. Shixin, "Performance of space-time block-coded MC-CDMA system in multipath fading channel," in *Microwave, Antenna, Propagation and EMC Technologies for Wireless Communications, 2005. MAPE 2005. IEEE International Symposium on*, 2005, pp. 1546-1550 Vol. 2.

[48] W. Xinsheng, Y. Wei, T. Zhenhui, and C. Shixin, "Performance of space-time block-coded multicarrier DS-CDMA system in a multipath fading channel," in *IEEE 2005 International Symposium on Microwave, Antenna, Propagation and EMC Technologies for Wireless Communications, 8-12 Aug. 2005*, Piscataway, NJ, USA, 2005, pp. 1551-5.

[49] L. K. Bansal and A. Trivedi, "Performance study of space-time trellis coded MC-CDMA system employing different detection techniques," in *4th International Conference on Wireless Communication and Sensor Networks, WCSN 2008, December 27, 2008 - December 29, 2008*, Indore, India, 2008, pp. 137-140.

[50] Z. Fayong, "PIC Receiver for MIMO MC-CDMA Systems Based on LCRLSCMA," in *Wireless Communications, Networking and Mobile Computing, 2008. WiCOM '08. 4th International Conference on*, 2008, pp. 1-4.

[51] M. Vehkapera, D. Tujkovic, L. Zexian, and M. Juntti, "Receiver design for spatially layered downlink MC-CDMA system," *Vehicular Technology, IEEE Transactions on*, vol. 54, pp. 1042-1055, 2005.

[52] L. Hanzo, L.-L. Yang, M. Munster, and B.-J. Choi, "Recital on multicarrier communications: Space-time coded versus adaptive OFDM/MC-CDMA," in

SympoTIC'04 - Joint 1st Workshop on Mobile Future and Symposium on Trends in Communications - Proceedings, October 24, 2004 - October 26, 2004, Bratislava, Slovakia, 2004, pp. X-XXVIII.
[53] V. Le Nir, M. Helard, and R. Le Gouable, "Space-time block coding applied to turbo coded multicarrier CDMA," in *57th IEEE Semiannual Vehicular Technology Conference. VTC 2003, 22-25 April 2003*, Piscataway, NJ, USA, 2003, pp. 577-81.
[54] S. Phrompichai and P. Yuvapoositanon, "A space-time chip semiblind multiuser receiver based on LMS algorithms," in *Communications, 2008. APCC 2008. 14th Asia-Pacific Conference on*, 2008, pp. 1-5.
[55] B. Golkar and F. Danilo-Lemoine, "Space-Time Coding and Spatial Multiplexing in MIMO Multicarrier CDMA," in *Personal, Indoor and Mobile Radio Communications, 2007. PIMRC 2007. IEEE 18th International Symposium on*, 2007, pp. 1-5.
[56] Z. Cheng and Z. Cuifang, "Space-time multiuser detection for space-time block coded multicarrier CDMA systems," in *2006 International Conference on Communication Technology, ICCT '06, November 27, 2006 - November 30, 2006*, Guilin, China, 2006.
[57] J. Li, K. B. Letaief, and Z. Cao, "Space-time turbo multiuser detection for coded MC-CDMA," *IEEE Transactions on Wireless Communications*, vol. 4, pp. 538-549, 2005.
[58] S. Jamallulil, J. P. Cances, and V. Meghdadi, "Space-time-block-coded transmissions for downlink MC-CDMA transmissions over frequency-selective fading channels," *Wireless Personal Communications*, vol. 39, pp. 63-79, 2006.
[59] N. Kumaratharan, S. Jayapriya, and P. Dananjayan, "STTC based site diversity technique for MC-CDMA system," in *Control, Automation, Communication and Energy Conservation, 2009. INCACEC 2009. 2009 International Conference on*, 2009, pp. 1-5.
[60] N. Kumaratharan, S. Jayapriya, and P. Dananjayan, "STTC based STBC site diversity technique for MC-CDMA system," in *Computing Communication and Networking Technologies (ICCCNT), 2010 International Conference on*, 2010, pp. 1-6.
[61] S. Phrompichai and P. Yuvapoositanon, "A Time-Reversal Space-Time Chip Semiblind Receiver for TR-STBC Downlink MIMO MC-CDMA Systems," in *Wireless and Mobile Computing, Networking and Communications, 2009. WIMOB 2009. IEEE International Conference*, 2009, pp. 19-23.
[62] P. Yuvapoositanon and S. Suwannajan, "A time-reversal-based space-time block coded blind adaptive MC-CDMA receiver," in *2009 6th International Conference on Electrical Engineering/Electronics, Computer, Telecommunications and Information Technology (ECTI-CON), 6-9 May 2009*, Piscataway, NJ, USA, 2009, p. 4 pp.
[63] X. Hu and Y. H. Chew, "On the capacity of multicode and variable spreading gain multirate space-time block coded multicarrier CDMA systems over frequency selective Rayleigh fading channel," in *Vehicular Technology Conference, 2004. VTC2004-Fall. 2004 IEEE 60th*, 2004, pp. 353-357.
[64] N. Kumaratharan and P. Dananjayan, "STSIC Detection for multi-user MIMO MC-CDMA systems," in *TENCON 2008-2008 IEEE Region 10 Conference*, 2008, pp. 1-6.

[65] G. Senthilkumar and R. Amutha, "Capacity enhancement of multicarrier code division multiple access (MCCDMA) using orthogonal complete complementary codes and adaptive constellations," *Scientific Research and Essays,* vol. 9, pp. 153-161, 2014.
[66] C. Xu, M. El-Hajjar, R. G. Maunder, L.-L. Yang, and L. Hanzo, "Performance of the Space-Time Block Coded DS-CDMA Uplink Employing Soft-Output ACO-Aided Multiuser Space-Time Detection and Iterative Decoding," in *Vehicular Technology Conference (VTC 2010-Spring), 2010 IEEE 71st*, 2010, pp. 1-5.
[67] D. L. Nicholson, *Spread spectrum signal design. LPE and AJ systems*. Rockville, MD, USA: Computer Science Press, 1988.
[68] A. J. Viterbi, *CDMA: principles of spread spectrum communication*: Addison-Wesley Pub. Co., 1995.
[69] A. Viterbi, "Spread spectrum communications--Myths and realities," *Communications Magazine, IEEE,* vol. 17, pp. 11-18, 1979.
[70] A. J. Viterbi, "Spread spectrum communications: myths and realities," *Communications Magazine, IEEE,* vol. 40, pp. 34-41, 2002.
[71] R. C. Dixon, *Spread spectrum techniques*: IEEE Press : [distributed by Wiley], 1976.
[72] S. H. Mneney, "Wireless CDMA for rural application," in *AFRICON '96*, New York, NY, USA, pp. 408-13.
[73] R. C. Dixon, *Spread spectrum systems*, 2nd ed. Chichester, Sussex, UK: Wiley, 1984.
[74] N. Yee and J.-P. Linnartz, "BER of multi-carrier CDMA in an indoor Rician fading channel," in *Proceedings of the 27th Asilomar Conference on Signals, Systems & Computers, November 1, 1993 - November 3, 1993,* Pacific Grove, CA, USA, 1993, pp. 426-430.
[75] N. Yee, J.-P. M. G. Linnartz, and G. Fettweis, "Multi-carrier CDMA in indoor wireless radio networks," *IEICE Transactions on Communications,* vol. E77-B, pp. 900-904, 1994.
[76] T. C. D. Group, "4Q 2010 CDMA SUBSCRIBERS," ReportDec 2010 2010.
[77] L. A. A. F. Base. (2011, 27 October). *Fact Sheet: Pseudorandom Noise (PRN) Code Assignments* [World Wide Web]. Available: http://www.losangeles.af.mil/library/factsheets/factsheet.asp?id=8618
[78] N. Moodley and S. H. Mneney, "Recurrent neural networks for sub-optimal multiuser detection," *Transactions of the South African Institute of Electrical Engineers,* vol. 97, pp. 105-111, 2006.
[79] H. Hashemi, "The indoor radio propagation channel," *Proceedings of the IEEE,* vol. 81, pp. 943-968, 1993.
[80] M. B. Mollah and M. R. Islam, "Comparative analysis of Gold Codes with PN codes using correlation property in CDMA technology," in *Computer Communication and Informatics (ICCCI), 2012 International Conference on*, 2012, pp. 1-6.
[81] P. Samundiswary and P. Viswa Kalyan, "Performance Analysis of WCDMA using Different Spreading Codes," *International Journal of Computer Applications,* vol. 38, pp. 8-11, 2012.
[82] G. Suchitra and M. L. Valarmathi, "Performance of Concatenated Complete Complementary code in CDMA systems," in *Cognitive Wireless Systems (UKIWCWS), 2009 First UK-India International Workshop on*, 2009, pp. 1-5.

[83] A. Ziani and A. Medouri, "Analysis of different Pseudo-Random and orthogonal spreading sequences in DS-CDMA," in *Multimedia Computing and Systems (ICMCS), 2012 International Conference on*, 2012, pp. 558-564.

[84] D. Muirhead and M. A. Imran, "Alamouti Transmit Diversity for Energy Efficient Femtocells," in *2011 IEEE 73rd Vehicular Technology Conference (VTC Spring), 15-18 May 2011*, Piscataway, NJ, USA, 2011, p. 5.

[85] V. V. Barinov, V. S. Kuznetsov, and M. V. Lebedev, "Spreading ensembles with improved correlation properties for multiple access," in *Personal, Indoor and Mobile Radio Communications, 2005. PIMRC 2005. IEEE 16th International Symposium on*, 2005, pp. 1081-1085 Vol. 2.

[86] Z. Gu, S. Xie, S. Rahardja, E. T. Sze, and Y. Xin, "Performance Comparison of Spreading Sequences in Synchronous MC-CDMA Systems," in *Information, Communications and Signal Processing, 2005 Fifth International Conference on*, 2005, pp. 633-637.

[87] G. V. S. Raju and J. Charoensakwiroj, "Orthogonal codes performance in multi-code CDMA," in *Systems, Man and Cybernetics, 2003. IEEE International Conference on*, 2003, pp. 1928-1931 vol.2.

[88] C. C. Chen, K. Yao, and E. Biglieri, "Optimal spread spectrum sequences-constructed from Gold codes," in *Global Telecommunications Conference, 2000. GLOBECOM '00. IEEE*, 2000, pp. 867-871 vol.2.

[89] M. Pal and S. Chattopadhyay, "A novel orthogonal minimum cross-correlation spreading code in CDMA system," in *Emerging Trends in Robotics and Communication Technologies (INTERACT), 2010 International Conference on*, 2010, pp. 80-84.

[90] J. Bi, Y. Wang, H. Tian, and K. Yi, "A new method to design CDMA spreading sequences," in *Communication Technology Proceedings, 2000. WCC - ICCT 2000. International Conference on*, 2000, pp. 526-529 vol.1.

[91] K. Khoongming, G. Guang, and D. R. Stinson, "A new family of Gold-like sequences," in *Information Theory, 2002. Proceedings. 2002 IEEE International Symposium on*, 2002, p. 181.

[92] L. Yu and J. Hu, "An improved Gold code for MC-CDMA system," in *Communications, 1999. APCC/OECC '99. Fifth Asia-Pacific Conference on ... and Fourth Optoelectronics and Communications Conference*, 1999, pp. 644-648 vol.1.

[93] D. Kedia, M. Duhan, and S. L. Maskara, "Evaluation of correlation properties of Orthogonal spreading codes for CDMA wireless mobile communication," in *Advance Computing Conference (IACC), 2010 IEEE 2nd International*, 2010, pp. 325-330.

[94] M. Akhavan-Bahabdi and M. Shiva, "Double orthogonal codes for increasing capacity in MC-CDMA systems," in *Wireless and Optical Communications Networks, 2005. WOCN 2005. Second IFIP International Conference on*, 2005, pp. 468-471.

[95] M. Moinuddin, M. Deriche, A. U. H. Sheikh, and A. Zerguine, "Analysis of multiple access interference in synchronous downlink CDMA systems with random signature sequences in AWGN and fading environments," in *Signal Processing and Its Applications, 2007. ISSPA 2007. 9th International Symposium on*, 2007, pp. 1-4.

[96] A. A. Khan, S. Bashir, and S. I. Shah, "An analysis of the effects of multiple access interference in DS-CDMA reverse link," in *Emerging Technologies, 2005. Proceedings of the IEEE Symposium on*, 2005, pp. 182-187.

[97] D. Carey, D. Roviras, and B. Senadji, "Comparison of multiple access interference in asynchronous MC-CDMA and DS-CDMA systems," in *Signal Processing and Its Applications, 2003. Proceedings. Seventh International Symposium on*, 2003, pp. 351-354 vol.2.

[98] R. H. Mahadevappa and J. G. Proakis, "Mitigating multiple access interference and intersymbol interference in uncoded CDMA systems with chip-level interleaving," *Wireless Communications, IEEE Transactions on*, vol. 1, pp. 781-792, 2002.

[99] W. M. Jang, L. Nguyen, and P. Bidarkar, "Multiple access and inter-carrier interference in OFDM-CDMA with random sequences," *Communications and Networks, Journal of*, vol. 7, pp. 21-28, 2005.

[100] L. Xuan and B. Senadji, "Multiple Access Interference Analysis in Asynchronous GSFH/MC-CDMA Systems," in *Wireless Communications and Networking Conference, 2007.WCNC 2007. IEEE*, 2007, pp. 197-201.

[101] S. Nagaraj and M. Bell, "Multiple Sequence Multicarrier CDMA for Interference-free Multiple Access," in *Wireless Telecommunications Symposium, 2006. WTS '06*, 2006, pp. 1-4.

[102] S. Sung-Hyuk and P. J. Voltz, "A multiple-access interference suppression technique employing orthogonal/random spreading sequences and a novel decentralized receiver for B-CDMA forward link systems in multipath channels," in *Circuits and Systems, 1998. ISCAS '98. Proceedings of the 1998 IEEE International Symposium on*, 1998, pp. 550-553 vol.4.

[103] E. M. Abu Anas and A. K. Mostafa, "A new approach to reduce multi-access interference in DS-CDMA," in *Ubiquitous and Future Networks, 2009. ICUFN 2009. First International Conference*, 2009, pp. 16-21.

[104] C. Hsiao-Hwa, C. Shin-Wei, and M. Guizani, "On Next Generation CDMA Technologies: The REAL Approach for Perfect Orthogonal Code Generation," *Vehicular Technology, IEEE Transactions on*, vol. 57, pp. 2822-2833, 2008.

[105] I. Mahalakshmi and S. Karunakaran, "Review on codes for multiple access communications," in *Electromagnetic Interference and Compatibility, 2003. INCEMIC 2003. 8th International Conference*, 2003, pp. 213-220.

[106] S. Coleri, M. Ergen, A. Puri, and A. Bahai, "A study of channel estimation in OFDM systems," in *56th Vehicular Technology Conference, September 24, 2002 - September 28, 2002*, Vancouver, BC, Canada, 2002, pp. 894-898.

[107] A. L. Intini, "Orthogonal Frequency Division Multiplexing for Wireless Networks - Standard IEEE 802.11a," University Of California, Santa Barbara, ReportDec 2000 2000.

[108] Y. Bar-Ness, J. P. Linnartz, and L. Xiangqun, "Synchronous multi-user multi-carrier CDMA communication system with decorrelating interference canceler," in *Personal, Indoor and Mobile Radio Communications, 1994. Wireless Networks - Catching the Mobile Future., 5th IEEE International Symposium*, 1994, pp. 184-188 vol.1.

[109] L. Vandendorpe, "Multitone spread spectrum multiple access communications system in a multipath Rician fading channel," *IEEE Transactions on Vehicular Technology*, vol. 44, pp. 327-337, 1995.

[110] S. Hara and R. Prasad, "DS-CDMA, MC-CDMA and MT-CDMA for mobile multi-media communications," in *Proceedings of Vehicular Technology Conference - VTC, 28 April-1 May 1996*, New York, NY, USA, 1996, pp. 1106-10.

[111] Q. M. Rahman, A. B. Sesay, and M. Hefnawi, "Two-stage maximum likelihood estimation (TSMLE) for MT-CDMA signals in the indoor environment," *Eurasip Journal on Wireless Communications and Networking*, vol. 2004, pp. 55-66, 2004.

[112] Q. M. Rahman and A. B. Sesay, "Data sequence detection for MT-CDMA signals," in *Electrical and Computer Engineering, 2002. IEEE CCECE 2002. Canadian Conference*, 2002, pp. 1400-1405 vol.3.

[113] Q. M. Rahman and A. B. Sesay, "Noncoherent MT-CDMA system with post-detection diversity combining," *Electrical and Computer Engineering, Canadian Journal of*, vol. 28, pp. 81-88, 2003.

[114] S. Hara and R. Prasad, "Design and performance of multicarrier CDMA system in frequency-selective Rayleigh fading channels," *Vehicular Technology, IEEE Transactions on*, vol. 48, pp. 1584-1595, 1999.

[115] Q. M. Rahman and A. B. Sesay, "Performance evaluation of non-coherent multi-tone CDMA system," in *2000 Canadian Conference on Electrical and Computer Engineering Conference Proceedings. Navigating to a New Era, 7-10 March 2000*, Piscataway, NJ, USA, 2000, pp. 245-9.

[116] Q. M. Rahman and A. B. Sesay, "Performance evaluation of non-coherent multi-tone CDMA system," in *Electrical and Computer Engineering, 2000 Canadian Conference*, 2000, pp. 245-249 vol.1.

[117] Q. M. Rahman and A. B. Sesay, "Post-detection diversity combining for non-coherent MT-CDMA system in a Rician fading channel," in *IEEE 54th Vehicular Technology Conference (VTC FALL 2001), October 7, 2001 - October 11, 2001*, Atlantic City, NJ, United states, 2001, pp. 1034-1038.

[118] Q. M. Rahman and A. B. Sesay, "Diversity combining for MT-CDMA signals in a fading channel," in *Communications, Computers and signal Processing, 2001. PACRIM. 2001 IEEE Pacific Rim Conference on*, 2001, pp. 140-143 vol.1.

[119] Q. M. Rahman and A. B. Sesay, "Post-detection diversity combining for non-coherent MT-CDMA system in a Rician fading channel," in *Vehicular Technology Conference, 2001. VTC 2001 Fall. IEEE VTS 54th*, 2001, pp. 1034-1038 vol.2.

[120] Q. M. Rahman and A. B. Sesay, "TSMLE-based MT-CDMA system in Rician Fading Channel," in *2002 IEEE Canadian Conference on Electrical and Computer Engineering, May 12, 2002 - May 15, 2002*, Winnipeg, Manitoba, Canada, 2002, pp. 1386-1391.

[121] B. Y. Sang, Y. P. Seung, and G. K. Chung, "Multi-carrier parallel combinatory DS/CDMA system: bandwidth efficient multiple access scheme for indoor wireless communication," in *Universal Personal Communications Record, 1997. Conference Record., 1997 IEEE 6th International Conference*, 1997, pp. 470-474 vol.2.

[122] L. Vandendorpe and O. van de Wiel, "Fractionally spaced decision feedback joint detection for multitone CDMA systems," in *Spread Spectrum Techniques and Applications Proceedings, 1996., IEEE 4th International Symposium*, 1996, pp. 1361-1365 vol.3.

[123] N. Yee and J.-P. Linnartz, "Controlled equalization of multi-carrier CDMA in an indoor Rician fading channel," in *Proceedings of the 1994 IEEE 44th Vehicular Technology Conference. Part 3 (of 3), June 8, 1994 - June 10, 1994*, Stockholm, Swed, 1994, pp. 1665-1669.

[124] S.-B. Yun, S. Y. Park, and C. G. Kang, "Multi-carrier parallel combinatory DS/CDMA system: Bandwidth efficient multiple access scheme for indoor wireless communication," in *Proceedings of the 1997 IEEE 6th International Conference on Universal Personal Communications, ICUPC'97. Part 1 (of 2), October 12, 1997 - October 16, 1997*, San Diego, CA, USA, 1997, pp. 470-474.

[125] R. Ganesh and K. Pahlavan, "Statistical characterisation of a partitioned indoor radio channel," *IEE Proceedings I (Communications, Speech and Vision),* vol. 139, pp. 539-545, 1992.

[126] A. A. Saleh and R. A. Valenzuela, "A statistical model for indoor multipath propagation," *Selected Areas in Communications, IEEE Journal*, vol. 5, pp. 128-137, 1987.

[127] T. S. Rappaport, "Characterization of UHF multipath radio channels in factory buildings," *Antennas and Propagation, IEEE Transactions on,* vol. 37, pp. 1058-1069, 1989.

[128] C. C. Huang and R. Khayata, "Delay spreads and channel dynamics measurements at ISM bands," in *Communications, 1992. ICC '92, Conference record, SUPERCOMM/ICC '92, Discovering a New World of Communications., IEEE International Conference on*, 1992, pp. 1222-1226 vol.3.

[129] I. B. Oluwafemi and S. H. Mneney, "Review of Space‐time Coded Orthogonal Frequency Division Multiplexing

Systems for Wireless Communication," *IETE Technical Review (Medknow Publications & Media Pvt. Ltd.),* pp. 417-426, 2013.

[130] S. Alamouti, "A simple transmit diversity technique for wireless communications," *Selected Areas in Communications, IEEE Journal on,* vol. 16, pp. 1451-1458, 1998.

[131] V. Tarokh, H. Jafarkhani, and A. R. Calderbank, "Space-time block codes from orthogonal designs," *Information Theory, IEEE Transactions,* vol. 45, pp. 1456-1467, 1999.

[132] V. Tarokh, H. Jafarkhani, and A. R. Calderbank, "Space-time block coding for wireless communications: performance results," *Selected Areas in Communications, IEEE Journal on,* vol. 17, pp. 451-460, 1999.

[133] V. T. Vakili and M. T. Mohebbi, "A new scheme for signal reception in MC-CDMA systems with space-time block coding," in *2005 International Conference on Wireless and Optical Communications Networks, 6-8 March 2005*, Piscataway, NJ, USA, 2005, pp. 463-7.

[134] B. Seo and J. Y. Ahn, "LMS adaptive receiver for uplink space-time coded MC-CDMA systems," in *12th International Conference on Advanced Communication Technology: ICT for Green Growth and Sustainable Development, ICACT 2010, February 7, 2010 - February 10, 2010*, Korea, Republic of, 2010, pp. 839-843.

[135] H. Li, W. Yang, Z. Tan, and S. Cheng, "Performance of space-time block-coded MC-CDMA system in multipath fading channel," in *MAPE2005: IEEE 2005 International Symposium on Microwave, Antenna, Propagation and EMC Technologies for Wireless Communications, August 8, 2005 - August 12, 2005*, Beijing, China, 2005, pp. 1546-1550.

[136] L. K. Bansal and A. Trivedi, "Comparative study of space-time trellis code concatenated with space-time block code MC-CDMA system," in *2009 IEEE International Advance Computing Conference. IACC 2009, 6-7 March 2009*, Piscataway, NJ, USA, 2009, pp. 1099-102.

[137] R. C. Dixon, *Spread Spectrum Signals and Systems*: IEEE, 1985.

[138] J. G. Proakis and M. Salehi, *Digital communications*, 2th ed.: McGraw-Hill, 1989.

[139] R. Gold, "Maximal recursive sequences with 3-valued recursive cross-correlation functions (Corresp.)," *Information Theory, IEEE Transactions on,* vol. 14, pp. 154-156, 1968.

[140] R. Gold, "Optimal binary sequences for spread spectrum multiplexing (Corresp.)," *Information Theory, IEEE Transactions on,* vol. 13, pp. 619-621, 1967.

[141] R. C. Dixon, *Spread Spectrum Systems*, 2nd ed.: Wiley John + Sons, 1984.

[142] D. V. Sarwate and M. B. Pursley, "Crosscorrelation properties of pseudorandom and related sequences," *Proceedings of the IEEE,* vol. 68, pp. 593-619, 1980.

[143] E. H. Dinan and B. Jabbari, "Spreading codes for direct sequence CDMA and wideband CDMA cellular networks," *Communications Magazine, IEEE,* vol. 36, pp. 48-54, 1998.

[144] O. B. Wojuola and S. H. Mneney, "Performance of even-and odd-degree Gold codes in a multi-user spread-spectrum system," in *Wireless Communications, Vehicular Technology, Information Theory and Aerospace & Electronic Systems (VITAE), 2014 4th International Conference*, Aalborg, Denmark, 2014, pp. 1-5.

[145] O. B. Wojuola and S. H. Mneney, "Multiple-access interference of Gold codes in a DS-CDMA system," *SAIEE African Research Journal,* vol. Volume 106, pp. 4-10, 2015.

[146] A. Goldsmith, *Wireless communications*: Cambridge university press, 2005.

[147] B. Vucetic and J. Yuan, *Space-time coding*: John Wiley & Sons, 2003.

[148] H. Jafarkhani, *Space-time coding: theory and practice*: Cambridge university press, 2005.

[149] I. B. Oluwafemi, "Super-orthogonal space-time turbo-coded OFDM systems," PhD, School of Engineering, University of KwaZulu-Natal, Durban, 2012.